# LITHOSTRATIGRAPHY AND PROVENANCE

# of the

# NEOARCHEAN McKELLAR HARBOUR SEQUENCE,

# SUPERIOR PROVINCE,

# ONTARIO, CANADA

by

ROBERT H. PURDON ©

A Thesis Submitted in Partial
Fulfilment of the Requirements
for the Degree of Master of Science

Lakehead University

November, 1995

ISBN 0-612-09233-X

## ABSTRACT

The McKellar Harbour Sequence is located on the shore of Lake Superior approximately 40 km west of the town of Marathon, Ontario. The Sequence was examined in detail through stratigraphic and geochemical investigations in order to determine the depositional environment and provenance of these rocks.

Four subsequences were identified in the McKellar Harbour Sequence, consistent with the facies associated with a distal submarine ramp environment. The Sequence shows thickening and coarsening upward trends, indicative of progradation of the ramp onto the basin floor. This indicates that the rocks of the McKellar Harbour Sequence are the distal equivalents of the proximal submarine ramp facies identified in the Beardmore-Geraldton and Quetico terranes to the north of the study area. Sedimentary strata from other potential source regions did not exhibit the characteristic features of a submarine ramp, and were likely deposited through different processes. Insufficient data were collected to determine the depositional environment for these units.

Geochemical analyses indicate that the rocks of the McKellar Harbour Sequence have immobile element chemistry that is very similar to that of the Beardmore-Geraldton and Quetico terranes, and that a continuum of deposition from north to south is present. Sediments generated in the Beardmore-Geraldton terrane were transported to small basins associated with the Schreiber-Hemlo volcanic island system by a submarine ramp.

# ACKNOWLEDGEMENTS

I would like to thank Dr. Phil Fralick for his support and patience in the completion of this project, which was partially funded by the Centre for Northern Studies and NSERC. Reino Viitala and Anne Hammond prepared the thin sections and Elenor Jensen assisted with the analyses.

Trow Consulting Engineers Ltd. provided drafting supplies, time, a regular paycheck and a career.

Most of the credit should, however, go to my wife Christina and daughter Leslie who inspired me to finish despite the commitments of fatherhood and a full-time job. This manuscript is dedicated to you both, without whom it would never have been completed.

TABLE OF CONTENTS

List of Attachments

# 1.0 INTRODUCTION

## 1.1 Purpose

This study is an attempt to establish the origin of the Late Archean metasedimentary rocks in the Jackfish-Middleton area through lithostratigraphic interpretation, provenance studies, and paleoenvironmental reconstruction. The study area has received little attention of this sort, with most previous work focusing on the nature of the gold mineralization at Hemlo. Within the study area there are several good exposures of sedimentary rock that contain information on the lithofacies present. Using lithofacies associations, the depositional environments for these specific locations can be determined. The best exposure of sedimentary strata in the study area lies on the shores of McKellar Harbour. This sequence provides an excellent opportunity to perform both provenance studies and compilation of data for paleoenvironmental interpretation. To gain a regional perspective, it is necessary to acquire sedimentological and geochemical data from any possible source areas that may have provided sediment to the McKellar Harbour Sequence. One possible source area (the Quetico Subprovince) has a substantial data base. Additional sedimentary exposures in the Winston Lake, Schreiber, Lake Superior, Pukaskwa, Hemlo, and Amwri Lake areas were examined as part of this study. The depositional environments and geochemical signatures of the various regions can then be compared in order to develop a regional reconstruction of depositional environments, providing an overview of the tectonic processes at work during the time of deposition. This type of study has not been attempted in the area as yet, and will yield significant information regarding the history of the region.

1.2 Location and Access

The study area is located within the District of Thunder Bay, between the town of Schreiber to the west, and White Lake Provincial Park to the east (Figure 1). The rocks within the study area consist of metavolcanic and metasedimentary supracrustal units in the Wawa Subprovince of the Superior Province, Canadian Shield. The area has been subdivided into smaller regions (Schreiber -Winston Lake, Jackfish - Middleton, and Heron Bay - Hemlo) to ease discussion (Figure 1). Access is gained primarily by Highway 17 (the Trans-Canada Highway, Lake Superior Route) which traverses east-west through the area. Several smaller dirt roads, and the Whitesand-Winston Road provide additional access off this main route The C.P.R. railway tracks also provide good access to the shore of Lake Superior at several points, and a boat launch can be used at Neys Provincial Park to enable water access to the McKellar Harbour area.

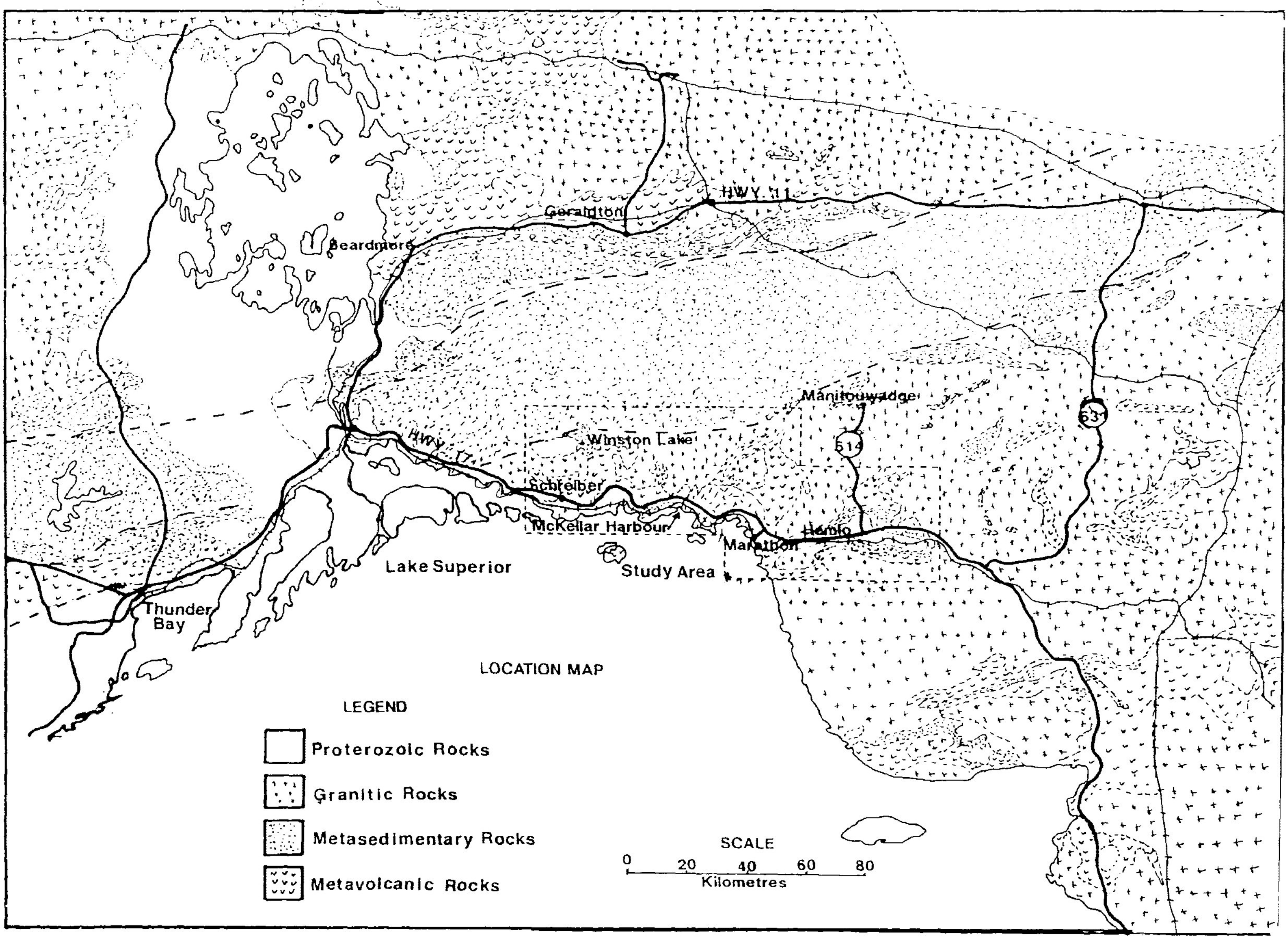


Figure 1: Study Area and General Geology

Due to the complexities introduced through metamorphism and deformation, interpretation of the data was made with caution. Deformation can produce features that are quite similar to primary sedimentary features, in addition to obliterating or complicating existing primary sedimentary structures. Thus, this study concentrates on the description and interpretation of small scale (i.e. individual lithofacies) observations, and lithofacies associations. Where possible, relatively less-deformed rocks were used to give insight into the understanding of more deformed rocks. For instance, in the McKellar Harbour section there was evidence deformation had occurred, causing the vertical attitudes of the units and the rare presence of minor Z type folds (or kinks) in some beds, but there were no bedding reversals or outcrop scale folded (i.e. synforms or antiforms) structures in over 850 m of section. These rocks would classify as "less-deformed" for the purposes of this discussion.

## 1.3 Previous Geological Work

The eastern portion of the study area received little attention prior to the discovery of gold in the Hemlo camp. Reconnaissance mapping was conducted by the Ontario Department of Mines (ODM) (now the Ontario Geological Survey (OGS)) in 1931 and 1932 by J.E. Thomson (Thomson 1931, 1933). Discovery of gold mineralization in what is now the Hemlo Camp, prompted mapping by M.W. Bartley and T.W. Page in 1947 for the Lake Superior Mining Corporation Ltd. (Page, 1947). These two workers continued mapping during the early 1950's for the Department of Industrial Development of the Canadian Pacific

Railway (Bartley and Page, 1957, 1958). V.G. Milne of the ODM mapped the Cirrus Lake-Bamoos Lake Area north of Marathon in 1963, and the Black River Area to the east in 1964, 1965 (Milne, 1968). The Heron Bay and Hemlo Areas were mapped by T.L. Muir of the OGS in 1977 and 1978, respectively (Muir, 1982a,b). Muir conducted a more detailed examination of the structure and stratigraphy of the Hemlo Camp in 1983 (Muir, 1984). Muir also produced detailed lithological and structural maps of the Hemlo Camp in 1990 and 1991. G.M. Siragussa of the OGS mapped to the east of Muir in 1983 (Siragussa, 1984a, b), and continued mapping to the east and northeast of the Camp in 1984 and 1985 (Siragussa, 1985a,b). Mann (1986) examined the lithostratigraphy of the Moose Lake Formation. Pan and Fleet (1989) conducted a study of the metamorphic petrology and gold mineralization of the White River gold prospect and examined the Cr-rich silicates of the Hemlo area. These workers also studied much of the geochemistry, alteration and metamorphism of the Hemlo camp. Pan (1990) also completed a Ph.D. thesis studying the metamorphic petrology and gold mineralization in the Camp. Pan, Fleet, and Stone (1991) looked at the calc-silicate alteration in the Hemlo deposit, the geochemistry of metasedimentary rocks in the Hemlo-Heron Bay greenstone belt, and skarn mineralization at the White River property in the Hemlo area. Corfu and Muir (1989) determined U-Pb ages in the Hemlo Camp.

The area to the west of the Coldwell Alkalic Complex (the Schreiber-Middleton Region) has received comparatively little attention. The Jackfish-Middleton Area was mapped at a scale of 1:31,680 by Walker (1967). The Big Duck Lake Area (Winston Lake Area) was mapped by Pye (1967). The Winston Lake VMS deposit was the subject of a paper by Balint et. al. (1986). Iron formations and associated rocks of the Lower Steel River - Little Steel lake area were the subject of a M.Sc. thesis by Schnieders (1987). Carter (1988) described the geology of the Schreiber - Terrace Bay Area. An occurrence of sulphide-facies iron formation southeast of Schreiber (the Morley Occurrence) was the subject of a study by Fralick et al (1989). The area was also given an overview in a field trip guide by Fralick and Barret, (1991), and the tectono-stratigraphic synthesis is discussed in Erickson, Krapez and Fralick (1994, in press).

# 2.0 GENERAL GEOLOGY

## 2.1 Introduction

The study area is bounded by rocks of the Quetico Subprovince to the north, and by rocks of the Pukaskwa Gneissic Complex to the south. The area is also effectively bisected by rocks of the Coldwell Alkalic Complex. The geologic discussions will deal with the rocks of the Schreiber - Winston Lake Region, Jackfish - Middleton Region, and the Heron Bay - Hemlo Region separately (refer to Figure 1 for the location of these regions within the study area). Most rocks in the study area have been subjected to at least greenschist facies metamorphism, thus to reduce repetitive usage, the prefix "meta" will be dropped and the lithologies described with their original nomenclature.

## 2.2 Schreiber - Winston Lake Region

The Winston Lake region consists of mainly mafic volcanic rocks in the southern portion. Intermediate to felsic volcanic rocks intercalated with sedimentary rocks occur interlayered with mafic flows in the north (Pye, 1967, Carter 1988), particularly in the vicinity of the Winston Lake Mine. Felsic Volcanic rocks associated with the Winston Lake Mine have been dated at 2723+/-2Ma (Schandl et al., 1991). The volcanic rocks have been intruded by granitic rocks of the Crossman Lake Batholith in the north, the Whitesand Lake Batholith to the west, and the Terrace Bay Batholith to the southeast. Rocks of the mine area are also intruded by a gabbroic sill.

The Schreiber - Terrace Bay Area is underlain by two cycles of volcanic rocks separated by sulphide-facies iron formation (Carter, 1988). The southern series of rocks is dominated by pillowed mafic flows, pillowed andesitic flows, and lesser amounts of rhyolite. This 2000m thick sequence gives way to 242m of felsic tuff and lapilli tuff, followed by 120m of iron formation (Carter, 1988). To the east, rocks below the iron formation marker horizon consist of a 3900m thick structureless package of intermediate calc-alkalic pyroclastic rocks. Above the iron formation, which Carter (1988) interprets as the top of the lower sequence, there occurs a 5230m thick sequence of iron-rich, pillowed tholeiitic mafic volcanic flows that are interlayered with thin units of clastic and chemical sedimentary rocks, as well as relatively thin (60m) andesitic and rhyolitic units. Overall, in the Schreiber - Winston Lake Area, the volcanic assemblages make up a much larger proportion of the rocks present than do the sedimentary rocks.

### 2.3 Jackfish-Middleton Region

The Jackfish - Middleton region is underlain by Archean supracrustal rocks consisting of a volcanic-sedimentary sequence that has been intruded by granitic to syenitic plutons, as well as mafic to ultramafic dikes and sills (Schnieders, 1987). Volcanic rocks include massive to pillowed mafic flows, and intermediate to felsic tuffs and pyroclastic rocks. Sedimentary rocks consist predominantly of graded turbidites with minor conglomerate and iron formation (Schnieders, 1987, Walker, 1967). Sedimentary rocks, although not dominating the sequence in this area, make up a substantially larger portion of the overall succession than in the Schreiber - Winston Lake Area.

Mafic intrusions include gabbroic and dioritic with minor ultramafic sills, dikes, and stocks (Schnieders, 1987). The relationship of these rocks to the host volcanic/sedimentary sequence (i.e. feeders, sub-volcanic intrusions, coarse-grained flows, etc.) is unknown (Walker, 1967).

The Paleoproterozoic Animikie Group (including the Gunflint and Rove Formations) overlies the Archean supracrustal rocks and consists of conglomerate, greywacke, algal chert, iron and dolomitic chert-carbonates ("Superior-Type" iron formation, [Schnieders, 1987]) black pyritic shale, argillite, tuff, and minor basalt.

The Sibley Group (consisting of the Pass Lake, Rossport, and Kama Hill Formations) represents Mesoproterozoic sedimentary rocks (conglomerate, sandstone, dolomite, chert, and mudstone) that disconformably overlie the shales of the Animikie Group. Keweenawan rocks consist of diabase, gabbro, peridotite, and the Osler Group volcanic rocks (tholeiitic basalts with minor rhyolite and interflow conglomerate). The Coldwell Alkalic Complex is a Late Precambrian intrusive that forms the eastern boundary of the Schreiber-Middleton area. Other intrusive rocks of the Late Precambrian that occur within the study area include the Prairie Lake Carbonatite and mafic to felsic dikes (geology summarized by Schnieders, 1987).

## 2.4 Heron Bay - Hemlo Region

The Hemlo region is underlain by supracrustal rocks that have been interpreted as part of the Schreiber-White River section of the Wawa Subprovince, Superior Province. These rocks are Late Archean in age (2800-2600 Ma: Corfu and Muir, 1989a,b), have been intruded by the Proterozoic Coldwell Alkalic Complex to the west, and other granitic bodies. The Gowan Lake Pluton in the vicinity of the Hemlo Mining Camp is 2678+/-2 Ma B.P. (Corfu and Muir, 1989).

The metavolcanic rocks of this portion of the greenstone terrane have been subdivided into two major groups based on geochemical analysis and location (Muir 1982a,b): The Playter Harbour Group lies to the south (Figures 2, 2A) and consists of massive and pillowed tholeiitic basalt flows (locally variolitic) with minor intercalations of intermediate to felsic pyroclastic rocks and siltstone units. Thin interflow units of chert, amphibolite and magnetite iron formation plus graphitic mudstone with pyrite, pyrrhotite, and chalcopyrite are also present (Muir, 1982a, b). The Heron Bay Group lies to the north of the Plater Harbour sequence and consists of the bulk of the supracrustal rocks in the Hemlo-Heron Bay greenstone terrane. These rocks host the gold deposits of the Hemlo Camp and consist of mainly dacitic with minor rhyolitic, calc-alkalic pyroclastic rocks with some calc-alkalic and basaltic, pyroclastic rocks, and minor tholeiitic basalt flows (Muir, 1982a,b). Muir (ibid) has identified a lateral facies transition within the Heron Bay Group as follows: coarse pyroclastic breccia occurs in the vicinity of Heron Bay, with blocks measuring up to 2 m in diameter. Fragment size decreases gradually to the east, with lapilli tuff and tuff dominating. East of Rous Lake, volcaniclastic sedimentary rocks become increasingly more prevalent, and to the east of the mine sites clastic sedimentary rocks (wacke and siltstone) predominate. This facies transition indicates the presence of a volcanic centre to the west in the vicinity of Heron Bay, and another possible minor centre in the area of the mining camp. Siragusa (1984) suggests the presence of another centre further to the east, where coarse pyroclastic rocks are found associated with pebbly arenite, which passes laterally to fine-grained sedimentary rocks to the west.

A fourth volcanic centre has been identified by Milne (1968) to exist north of the Musher Lake pluton. This is based on the apparently continuous sequence (from north to south) of mafic pillowed volcanic rocks, silicic pyroclastic rocks with minor intercalated mafic flows, conglomeratic sedimentary rocks, and then finer-grained sedimentary rocks.

FIGURE 2. Geology of the Heron Bay - Hemlo Region

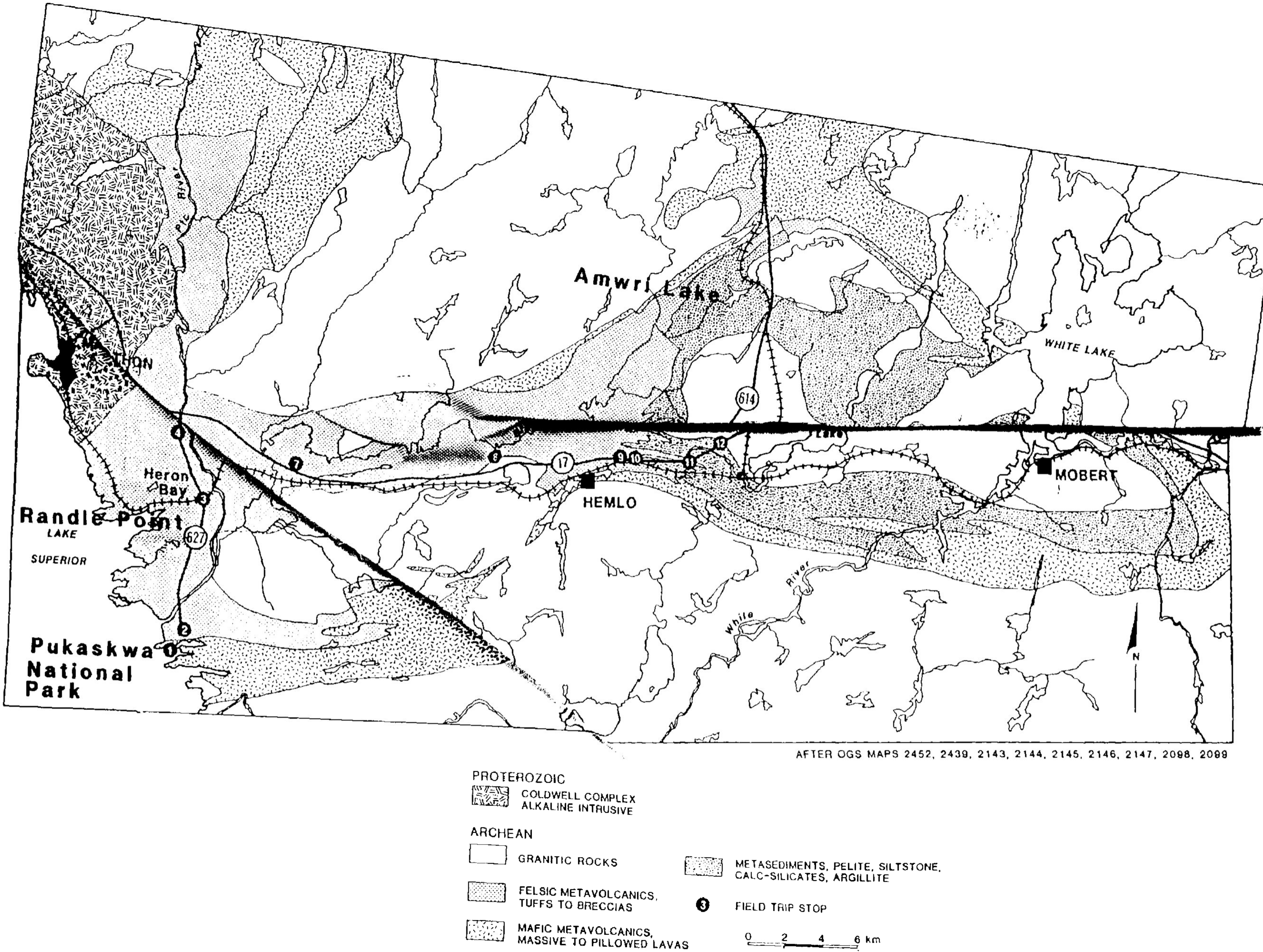


*Figure 2. Regional Geology of the Hemlo Area.*
**(reproduced from Patterson, 1984)**

Mafic and ultramafic intrusive rocks (gabbro, peridotite, and pyroxenite) have been emplaced into the volcanic and sedimentary rocks, and are located primarily in the Playter Harbour Group, and in the northern portions of the Hemlo region (Milne, 1968, Muir, 1982a,b). Some may have been comagmatic with the host mafic volcanic rocks (Muir, 1982a).

Several granitic bodies have also intruded the supracrustal assemblage. These form a series of hornblende-biotite granodiorite intrusions (Milne, 1968, Muir 1982a) and include the Heron Bay Pluton to the southwest, the Cedar Lake Pluton and Cedar Lake Stock in the centre, and the Mosher Lake Pluton to the north. Surrounding the supracrustal rocks are granitic gneiss of the Gowan Lake Pluton to the north, a portion of the Quetico Metasedimentary Belt (consisting primarily of quartz monzonite, Milne, 1968), the White Lake Gneissic Complex to the east, and the Pukaskwa Gneissic Complex to the south. The White Lake Gneissic Complex and Pukaskwa Gneissic Complex both consist of trondjhemite, granodiorite, and minor quartz monzonite (Muir, 1982a,b).

Feldspar porphyry dikes and sills are common locally, within both the volcanic and sedimentary rocks, some of which may be synvolcanic, and some related to the younger granitic intrusions (Muir, 1982a,b, Siragusa, 1984).

Two, and possibly more ages of Archean diabase dikes are present throughout the Heron Bay-Hemlo region, intruding all previously mentioned rock types, and occasionally each other (Muir, 1982a,b). Proterozoic diabase dikes are also present, as is lamprophyre, again cross-cutting all lithologies (Muir, 1982a,b).

## 2.5 Structural Geology

### 2.5.1 Schreiber - Winston Lake Region

The structural geology of the Big Duck Lake Area was discussed by Pye (1964). Pye describes the rocks as striking east-northeast in the east, with steep (60-90°) northerly dips. This strike changes to west near Big Duck Lake, and to the northwest in the Winston Lake Area. As the strike changes, the dips of beds were observed to flatten to 35-60° to the northeast. Pye (1964) interprets this as representing a possible syncline, or as being the result of crossfolding, but did not undertake a detailed structural study.

The structure of the Schreiber - Terrace Bay Area has been described by Carter (1988). The upper (Cycle II) volcanic/sedimentary assemblage in the Schreiber -Terrace Bay Area has been folded about east-southeasterly plunging axes (Carter, 1988), while the southern (lower Cycle I) volcanic sequence is homoclinal in nature. Deformation has produced a regional fabric that is generally parallel to the lithological trends, but is observed to "wrap around" the granitic intrusions locally. The rocks of this area have also been cut by faults that generally trend to the northwest.

### 2.5.2 Jackfish - Middleton Area

Walker (1967) based on reconnaissance scale mapping, found no reliable marker horizons, and iron formations to only represent the general structure locally . These formations were not continuous nor distinctive enough to use as markers. Walker (1967) also reports a northeast to east structural trend between Jackfish and Middleton that changes to a northwest trend between Santoy Lake and the Aguasabon River. In addition to this trend, he found easterly trending isoclinal folds, with sub-horizontal fold axes. In the Bottle Point and Kingdom Area, Walker (1967) suggests that the volcanic rocks overlie the sedimentary rocks based on local top indicators. Walker also identified an easterly plunging anticline in the mafic pillowed volcanic rocks between Jackfish Bay and the lower Steel River. This structure is upright south of Jackfish, and is overturned to 60° to the south east of Little Santoy Lake.

Schnieders (1987) undertook a more detailed but more localized examination of the structure in this area. He examined in detail the structural elements in four areas: Kingdom, Lawson Island, Steel River, and Blackfox (Figure 3). Schnieders concluded that the rocks of his study area were subjected to two separate folding events, or a complex progressive deformation during one event. The presence of structural facing reversals, and younging direction reversals indicates a more complex structural setting than that envisioned by Walker (1967). Schnieders (1987) shows that, in the Kingdom Area, the volcanic rocks lie stratigraphically below the sedimentary rocks, and that the iron formation marks the transition from active volcanism to turbiditic sedimentation.

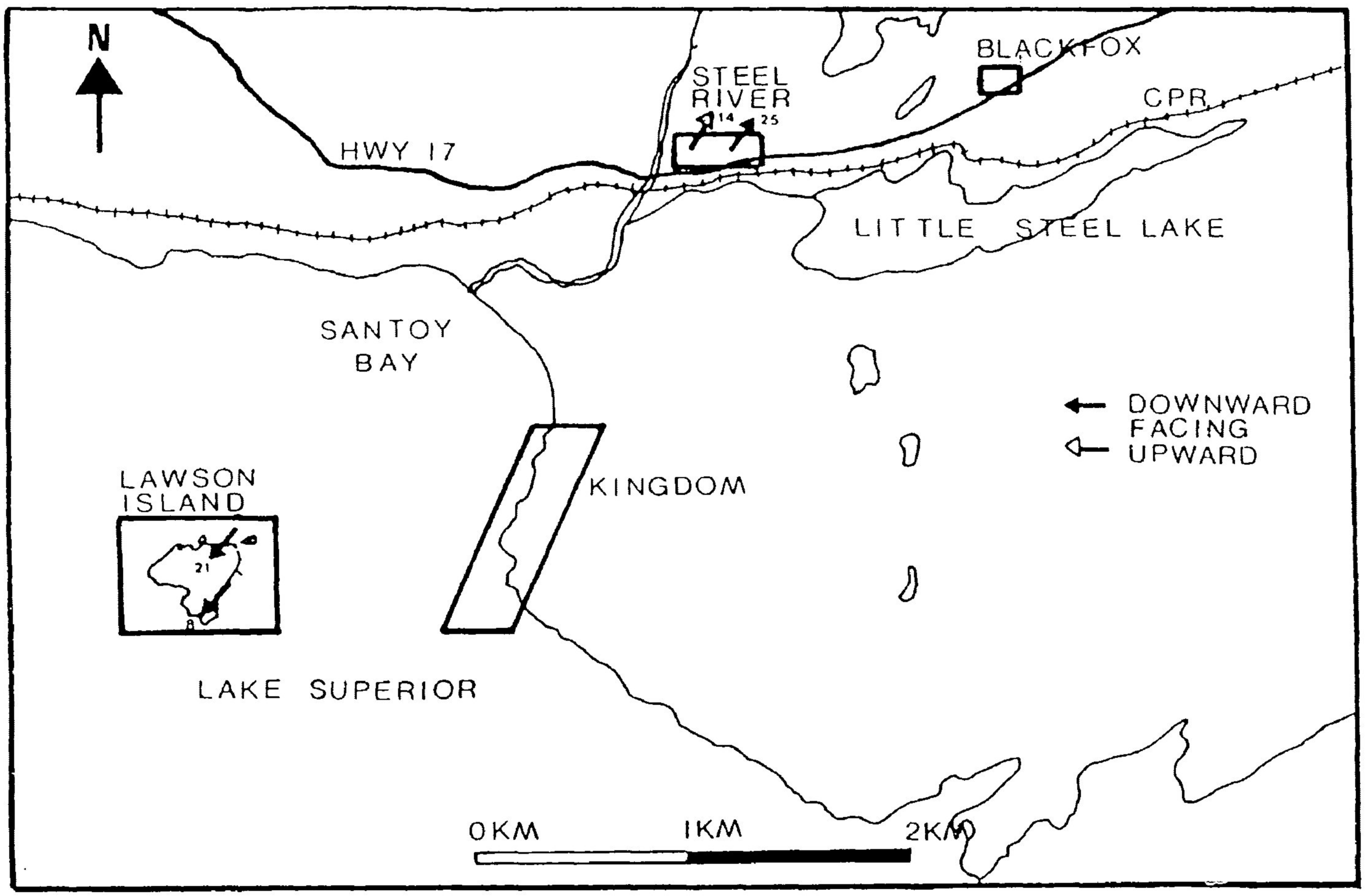


FIGURE 3. Schnieders' (1987) Study Areas.

### 2.5.3 Heron Bay - Hemlo Area

The structure of the Hemlo region has been examined by many workers. Patterson (1984) and Quartermane (1985) describe the large-scale structure as a synform with granitic intrusions along the fold axis. West and South of the Cedar Lake Pluton, rock lithologies strike generally E-W to ESE-WNW and are observed to dip moderately to subvertically to the north (Muir 1982b, Siragusa, 1984a,b). North of the Cedar Lake Pluton, the rocks strike NW-SE and dip subvertically or steeply to the southwest (Milne, 1968, Siragusa 1984a,b). This led Siragusa (1984a) to conclude that the rocks surrounding the Cedar Lake Pluton are downward converging structures, and were likely joined before the emplacement of the Cedar Lake Pluton; further work (Siragusa, 1984a) indicates that the two "belts" (one to the north, one to the west and south of the Cedar Lake Pluton) may be the limbs of a fold around the Cedar Lake Pluton, with the closure intruded by pegmatitic granite in the Bremner River area. The Hemlo region was subjected to polyphase deformation, or at least a very complex progressive deformation as indicated by the presence of up to three structural fabrics (Muir, 1985).

## 2.6 Metamorphism

### 2.6.1 Schreiber - Winston Lake

In the Winston Lake Area, the rocks have been subjected to a relatively high grade of metamorphism. Garnet-hornblende-biotite assemblages occur in the vicinity of the Winston Lake Mine, and within 1600m of the Quetico-Abitibi subprovince boundary throughout the Big Duck Lake Area, suggesting that this amphibolite-facies metamorphism is related to the subprovince boundary (Carter, 1988).

### 2.6.2 Jackfish - Middleton

The rocks of this area have generally been subjected to greenschist facies metamorphism (Walker, 1967) with corresponding local increases adjacent to intrusions. The contact aureole of the Coldwell Alkalic Complex was found by Walker (1967) to extend to 1.6 km (1 mile) from the contact with the intrusion in the Dead Horse Creek area. This aureole shows an increase in grade from the regional metamorphic grade to upper amphibolite facies.

### 2.6.3 Heron Bay - Hemlo

Generally, the regional metamorphic grade is thought to be of low greenschist facies (Muir, 1982 a,b). This assumption is based on the metamorphic grade of a large variolitic mafic volcanic unit north of Heron Bay that is relatively removed from the influence of any of the large intrusive bodies in the region which increase the local metamorphic grade. Contact metamorphism reaches upper amphibolite facies , and the effects of contact metamorphism can extend up to 1.7 km from the larger plutons (i.e. the Coldwell Alkalic Complex) (Muir, 1982b). The regional metamorphism affects all rock types except the Late Precambrian alkalic intrusive rocks, and possibly the Middle Precambrian diabase dikes (Muir 1982b). Smaller mafic to ultramafic intrusions also can increase the local metamorphic grade to lower amphibolite facies (Muir 1982b). Muir (1982a) has defined the regional metamorphic conditions as 3 to 3.4 kbars and 510 to 530 °C based on the mineralogy of a pelitic schist. Quartermain (1985) puts the conditions at 5 kbar and 600 °C based on the mineralogy of a pelite near the mining camp.

To the east of the Hemlo Camp, Siragusa (1983, 1984a,b) found the supracrustal sequence to have been subjected to amphibolite grade regional metamorphism, with local contact metamorphic aureoles adjacent to intrusive bodies. Siragusa (ibid) also found silicification along fractures and joints, particularly in the sediments proximal to the large granitic intrusions (i.e. the Cedar Lake Pluton). Milne (1967) found the rocks to the northwest of Hemlo (the Cirrus Lake - Bamoos Lake area) to have been subjected to hornblende-hornfels metamorphism or phases intermediate between hornblende-hornfels and almandine-amphibolite. Milne (1967) also noted retrograde effects in the presence of sericitization of andalusite, or sericitization and sausseritization of feldspar in amphibolite rocks.

To the northeast, (Black River Area) Milne found almandine-amphibolite grade metamorphism, along with retrograde effects.

The supracrustal rocks of the Heron Bay - Hemlo region can therefore be said to have been subjected to an average metamorphic grade of lower to middle amphibolite facies, with local increases or decreases in grade due to the proximity or distance to intrusive bodies, and retrograde metamorphism from amphibolite facies to greenschist facies appears to be relatively common.

# 3.0 LITHOFACIES ASSOCIATIONS - STUDY AREA

## 3.1 Introduction

In this section, sedimentary rocks of the Jackfish-Middleton region are described first, as they form the units whose depositional environments and provenance are being investigated. Sedimentary sequences in the surrounding areas are then described under the heading "Possible Source Areas", as a regional context is required for proper environmental and provenance reconstruction.

The following lithologies were recognized in the region:

1. Conglomeratic/Pyroclastic Rocks
2. Sandstone
3. Siltstone
4. Mudstone/Shale (including graphitic shale)
5. Chemical Sedimentary Rocks
   a. iron formation
   b. calc-silicate units
   c. barite horizons
6. Associated Volcanic Rocks
   a. mafic volcanic rocks
   b. intermediate to felsic volcanic rocks

The lithofacies will be discussed in terms of field and petrographic microscope examination. Where one or more of these lithofacies is not present for a specific area, it will be omitted from discussion. The Conglomeratic/Pyroclastic lithology is a broad classification that will be more clearly defined as the rocks from each area are described. Due to the effects of metamorphic recrystallisation and/or grain size reduction, with some rocks (the sandstone, siltstone, or mudstone lithofacies) nomencalture has been assigned through field observation, lithofacies association, and geochemical evidence rather than strictly by grain size. The inclusion of the volcanic rocks in the discussion of the sedimentary rocks is necessary due to the close association (particularly of the intermediate to felsic pyroclastic units which are often interstratified with the sedimentary units) of these two rock types. The correct interpretation of the depositional system requires that the relationship between the volcanic and sedimentary rocks be fully understood.

Ghibaudo (1992) has developed a classification system for subaqueous sediment gravity flows that allows more descriptive detail to be included in the nomenclature. When describing the sedimentary rocks in the study area formed by subaqueous processes, this classification system will be used in conjunction with that of Bouma (1962). The names and letter codes of Ghibaudo's classification system are presented in Appendix A.

## 3.2 Jackfish - Middleton Region

The Jackfish - Middleton Region has been divided into the Jackfish Area, which was examined by Schnieders (1987), and the McKellar Harbour Area which was examined as part of this study. The general geology of and sample locations in the McKellar Harbour Area are illustrated on Figure 4.

### 3.2.1 Jackfish Area

At the Steel River bridge on Highway 17, Schnieders (1987) describes turbiditic sandstones ranging from "ABCBCD and ABCBCDE (near complete turbidites, Bouma, 1967) to AE, (proximal) CDE, and BDE (medial-distal), and DE (distal-pelagic) types". These have been interpreted as representing deposition in channels (AE and AA turbidites), and on fan lobes (ABCDE turbidites) of the submarine fan model (Walker, 1976). Stratigraphic sections (Figures 4 and 5) from the Steel River Bridge have been interpreted as thinning upwards (Figure 4) and thickening upwards (Figure 5). Schnieders (1987) favours deposition on a submarine fan using Walker's (1978) model, but also suggests that deposition could have occurred in an arc-trench system with the progradation of small fan lobes along the floor of the trench.

Schnieders (1987) also examined the nature and chemistry of iron formation in the Jackfish Area in detail. They occur as units of varying thickness and commonly mark the contact between volcanic and sedimentary successions. They are often interbedded with carbonaceous slates underlying the turbidites (Schnieders, 1987).

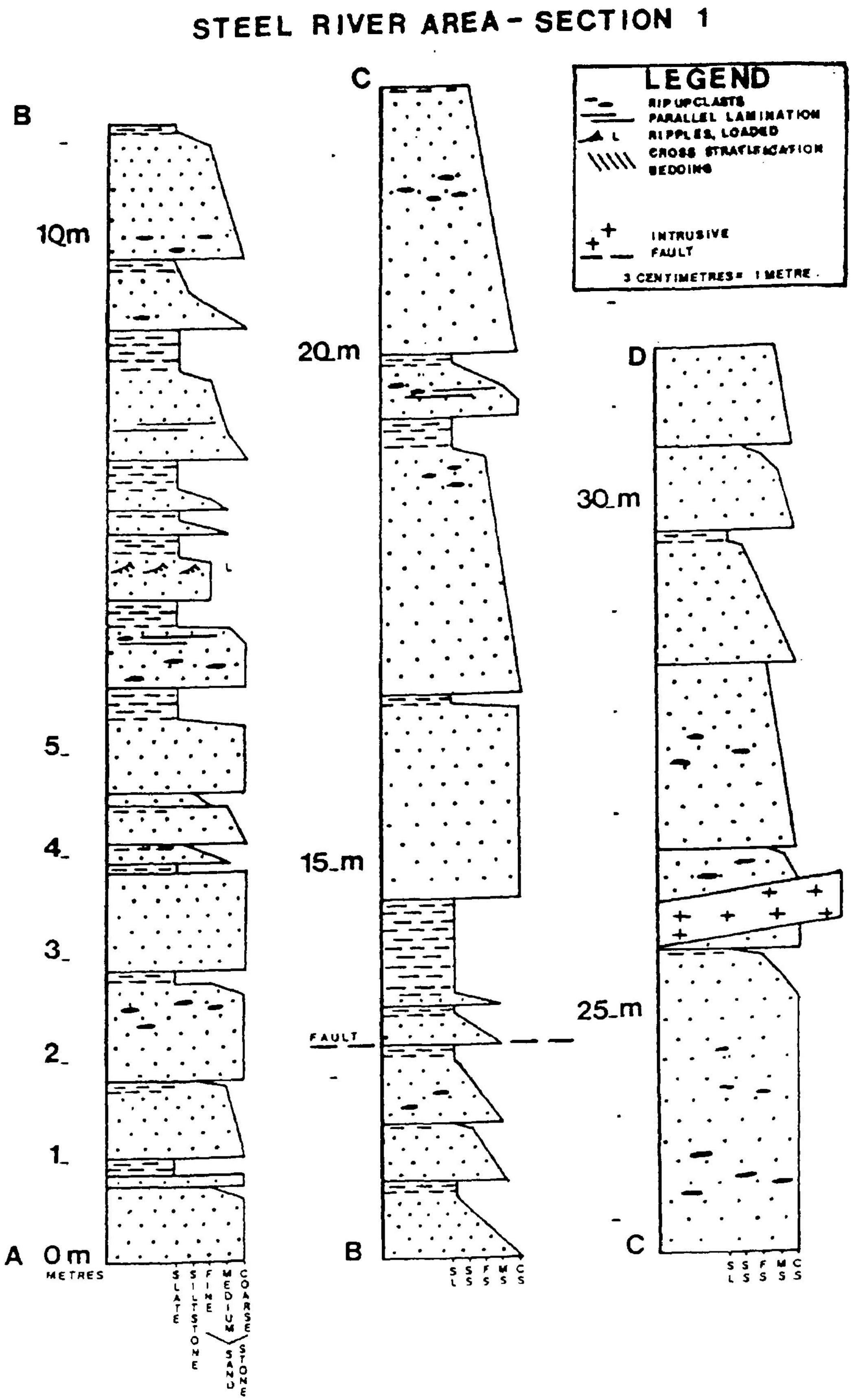


FIGURE 4. Steel River Section 1 (Schnieders, 1987)

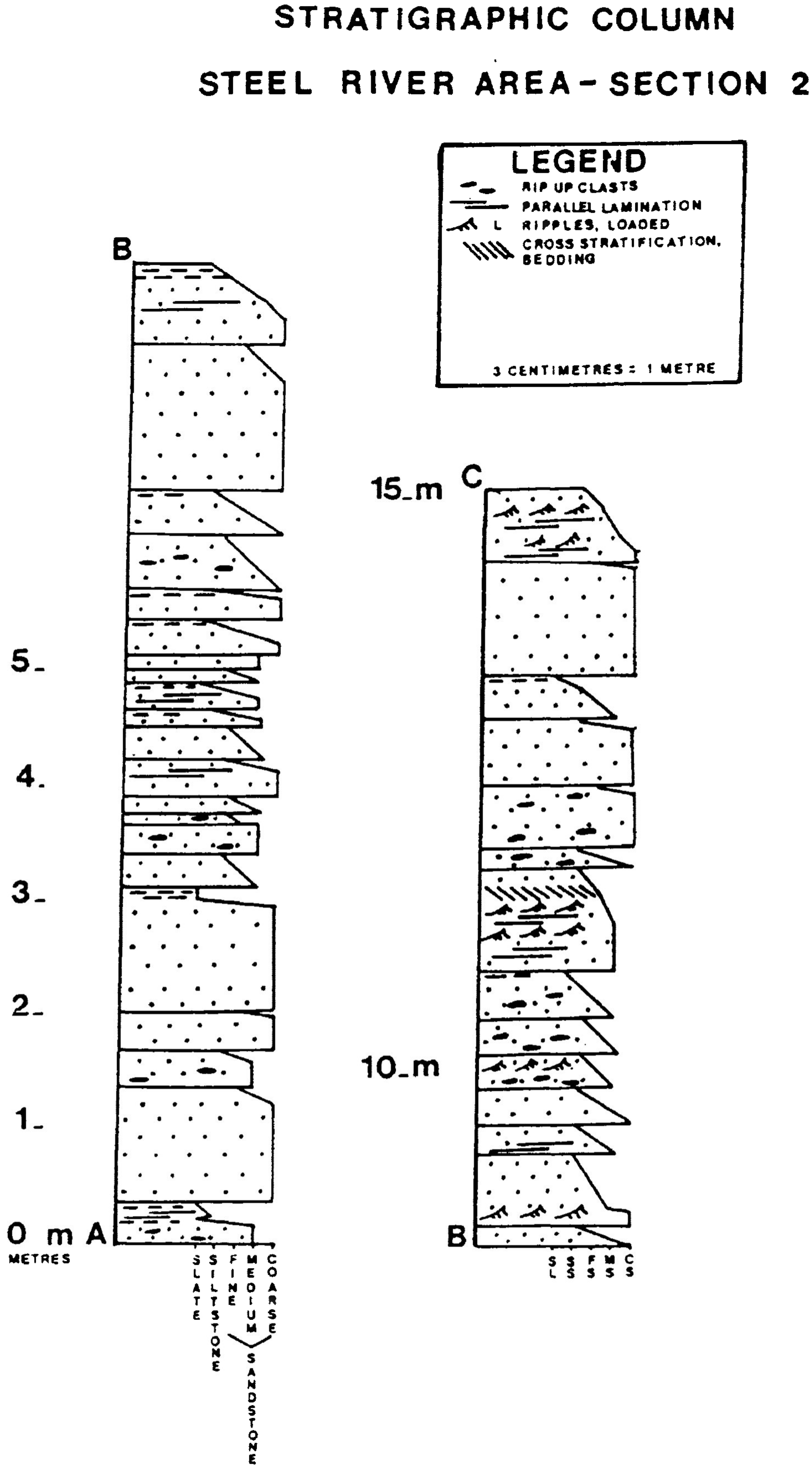


FIGURE 5: Steel River Section 2 (Schnieders, 1987)

Mafic (pillowed, massive, porphyritic and amygdaloidal) volcanic rocks are the predominant lithology associated with the iron formations of the Jackfish Area (Schnieders, 1987). In the Jackfish-Middleton region, mafic volcanic rocks consist of pillowed, sometimes variolitic, sometimes amygdaloidal, tholeiitic and minor calc-alkalic flows. One outcrop to the east of the Steel River on Hwy 17 shows an excellent exposure of spherulitic basalt . These spherules consist mainly of carbonate, giving the rock a higher than average $CO_2$ (up to 5%) content. These mafic rocks also have a lower $SiO_2$ content (47-52%) compared with other volcanic rocks from this portion of the study area which tend to have $SiO_2$ contents on the order of 60-69% (i.e. Samples BRS-14, BRS-15, BRS-16, data from Schnieders, 1987).

Graphitic slates were observed, primarily in the McKellar Harbour area, and consist of thin <1m beds of schistose, graphitic shale/slate often separating individual turbidites (McKellar Harbour Section, Appendix B). No calc-silicate units were observed in this portion of the study area.

In the Jackfish-Middleton portion of the study area, intermediate to felsic volcanic rocks occur as a large package to the north of the sedimentary units logged in the McKellar Harbour area. Walker (1967) describes these as tuff, lapilli tuff, agglomerate, crystal tuff and porphyritic lava. These rocks were not examined as part of this study.

### 3.2.2 McKellar Harbour Area

#### Coarse-Grained Lithologies

In the McKellar Harbour area, only one thin (5-10 cm) conglomeratic unit was located. This unit is consists of felsic and intermediate volcanic clasts in a fine-grained sandy matrix. It can be classified as facies Mgys using the nomenclature of Ghibaudo (1992). The clasts are angular and elongate parallel to bedding, with an average size of about 2X4 cm. No sedimentary structures were observed in the unit, and in thin section, the sandy matrix consists of mainly quartz with lesser amounts of feldspar and minor biotite. This unit occurs at the base of a Type 1 Subsequence (see below).

#### Medium-Grained Lithologies

The best occurrences of sandstone in this area are located within the sedimentary rocks that crop out in McKellar Harbour. A composite section was logged along the shore of Lake Superior, giving approximately 850 m of nearly continuous section (Appendix B). The sequence consists of mainly medium- to fine-grained turbiditic sandstones in conjunction with generally thinner siltstone/shale units in AE, AD, BE, ABE, CE, CD, DE, and rarely ABCDE (Bouma, 1962) arrangements. These units can also be described as facies gSM, glSM, lSM, xSM, tgSM, and trSM (Ghibaudo, 1992). The sandstone beds range in thickness from 10 cm to over 2 m, and usually possess parallel laminations of finer, but sometimes coarser sand. Other internal primary structures observed were: ripple cross-lamination, scour structures, suspended ripples, loaded ripples, convoluted bedding, siltstone/mudstone rip-up clasts, and occasional dewatering features such as sandstone dikes. Coarse-tail grading was noted at a few locations. Some beds of medium-grained sand contain laminations of medium- to coarse-sand- sized lithic fragments (usually granitic, but occasional volcanic in composition). Isolated, loaded, sandy ripples occur within some shale/mudstone units. Sedimentary structures define the individual lithofacies associations and will be discussed in more detail in the relevant section.

Fine-Grained Lithologies

Siltstone units were observed in the McKellar Harbour area most often as the C or D division of CE and DE turbidites (Bouma, 1962). These correspond to facies lTM and gTM of Ghibaudo (1992). However, Ghibaudo does not include a classification for rippled silt-mud couplets (CE turbidites). Using the same format as Ghibaudo, they can be given the letter-code rTM.

The silt-mud couplets observed in the McKellar Harbour Sequence range in thickness from < 1 cm to 25 - 30 cm. They are commonly bounded by sharp contacts, especially between individual turbidites. Within a single turbidite, the contact between the underlying siltstone and the overlying mudstone is somewhat more gradual, but still makes a sharp transition in grain size. The siltstone units commonly show parallel lamination (D division), but some beds show cross-stratification, and some contain ripples, classifying them as the C division of a CE turbidite (facies rTM). At times the siltstone units scour into underlying units, or in turn are scoured into by overlying units. Shale rip-up clasts are occasionally present within siltstone units. Silty material is also present as loaded or isolated ripples in the mudstone E divisions of some turbidites. Siltstones occur in Subsequence Types 1 and 2 (see below for their association with the sandstone lithologies).

In the Jackfish - Middleton area mudstone units usually occur as the E division in DE, BE, and CE turbidites (Bouma, 1962) or facies ITM, gTM or rTM (Ghibaudo, 1992) within Subsequence Types 1 and 2. Rare isolated siltstone/shale beds were observed. Thickness varies from <1 cm to >1 m. Sharp contacts usually exist between shale units and the surrounding beds, both within a single DE turbidite, and a sharp contact defines the top of one DE sequence and the beginning of the next. However, within an individual DE sequence, the contact between the shale E division and the underlying sandstone or siltstone D division is generally more gradual than that between separate DE sequences. Individual shale units (facies IgM or gM, Ghibaudo, 1992) also occur, often separating coarser sandstone units, but not as part of a turbidite deposit. The shale in these units is black in appearance, and usually has a well-developed planar fabric parallel to bedding. These individual shale units are interpreted to represent the top of Subsequence Type 3. Commonly, wisps of fine sand, and more rarely, isolated ripples of fine sand occur within the shale units. Overlying sandstone units often scour into underlying shale units (especially between separate turbidite sequences), and shale rip-up clasts are common within sandstone units.

### 3.2.3 Sequence Organization

The McKellar Harbour sequence can be divided into 4 types of subsequences, or lithofacies associations, based on the types of sedimentary structures present within individual layers, the relative thickness and grain size of the units, and their association with one another. There is a general lack of organization of the sequence into definitive cycles, but an attempt has been made to group units of a similar nature into their respective subsequences. The Subsequence Types 1, 2, and 3 are similar in appearance, but when examined in detail section (Appendix B) the differences in bed thickness, combined with the presence or absence of beds with specific sedimentary structures enables distinction to be made. Subsequence Type 4 is significantly different than the other Subsequences, making recognition easier, but only one occurrence of this Type was noted in the McKellar Harbour Area. Once one is familiar with the Subsequences, it is possible to recognize them in the field. The Subsequence nomenclature used herein has been developed based on data collected from McKellar Harbour, and is used only as a tool to aid in the description of the McKellar Harbour Sequence. The portions of the stratigraphic sections presented in this chapter use the legend as presented in Appendix B.

#### Type 1 Subsequence

This subsequence (Figure 6, Photograph 1) is the second most common within the Mckellar Harbour Sequence and consists of relatively thick (1 - 1.5 m) AE, BE and CE turbidites (facies gsS, gsxS, gslS,etc of Ghibaudo (1992).

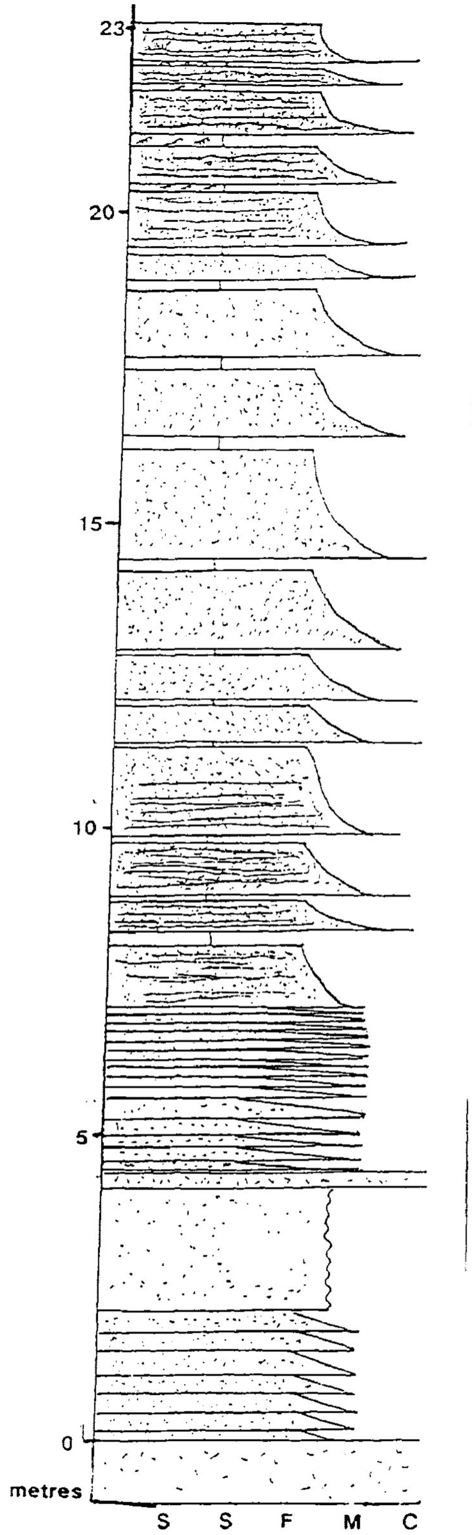


FIGURE 6: Type 1 Subsequence.

PHOTOGRAPH 1: Type 1 Subsequence.

The A/B/C divisions show medium to coarse bases that rapidly grade upwards to fine sand, usually in the first 10 to 20 cm. Lithic fragments (coarse sand-sized) are common in the bases, and petrographic examination has shown that mono or polycrystaline quartz dominates, but granitic fragments are common, and volcanic fragments form a minor component. In some beds, the lithic fragments or coarse sand grains are observed to float in a matrix of finer sand. The sand units are commonly parallel laminated (facies glS), with the laminations concentrated near the bottoms of the beds, becoming less frequent towards the tops of the beds. Other internal sedimentary structures consist of: shale rip-up clasts (usually but not always located near the bottom of beds); isolated ripples of coarser sand located sporadically throughout the unit; ripple cross-stratification (usually located in the upper portions of beds); scours into underlying units; convoluted lamination (disrupting the parallel-laminated portions of the beds); and sandstone dikes into overlying units. The last two dewatering features occur less frequently than the other features. Sedimentary structures usually occur only in the thickest units, with the exception of parallel lamination. The top of the sand unit is marked by a sharp contact, followed by 1 to 20 cm of silty shale, then a sharp contact with the overlying turbidite. Sometimes the E division silty shale contains isolated ripples of fine sand, or is scoured into by the overlying unit. The contact between the fine and coarse divisions of a single turbidite is generally not as sharp as that between separate turbidites, allowing them to be distinguished in the field.

Type 1 Subsequences vary in thickness from several metres to tens of meters, and often show a gradual upwards transition into other subsequences, but the upwards transition can be quite abrupt. The lower transition is almost always sharp. Within this Subsequence, the beds are usually observed to thin upwards, particularly when a transitional boundary exists between Type 1 and Type 2 (below) Subsequences.

Type 2 Subsequence

This subsequence (Figure 7, Photograph 2) dominates the McKellar Harbour Sequence. It consists mostly of AE, BE, CE, CD, BDE, ADE, and rarely ABCDE turbidites or facies gSM, lSM, glSM, gxSM, rSM, and rgSM of Ghibaudo (1992). These units are thinner (usually <1 m) than those included in the Type 1 Subsequence, but possess the same general appearance as they have a medium- to coarse-grained sand base which grades rapidly (within the first few cm) to fine-grained sand. The sand units also possess the same types of sedimentary structures as the Type 1 Subsequence. This Subsequence consists of relatively thinner

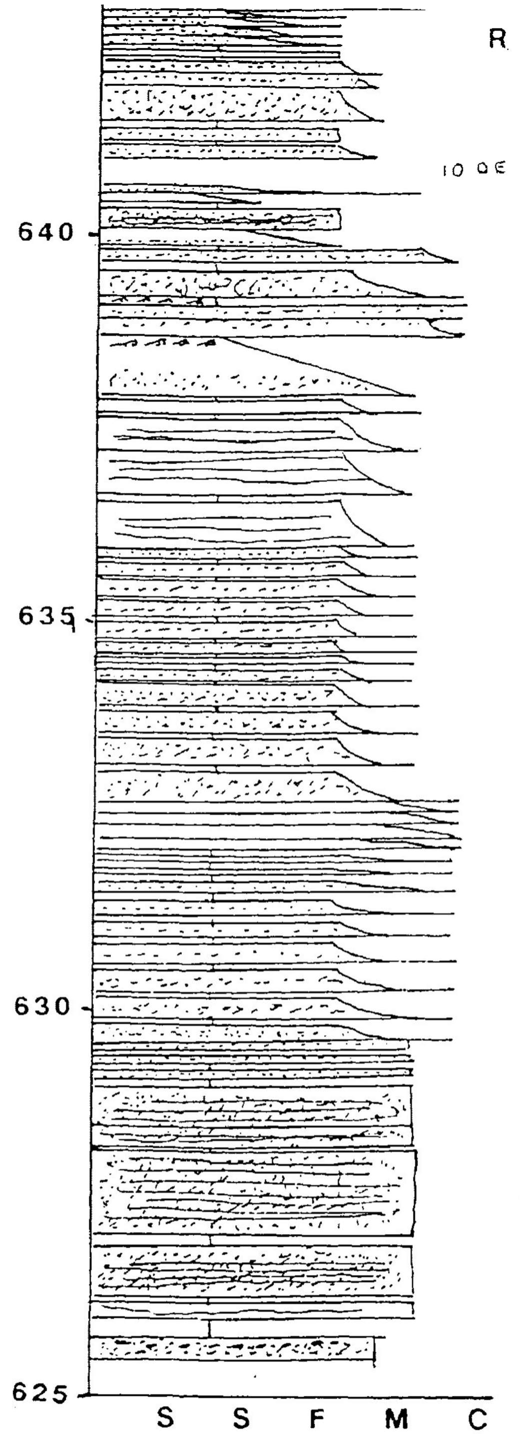


FIGURE 7: Type 2 Subsequence.

PHOTOGRAPH 2: Type 2 Subsequence.

units however, and sedimentary structures other than parallel lamination occur less frequently than in the Type 1 Subsequence. Shale rip up clasts appear more frequently in Type 2 Subsequences than in Type 1. The E division (silty shale, facies T) is bounded by sharp contacts, as in the Type 1 Subsequence. Type 2 Subsequences range in thickness from several meters to several tens of meters, and dominate the middle portion of the McKellar Harbour Sequence. The lower boundaries of this Subsequence type are often hard to distinguish due to their transitional nature, but the upper boundary between this Subsequence and Types 1 and 3 is usually distinct due to changes in bed thickness.

Type 3 Subsequence

This Subsequence (Figure 8, Photograph 3) occurs less frequently than the Type 1 Subsequence, but is similar in that it consists of relatively thick (up to 3 m) sandstone units, but usually the silty shale E division (facies T or M), present in Type 1, is lacking. The sandstone units can grade rapidly from medium- to coarse-grained sand at the base to fine-grained sand within a few centimetres, (facies glS) but size grading is less apparent, and parallel lamination less common within this type of subsequence than with those previously described. Shale rip-up clasts are quite common within this Subsequence, and loaded ripples (facies grS, Ghibaudo, 1992) often occur at or near the top of individual beds. Several of these thick sand units will occur together, topped by a unit of black shale (facies lM, Ghibaudo, 1992) 0.5 to 1 m thick. These shale units mark the top of the Type 3 Subsequences. Type 3 Subsequences vary in thickness from 3 to 20 metres, appear to occur primarily in the top 1/3 of the McKellar Harbour Sequence, and are marked by sharp upper and lower transitions into other Subsequences.

Type 4 Subsequence

Only one Type 4 Subsequence (Figure 9, Photograph 4) was located in the McKellar Harbour Sequence, but because of its markedly different character, it deserves it's own classification. It consists of thick (1 - 2 m) beds of silty shale separated by thin (10 cm) fine-grained sand layers (facies mMS). One silt layer contains shale rip-up clasts, and one fine-grained sand layer contains ripples (facies rMS), but sedimentary structures are generally lacking within the Subsequence. This Subsequence is approximately 10 metres thick, and is bounded by sharp transitions with the overlying Type 3 and underlying Type 2 Subsequences. Subsequence development in the McKellar Harbour Sequence from bottom to top is shown in Table 1 below, omitting missing portions of the section. From this Table, it can be seen that the lower and middle parts of the McKellar Harbour Sequence are dominated by Type 1 and 2 Subsequences while the upper parts are dominated by Type 3 Subsequences, with one occurrence of a Type 4 Subsequence.

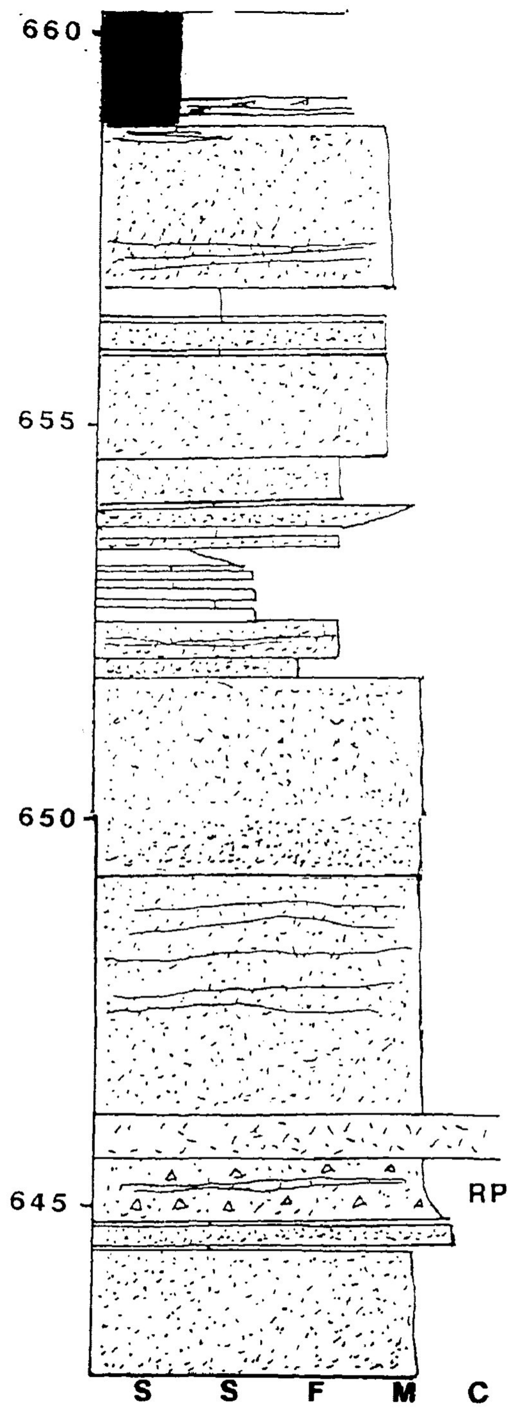


FIGURE 8: Type 3 Subsequence.

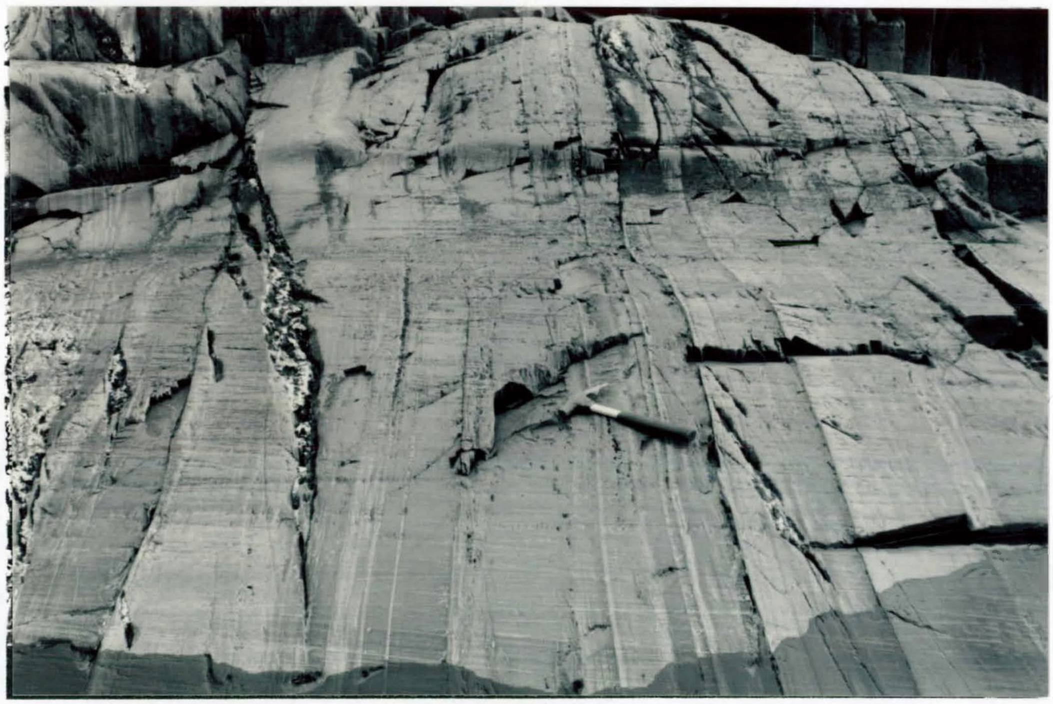

PHOTOGRAPH 3: Type 3 Subsequence.

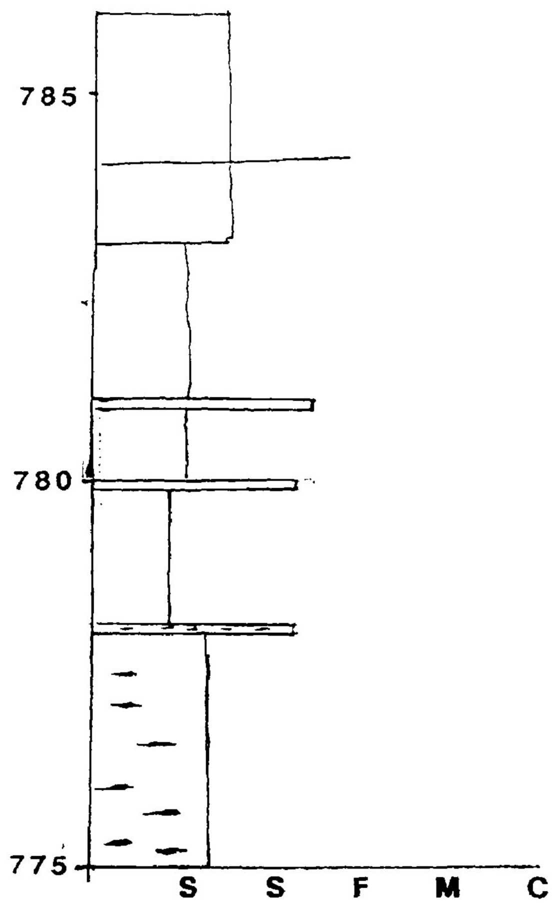


FIGURE 9: Type 4 Subsequence.

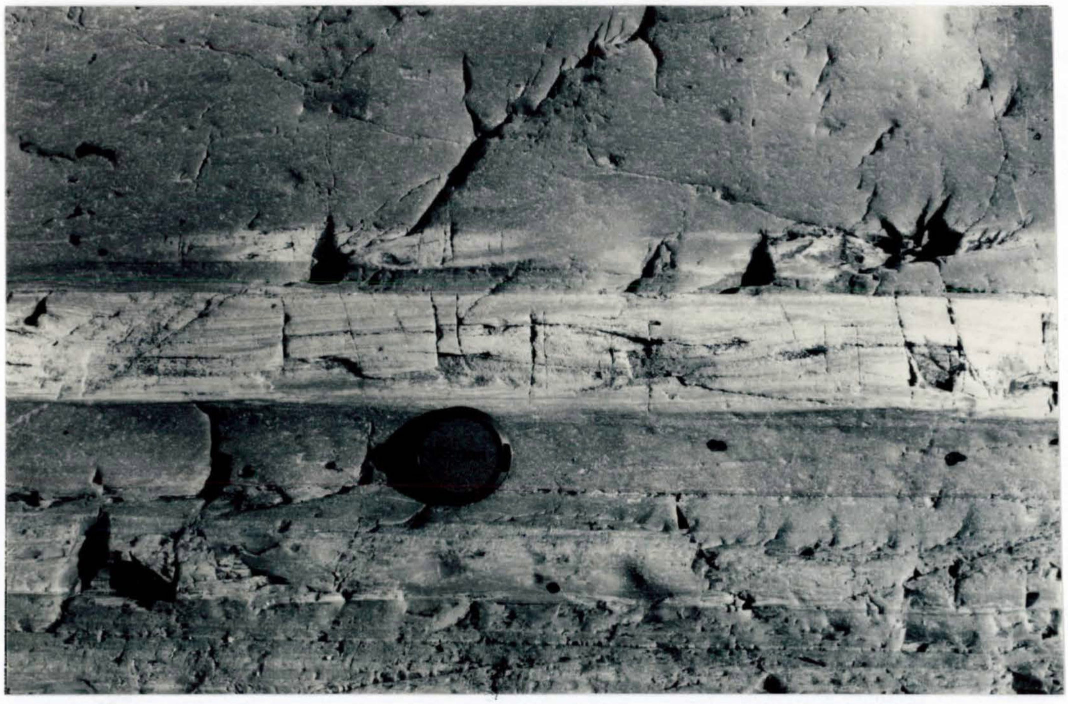

PHOTOGRAPH 4: Type 4 Subsequence.

FIGURE 10: Table 1- Sequence Organization.

| Stratigraphic Position | Subsequence Type |
|---|---|
| 0-40m | Type 1 |
| 40-42m | Transition to Type 2 |
| 42-72m | Type 2 |
| 72-99m | Type 1 Transitional to Type 2 |
| 99-124m | Type 1 Transitional to Type 2 |
| 124-154m | Type 1 Transitional to Type 2 |
| 154-236m | Type 1 |
| 236-246m | Type 2 |
| 246-265m | Type 1 |
| 265-325m | Quartz Diorite Intrusion |
| 325-366m | Type 1 Transitional to Type 2 |
| 366-403m | Type 1 |
| 403-491m | Type 1 Transitional to Type 2, Transitional back to Type 1 |
| 491-505m | Type 2 |
| 505-641m | Type 2 |
| 641-660m | Type 3 |
| 660-664m | Type 3 |
| 664-745m | Type 2 |
| 775-786m | Type 4 |
| 786-790m | Type 3 |
| 790-811m | Type 3 |
| 811-815m | Type 3 |
| 815-835m | Type 3 |
| 835-837m | Type 3 |
| 837-849m | Type 3 |
| 849-850m | Type 1 |

# 4.0 LITHOFACIES ASSOCIATIONS - POSSIBLE SOURCE AREAS

## 4.1 Quetico Subprovince

The rocks of the Quetico Metasedimentary Province have been described as a 70 km wide sequence consisting of "thinly bedded, feldspathic and lithic wackes containing abundant intraformational breccias, grainflows, rare ironstones, mixtites, and ultramafic sediments" (Percival, 1989, Williams, 1987a, 1989). The southern portion of the Subprovince (between Big Duck and Killalla Lake, immediately to the north of the Winston Lake area) contains a unit of "felsic volcanic breccia and derived conglomerate" (Williams, 1989) that can be interpreted as proximal facies derived from the Wawa Subprovince volcanic centres to the south. Workers in the Quetico Subprovince (Williams, 1987, 1989, 1990; Devaney and Williams, 1988, and Card, 1990) describe it as an accretionary prism lying between the Onaman-Tashota/Beardmore-Geraldton Terranes to the north, and the Wawa Terrane to the south . This prism was then subjected to high temperature (Abukuma Type) metamorphism (Card, 1990) during the conversion from a forearc setting to a back-arc setting as the oceanic basin between the northern (Onaman-Tashota/Beardmore-Geraldton) volcanic arc and southern (Wawa) volcanic arc closed.

Barret and Fralick (1989) and Fralick et al. (1992) have examined sedimentary rocks in the Beardmore-Geraldton and northern Quetico areas, and have concluded that a submarine ramp (Heller and Dickinson, 1985) was the depositional system. Felsic turbidites occur south of Beardmore in vertically structured successions of turbidites (Fralick et al, 1992).

The turbidites are organized into thick thinning- and fining-upwards sequences, and are topped by CDE and/or DE turbidites, with the overlying massive grainflows/high density turbidites marking the bottom of the next sequence.

4.2 Schreiber- Winston Lake Region

Conglomeratic rocks make up only a small proportion of the rocks observed in the Schreiber-Winston Lake area. To the north, adjacent to the Winston Lake Mine, there are units present that have been described as "pseudo-fragmental" (Balint et al, 1990). In the field the rocks have a sedimentary appearance, but this may be the result of post-depositional deformation, with the "pseudo-fragments" representing tectonically disrupted layers. Also at the Winston Lake Mine, units described as "pyroclastic" (Balint et al, 1990) occur several hundred metres south of the mine site. In thin section, the "clasts" in these units show an outer rim or rind of feldspar and quartz-rich material, with an inner rim of mafic minerals (hornblende and biotite). Inside this inner rim is a core of fairly coarse-grained (0.5mm) quartz. Little work has been performed on features of this sort, but it is thought that this core and rim structure suggests a metamorphic/tectonic origin for these "clasts" (Dr. G. Borradaile, pers. comm.).

At the Winston Lake Mine, the volcaniclastic rocks observed have been subjected to metamorphism, deformation and chemical alteration which makes lithofacies identification and original grain size determination difficult. They occur interbedded with pillowed mafic volcanic flows (Balint et al. 1990) and gabbroic intrusive rocks in units up to several metres in thickness. Each "unit" consists of beds or layers (Winston Lake Section, Figure 11) that vary in thickness from several centimetres to several tens of centimetres. Often the layers are disrupted, contorted, or crenulated, and occasional fish-hook folds were observed. Graded beds either did not exist, or these features have been obliterated due to combined deformation, metamorphism and alteration. To the west of the mine area, away from the alteration envelope, units of definite sedimentary origin occur. Unfortunately, these units are relatively poorly exposed, and no detailed stratigraphic work could be performed.

Adjacent to Hwy. 17, immediately to the east of the town of Schreiber, there occur several sedimentary units intercalated with intermediate volcanic rocks. These thin (<1 m) units consist of massive fine sandstone beds 10 to 20 cm thick, interbedded with graphitic shale. These sedimentary units make up a relatively small proportion of the rocks present.

Just west of the town of Schreiber, an excellent exposure of iron formation occurs, but it was not examined as part of this study. The Morley Pyrite Occurrence (located between Schreiber and Terrace Bay) was the subject of a study by Fralick et al. (1989). These workers found that the internal structure of the pyrite laminations indicates the presence of deep water organic mats adjacent to hydrothermal vents, and a possible modern analogue exists with the sulphidic sediments of the Red Sea brine deeps.

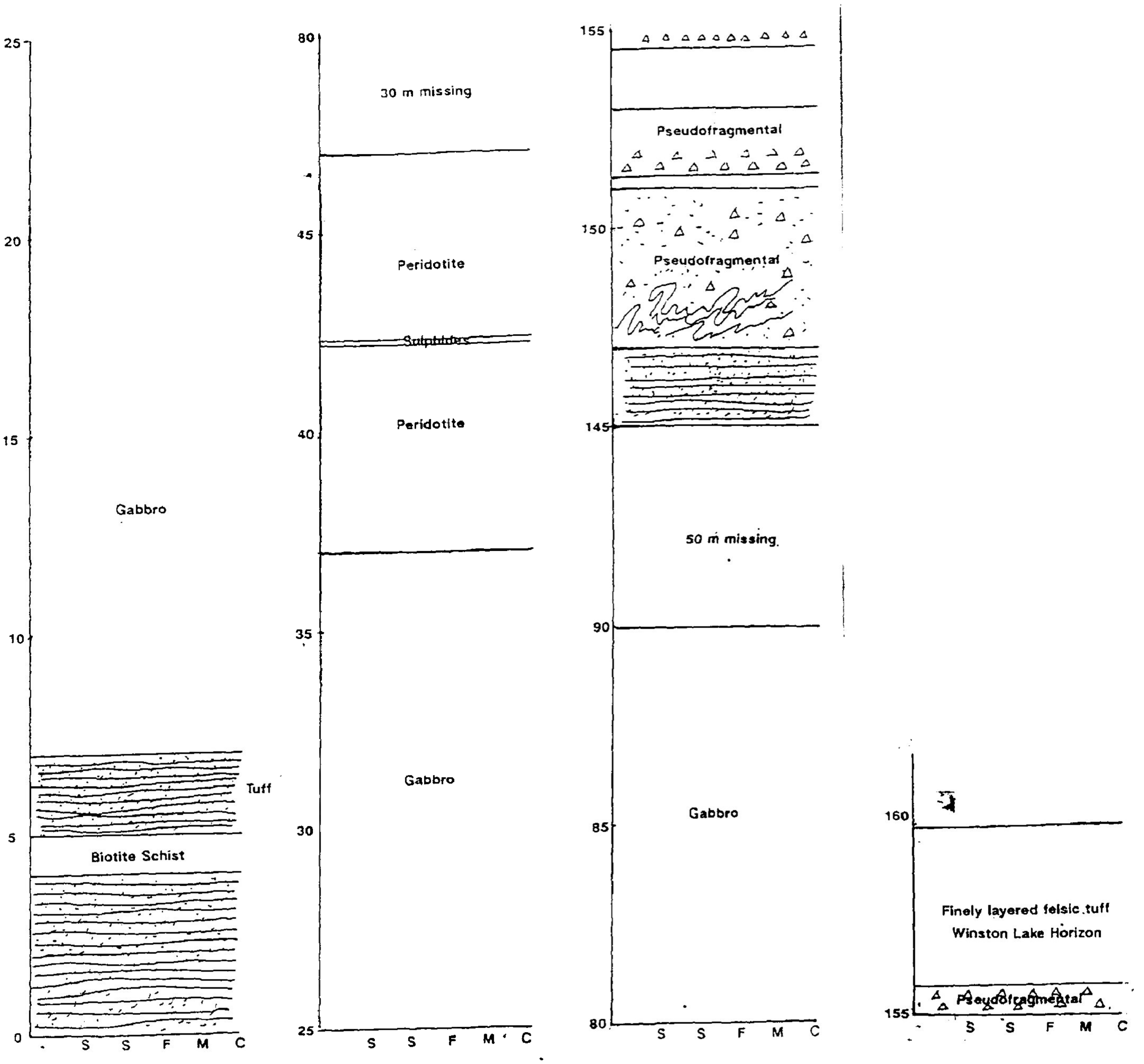


FIGURE 11: Winston Lake Section.

The mafic volcanic rocks examined near the Winston Lake Mine have been subjected to amphibolite-facies metamorphism (Carter, 1988). They are quite schistose, and appear black or dark green on fresh surface, but are grey to rusty on weathered surfaces. Some outcrops to the west of the mine site, removed from the alteration associated with the Winston Lake VMS deposit are pillowed, but generally these features are not present. Mineral assemblages consist predominantly of hornblende, plagioclase feldspar, +/- garnet, with minor quartz. Biotite develops along the planes of the schistosity.

Intermediate to felsic volcanic rocks exist in the Winston Lake Area as pyroclastic tuffaceous units. In the mine area it is difficult to determine the exact origin of these units.

## 4.3 Heron Bay - Hemlo Region

The Heron Bay - Hemlo Region consists of the Lake Superior Area, the Pukaskwa Area, the Hemlo Area, and the Amwri Lake Area (Figure 12). The region is dominated by volcanic rocks of the Heron Bay Group and the Playter Harbour Group (Muir,1982a,b), but sedimentary rocks do occur within the belt, and meaningful stratigraphic information could be obtained from these units.

### 4.3.1 Coarse-Grained Lithologies

Two occurrences of conglomeratic rocks were examined in the Hemlo - Heron Bay area as part of this study. The first is located just northwest of Amwri Lake (Figure 11), while the second is located on the Page-Williams mine site in the Hemlo Area. They are variable in composition and configuration, but possess an assortment of angular clast types and sizes. These rocks have been termed pebbly arenite and conglomerate (Siragusa, 1984a,b), conglomerate (Milne, 1968, Brown et. al. 1985), volcaniclastic conglomerate (Patterson 1984, Muir 1982b), polymictic paraconglomerate (Quartermain, 1985), agglomerate (Milne, 1968), and primary intraformational breccia (Muir, 1982b).

#### Amwri Lake Area

Conglomeratic rocks outcrop on the Amwri Lake sideroad which extends west from Highway 614, 14 km north of the Trans Canada Highway (Hwy. 17). Eleven small outcrops occur 3.4 to 3.8 km west of Hwy. 614. These outcrops are well-exposed, as they were stripped and cleaned by Noranda Exploration in 1983. The outcrops were carefully logged, the clast lithologies noted, and internal characteristics (i.e. thickness of fragment- and fragment-free layers, sorting and grading, etc.) recorded.

FIGURE 12: The Heron Bay - Hemlo Region.

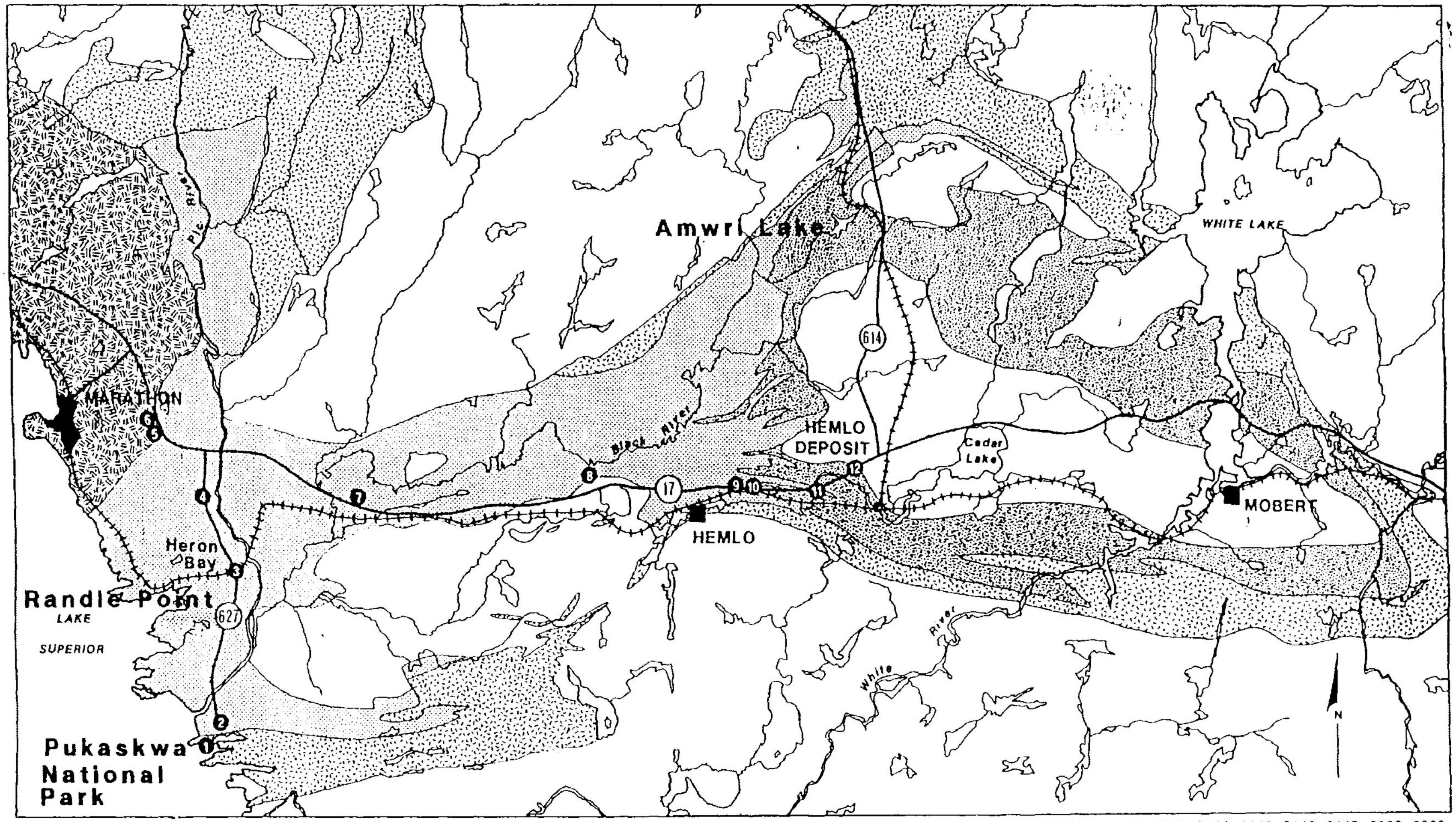


AFTER OGS MAPS 2452, 2439, 2143, 2144, 2145, 2146, 2147, 2098, 2099

PROTEROZOIC
- COLDWELL COMPLEX ALKALINE INTRUSIVE

ARCHEAN
- GRANITIC ROCKS
- FELSIC METAVOLCANICS, TUFFS TO BRECCIAS
- MAFIC METAVOLCANICS, MASSIVE TO PILLOWED LAVAS
- METASEDIMENTS, PELITE, SILTSTONE, CALC-SILICATES, ARGILLITE
- FIELD TRIP STOP

0 2 4 6 km

*Regional Geology of the Hemlo Area.*

**(Reproduced from Patterson, 1984)**

Five different clast lithologies are present. The most abundant is a feldspar-quartz porphyry of granitic composition. Feldspar phenocryst content generally exceeds quartz phenocryst content, and both average 1-3 mm in size. The matrix consists of fine-grained (< 1 mm) felsic material with minor mafic mineral grains. Somewhat less abundant are clasts of a feldspar +/- quartz porphyry which has a dioritic bulk composition, with a greater concentration of mafic mineral grains in the matrix. Although there is a gradation of fragment types between the two end members, most of the fragments can be placed within the category of one or the other end member. The third and fourth fragment lithologies consist of fine-grained mafic schists; either biotite schist (more common), or hornblende schist (less common). The fifth fragment lithology is an aphanitic, felsic (rhyolitic) type that occasionally contains small (< 1 mm) phenocrysts of feldspar, with occasional quartz. These clasts are identical in appearance to lapilli within felsic pyroclastic rocks to the west, and are interpreted as felsic volcanic clasts. The relative abundances of these fragment lithologies were determined by counting the number of each fragment type within a one metre square area on an apparently representative outcrop of the Amwri Lake conglomerate (Thomson, 1985, unpublished data). The outcrop was chosen for its good exposure, even clast size (to eliminate possible bias due to clast size), and its possession of clasts that appear to be representative of the unit as a whole.

Of 117 fragments counted, 59 (50%) were granitic feldspar-quartz porphyry; 44 (38%) were dioritic feldspar (=/- quartz) porphyry; 11 (9%) were biotite schist; 1 (1%) was a hornblende schist; and 2 (2%) were felsic volcanics (Table 2). These values tend to over-represent the volcanic and hornblende schist fragments, as only 8 volcanic fragments, and just several hornblende schist fragments were located during subsequent work in the area. It was also found that the proportion of dioritic porphyry fragments may locally exceed that of the granitic porphyry fragments. Several granitic porphyry clasts were observed to contain small somewhat angular inclusions of mafic material (biotite- and/or hornblende-rich) similar to the mafic schist clast types.

Size of the fragment types varies (Table 2), ranging from .01 x 1 cm to 16 x 100 cm. Generally the porphyry fragments are largest, the mafic schist fragments are intermediate in size, and the felsic volcanic fragments tend to be smallest. Fragment size distribution will be discussed later.

The long axis-short axis ratios for the fragments (as viewed in two dimensions) are also quite variable, and appears strongly dependent on fragment lithology. These data are presented in Table 2.

Table 2.

| Fragment Lithology | Relative Abundance % | Size Range cm | Axis Ratio |
|---|---|---|---|
| Quartz-Feldspar Porphyry (granitic) | 50 | 1.5 x 0.4 to 7.5 x 45 | 5.5:1 |
| Feldspar +/- Quartz Porphyry (dioritic) | 38 | 0.7 x 3 to 16 x 100 | 4.7:1 |
| Biotite Schist | 9 | 0.8 x 10 to 2 x 30 | 10.8:1 |
| Hornblende Schist | 1 | 0.7 x 8 to 3.5 x 34 | 9.7:1 |
| Felsic Volcanic (rhyolitic) | 2 | 0.1 x 1 to 1.5 x 30 | 18:1 |

This conglomeratic unit consists of fragmental layers ranging in thickness from 4 cm to almost 3 m with an average thickness of 1 m. Alternating with these are clast-free layers that range from several cm to over 1m, with an average thickness between 15 and 20 cm. The fragments are clast-supported. The coarser fragmental layers show, at best, poor sorting, and are generally unsorted. The finer units are moderately sorted, with rarer wel- sorted layers. Size grading is not common in this lithofacies, and is crude where present. Often, unsorted layers of coarser clasts alternate with finer clast-sized units that display very poor size grading. This can give the impression of a thicker, more sorted layer than those that actually exist. Fining is most commonly in a northern direction, but some layers exhibited coarsening to the centre, grading to finer material to both the bottom and top of the layer.

The clast-free layers interstratified with the conglomerate layers consist primarily of fine sand-sized (0.1 to 0.2 mm average, range is 0.4 to 0.6 mm) quartz and feldspar with lesser mafic minerals. Thin section study gave visual estimates of composition as follows: 45-50 % quartz, 10-20 % albitic plagioclase, 5 % microcline, 10-20 % biotite, 5-15 % hornblende, 1-3 % epidote, and 0-2 % chlorite. Two samples (Samples H53, H54) of clast-free layers from this lithofacies were analysed in order to determine their geochemical composition.

The internal structure of the clast-free layers of the conglomeratic lithofacies is somewhat variable. Some layers are not truly "clast free" but can contain minor accumulations or the occasional isolated small fragment of the same composition as those described above. These clasts are 0.1x1.0 cm to 0.3x2.0 cm in size, with occasional larger clasts (up to 5x15 cm).

The clasts can be sparsely, but equally distributed throughout the lithofacies, and thus the clast-poor layers are considered a clast-poor, matrix-supported variety of the unit. More commonly, the clasts are concentrated at what has been interpreted as the base of the layer, with poor grading into the clast-free upper portion of the layer. Clast- free sandstone is often massive and non-graded. Several layers do contain alternating laminations of felsic and mafic minerals on a mm scale which are restricted to the basal few centimetres of the layer. These laminated interlayers are usually finer grained than the remainder of the unit. Size grading (where present) is found to be restricted to the uppermost few cm's of the layer. Some of the thicker sandstone (clast-free) units have a finer grained, compositionally laminated base several cm's thick, followed by a succession of well-defined layers which fine-up (northward).

Hemlo Area

Two distinctly different types of conglomeratic rocks occur on the Page Williams mine site. The first is similar to that described above, and has been described as a heterolithic fragmental unit by Valliant et al. (1985) and Valliant (1986). This description is essentially meaningless, as all sedimentary rocks are made up of fragments of some sort, and an ordinary sandstone could be classified as a "heterolithic fragmental unit". It is concluded, based on field observation that Valliant is referring to a conglomeratic lithology. This unit is relatively poorly exposed, and, where present, relatively strongly deformed. Muir (1982b) places this unit at the core of a large reclined overturned syncline, introducing the possibility of bed repetition. With the poor exposure, little meaningful geological information could be obtained, and this unit was not examined to any great extent. A brief, description will, however, be given here.

As with the Amwri Lake area, this unit appears to contain two main clast lithologies. The first is a granitic feldspar (+/- quartz) porphyry, and the second is mafic schist (biotite with minor hornblende). The granitic porphyry fragments appear to predominate, but no clast counts were performed. Other clast types may occur, but were not located. Clast sizes are comparable to those in the Amwri Lake Area, and range in size from 0.7x3.5 cm to 3x16 cm, with occasional larger clasts up to 12x60 cm in size. The long axis:short axis ratios, (as seen in two dimensions) are in the order of 4:1 to 5:1 for the granitic fragments and 10:1 for the mafic schist fragments. The clasts from this unit show deformational features such as fishhook folds on the end of clasts, or in rare cases, the clast may itself be isoclinally folded. Some clasts show amoeboid shapes. The mafic schist clasts do not exhibit these features.

The internal structure of these units appear to differ from those in the Amwri Lake Area in that they are strongly matrix supported (<25% clasts by volume), and no evidence of size grading was found. Only several clast free units were located, and no evidence of size grading, or internal structures were present. A thin section of this clast-free unit showed a very fine-grained sandstone (0.05-0.06 mm in size) with 30% quartz, 45% plagioclase feldspar, 15% biotite, 5% chlorite, 4% calcite and 1% epidote. The composition of the Amwri Lake Area units appears to be less feldspathic and more quartz-rich.

The second type of conglomeratic unit located on the Page Williams Site is quite different. It has been referred to as an intraformational breccia (Muir, 1982b), possibly resulting from slump brecciation. It is 2-3 m thick and has been traced around the limb of the previously mentioned fold for 600 m. The intraformational nature of this conglomeratic unit is suggested by the clast lithologies which are identical to the thinly interstratified rock types surrounding it. The clasts consist of garnet and staurolite bearing pelitic material and calc-silicate rock containing chiefly calcic amphibole, plagioclase, and calcite. Biotite schist and biotitic sandstone clasts are relatively less abundant. The clasts are angular to subrounded, less commonly ellipsoid in shape. They rarely exceed 15 cm in length, and numerous clasts appear boudinaged or folded.

### 4.3.2 Sandstone

In the Hemlo area, sandstone units have been interpreted as having been derived from both unlithified volcanic sources, and from reworked material (Muir, 1982b). They range from thinly bedded fine- to medium-grained sandstone turbidites to thicker, graded layers. The sandstone units occur interbedded with calc-silicate horizons and with conglomeratic rocks similar to the Amwri Lake Area. The rocks in this area have been subjected to contact metamorphism due to their proximity to the Cedar Lake Pluton (Muir, 1982b), and sandstone units sometimes show metamorphically induced reverse grading. Their garnet-andalusite-staurolite-cordierite and minor sillimanite assemblage is representative of contact metamorphism (Muir, 1982b). Bedding in outcrops in the mine area is often hard to discern, or is obscured by metamorphism and/or deformation, making meaningful stratigraphic study difficult.

### 4.3.3 Siltstone

Siltstone units occur infrequently in the Heron Bay - Hemlo Region, and are seen as relatively thin units interbedded with the sandstone and only occasionally associated with conglomeratic units. Sedimentary features are usually not present, aside from parallel lamination, with some beds showing convolute lamination.

Shale is found interbedded with sandstone and siltstone units, as interflow sediment between volcanic flows, or associated with calc-silicate horizons. Generally these units do not exhibit sedimentary structures, but occasional wispy and or parallel lamination can be observed.

### 4.3.4 Chemical Sedimentary Rocks

Iron formation, graphitic shales/slates, calc-silicate units, and barite horizons are present in the Heron Bay - Hemlo Region. Iron formations occur as thin units intercalated with mafic volcanic rocks within the Playter Harbour sequence on the shores of Lake Superior (Muir, 1982a), and were not examined as part of this study. Graphitic shales appear as thin interflow type units within mafic volcanic successions. Calc-silicate units in the vicinity of the Hemlo mining camp have been interpreted as thin bedded marl that has been metamorphosed to calcium-rich plagioclase and amphibole (Patterson, 1984). These thinly bedded units are associated with volcaniclastic sediments and tuffs.

Barite horizons were studied by Gliddon (1985). They are found associated with DE turbiditic argillaceous siltstones (sometimes with green mica clasts), green mica schists, sericite carbonate schists, mafic metavolcanic fragmentals and flows, as well as minor tuffs and quartz-feldspar porphyry. Gliddon (1985) interprets these horizons as having a syngenetic chemical sedimentary origin. Gliddon (1985) interprets the sedimentary rocks as being indicative of a deep water, starved basinal setting.

4.3.5 Volcanic Rocks

Mafic volcanic rocks in this portion of the study area consist of massive to pillowed, mainly tholeiitic flows that are locally variolitic. Flow top and pillow breccias are also present (Muir, 1982a,b). Minor calc-alkalic flows also occur.

In the Heron Bay-Hemlo portion of the study area intermediate to felsic volcanic rocks occur commonly in the Heron Bay sequence and only rarely in the Playter Harbour sequence (Muir, 1982a). These rocks occur as tuffs, and lapilli tuffs, and often grade laterally into sedimentary units. Geochemically, these rocks are thought to represent calc-alkalic rhyolites (Muir, 1982a). In the vicinity of the Hemlo Mining Camp, felsic pyroclastic units and tuff are found interbedded with siltstones and calc-silicate units.

Pukaskwa Area

On the shore of Lake Superior in Pukaskwa National Park, conglomerate occurs intercalated with sandstones (Figures 13 and 14). These units consist of pebble-sized material supported by a matrix of coarse- to medium-grained sandstone. The pebbles range in size from .2 X .5 cm to 2 X 5 cm, and are usually graded. These units can be given the facies classification GyS (Ghibaudo, 1992). In one unit, at the top of Pukaskwa Section #2, pebbly medium/coarse sand occurs as lenses in massive silty shale. Ghibaudo (1992) does not have a classification for this type of unit. Clast types (in the order of relative abundance) were observed as follows: granitic/dioritic (which were the larger clasts), intermediate volcanic, and hornblende-biotite. The hornblende-biotite clasts were schistose, and may have been derived from either a volcanic or a sedimentary source.

A large proportion of volcanic clasts, with few (if any) intrusive or sedimentary clasts would be indicative of a pyroclastic origin for these rocks, but the proportionally larger number of granitic intrusive clasts relative to the volcanic clasts indicates that these units are not of pyroclastic origin, but are the result of the weathering of a granitic/volcanic terrane.

Sandstone units in the Pukaskwa area were observed to range in thickness from 5 cm to several meters, and are often graded from medium-grained sand at the base to fine sand at the top of individual units. They commonly occur as AE, DE, and BE turbidites, and as individual beds separating conglomerate units. These units correspond to facies glS or gslS. Several thick sandstone units containing lithic fragments of granitic, felsic volcanic and sedimentary material (Figure 11) were also observed. One of these units has a basal section where the lithic fragments are 0.5 cm in size. The thicker sandstone units tend to show parallel lamination, and to contain lithic fragments of mainly granitic composition with minor volcanic fragments. Three sandstone beds are trough cross-stratified (facies xS, Ghibaudo, 1992), and others are convolute bedded. Ghibaudo (1992) does not have nomenclature for convoluted bedding, but following his system it is proposed here to use the symbol "c" to indicate the presence of this sedimentary feature. Sandstone with convoluted bedding would then have the facies classification cS. Sandstone was also observed as lenses and loaded ripples within shale/siltstone units.

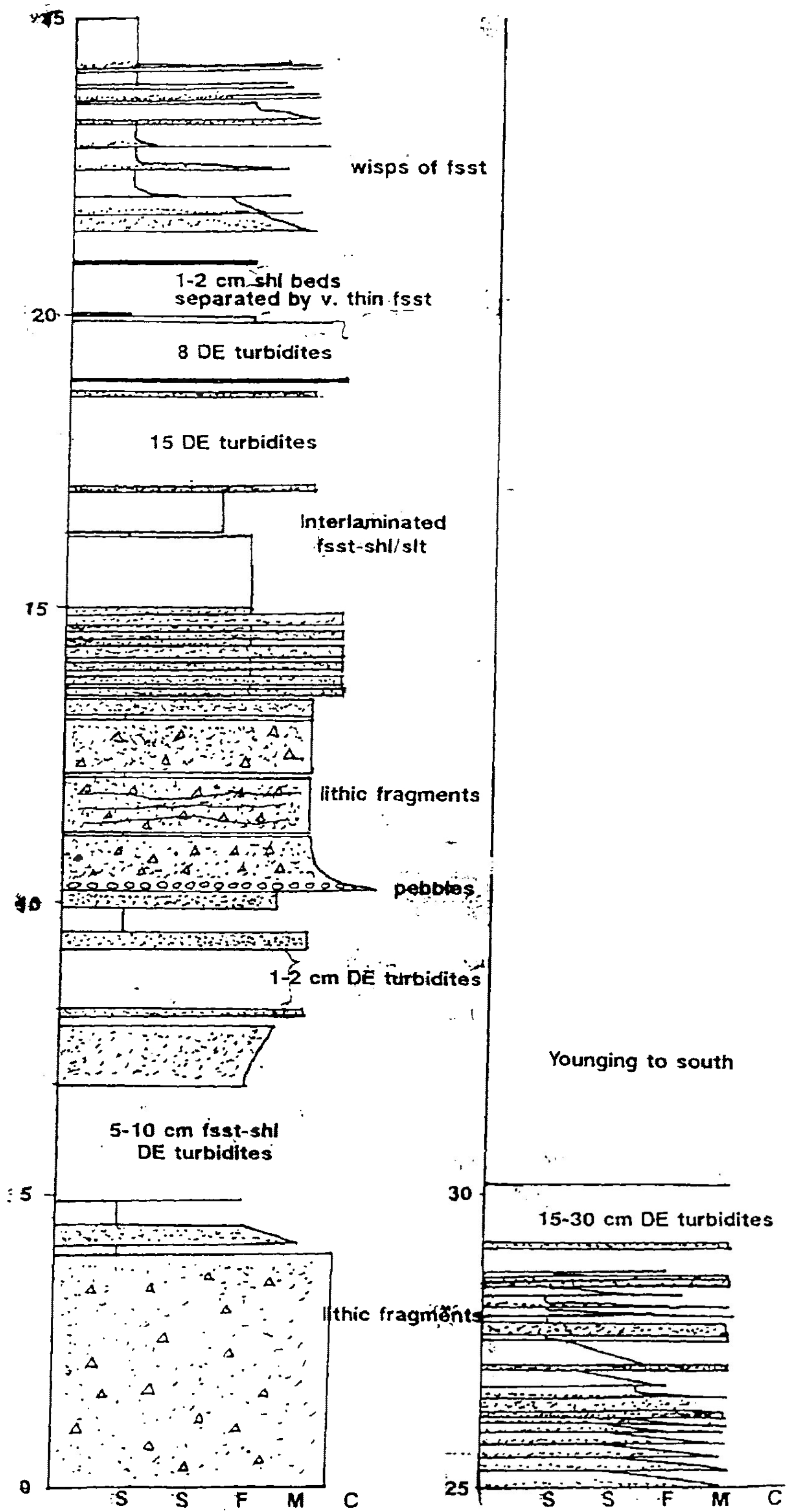


FIGURE 13: Pukaskwa Section 1.

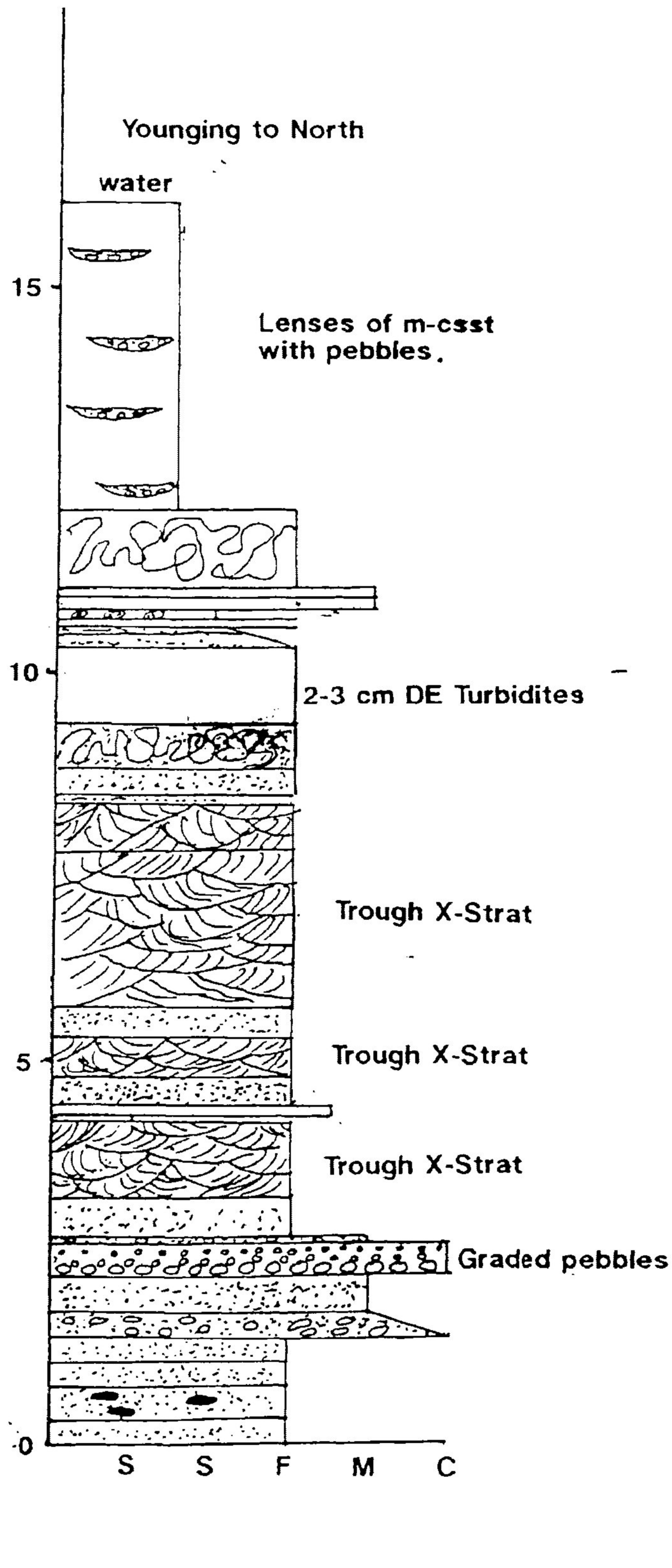


FIGURE 14: Pukaskwa Section 2.

The occurrence of siltstone beds in the Pukaskwa area is limited to relatively thin units interbedded with the coarser sandstone units. Siltstone units in this area commonly show parallel lamination, with minor convolute lamination, giving them the facies classification sT and cT.

Mudstone and pelitic rocks are found interbedded with the coarser sandstones, often as the E division of a DE turbidite (part of facies MS). They can occur as interflow units between volcanic flows, or as beds adjacent to calc-silicate units. They usually do not show any sedimentary features other than parallel lamination, with occasional wispy or convolute lamination.

Lake Superior Area

To the north of the sedimentary rocks observed in Pukaskwa National Park, north of Randle Point on Lake Superior, sandstone units are thicker and finer grained (Figure 15). More features indicative of slumping (convoluted bedding, slump folds, etc.) are found in these units. Pebbly sandstones were absent, but lithic fragments (mostly felsic volcanic) were present in some beds. The thicker beds do not show well-developed size grading, while the thinner units are generally graded (facies classifications cS,mS or gS [Ghibaudo, 1992]). There are also two thick units of felsic (rhyolite) tuffaceous material. Some shale/siltstone units contain sandstone as loaded or starved ripples (facies rSyM, Ghibaudo, 1992).

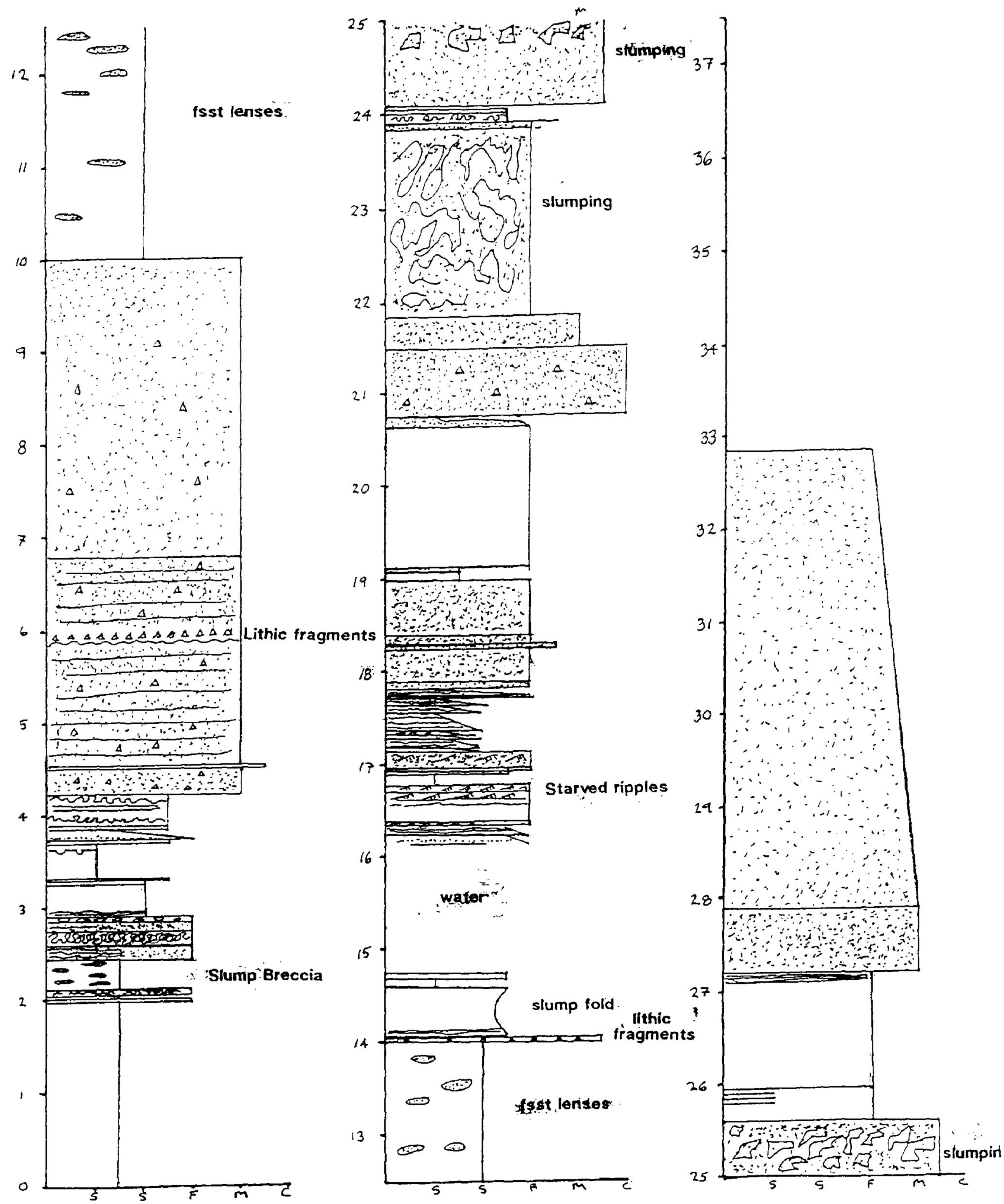


FIGURE 15: Lake Superior Section.

# 5.0 DEPOSITIONAL ENVIRONMENTS

## 5.1 Introduction

This chapter will provide a review of processes operative in sedimentary gravity flows, and how these were at work during the deposition of the McKellar Harbour Sequence. The depositional environments of the possible source areas will then be discussed, allowing subsequent interpretation of the provenance of the McKellar Harbour Sequence.

## 5.2 Sediment Gravity Flows

The deposition of turbidites is well-documented and described by Bouma, (1962). Bouma's work has been expanded on by workers such as Stow, (1985) to describe slump facies, debrites, coarse-grained turbidites, medium-grained or classical (as described by Bouma) turbidites, and fine-grained turbidites. Slumps occur in any lithology, can vary considerably in thickness, and in the types of deformational features present within individual beds. These are typically folds, thrusts, balls, fish-hook folds, rotational slumps. scars, etc.. Debrites consist of material ranging from mud to boulders, and can vary up to several tens of metres in thickness. They tend to be relatively unorganized and structureless. Turbidites have now been separated into three models, based on grain size and bedforms present. Coarse-grained turbidites are mainly deposited by high density turbidity currents, but the internal features generated are a result of grain flow, fluidized flow, or liquified flow mechanisms during the final stages of deposition (Lowe, 1982). Medium-grained turbidite facies develop usually as the classical Bouma (1962) sequence: Ta - massive to graded sand; Tb - parallel-laminated sand; Tc - cross-laminated and/or convolute sand; Td - parallel laminated fine sand and silt; and Te - bioturbated mud (in Phanerozoic and younger deposits). Fine-grained turbidites usually consist of graded silt-laminated mud passing upwards into graded and nongraded mud. With these general models in mind, it should be noted that complete sequences are rare, and that partial sequences are much more common.

Lowe (1982) describes deposition of sediment by both high and low density turbidity currents. Low density currents produce the facies already described (i.e. the "classic" Bouma (1962) model), with deposition occurring through suspension, followed by traction. High density turbidity currents occur as sandy flows (with grains supported by turbidity and hindered settling), or as gravelly flows (with sediment supported largely by dispersive pressure and matrix buoyant lift). The terms low density current and high density (Lowe, 1982) appear to be more reflective of the relative energy of the turbidity currents, as opposed to the actual density, and sandy high density flows are supported by much the same mechanisms as low density flows (turbidity and hindered settling). In low density turbidity currents the material tends to be finer (silt as opposed to sand), and thus requires less energy to keep the material in suspension. The deposition of sandy "high density turbidites" occurs through three stages (Lowe, 1982): 1) a traction sedimentation stage, 2) a traction-carpet stage, and 3) a suspension-sedimentation stage. Within a turbidite flow, material moves in traction at the base, with a plume of suspended material above and behind the body of the flow. The traction-carpet stage marks deposition of material through "freezing" below the flow (Lowe, 1982). The material deposited by traction is characteristically parallel laminated or cross-stratified, while deposition by the traction carpet results in layers of graded coarse sand (facies Ta of Bouma, 1962) at the base of the turbidite. Deposition of the suspended material above the flow typically shows grading, water escape structures, or can be reworked by residual currents operating after cessation of the initial flow. These residual, lower energy currents can produce an upper layer of planar-laminated or cross-stratified material typical of "low density" turbidity currents (Lowe, 1982).

Gravelly high density turbidity currents consist of a range of material from sand to gravel, with this gradation resulting in a range of depositional mechanisms. The coarser material in the base of the flow is "frozen" in place when the energy of the flow drops below that required to maintain dispersive pressure (Lowe, 1982), resulting in a basal, inversely graded traction carpet. This is in turn overlain by a normally graded suspension sedimentation unit (Lowe, 1982). This sequence is thought to represent more proximal facies, as flow unsteadiness will result in direct suspension sedimentation without traction carpet development (Lowe, 1982). Also, as the flow moves more distal to the source, much of the material that could be carried by traction carpet processes may have already been deposited through "freezing", leaving only that which can be transported through suspension.

### 5.2.1 Jackfish - Middleton Region

The Jackfish - Middleton Region is dominated by the rocks of the McKellar Harbour sequence. This is a relatively thick assemblage of turbiditic sandstone, siltstone, and mudstone. The McKellar Harbour Sequence does not exhibit any changes of younging direction, nor were any small-scale folds observed for over 800 meters of section. Some portions of the section are missing (covered by water or overburden), and this could mark the locations of folds or faults. However, as there is no evidence to the contrary, the McKellar Harbour Sequence will be treated as a continuous sequence for the purposes of this interpretation.

A submarine fan model incorporating three fan facies associations has been developed (Mutti and Ricci-Lucchi, 1978, Walker, 1978). The upper fan facies is characterized by channel (thick-bedded coarse-grained sandstone-conglomerate) and interchannel deposits (laminated or bioturbated mudstone-marlstone). Levee deposits are represented in this model by thin bedded, fine-grained turbidites. Middle fan facies consist of distributary channels (thinning upwards cycles), overlying the thickening upwards cycles representative of prograding lobes. In this mid-fan facies medium- and coarse-grained discontinuous turbidites and crevasse-splay sandstones, as well as hemipelagites occur in interchannel and distal lobe areas,. The lower fan facies consists of medium- and fine-grained laterally continuous turbidites and interbedded hemipelagites. Walker's (1978) model consists of inner, mid and outer facies consisting of debris flow conglomerates, slumped sandstones, and graded pebbly sandstones deposited in the inner fan, with "classical" turbidites occurring in the mid to lower fan. "Proximal" turbidites are thought to be thick bedded, while "distal" turbidites are thought to be thin bedded in this model. Both these models show that in modern and ancient submarine fans, a well-ordered, structured sequence develops. The McKellar Harbour Sequence does not show any of the structuring usually encountered in a submarine fan environment.

Relatively unordered stacking of turbiditic sandstones occurs in regions that have a submarine ramp environment (Heller and Dickinson, 1985). A submarine ramp is essentially a sandy submarine fan that has not developed any long-lasting channels. This lack of channelization tends to prohibit the development of suprafan lobes, which occur only locally in the ramp environment (Heller and Dickinson, 1985). Ramps are often fed by deltas prograding onto the basin floor, over the slope, from numerous points along the delta front (Heller and Dickinson, 1985). Figure 16 illustrates the differences between the "classic" submarine fan model of Mutti and Ricci-Lucchi (1978) and the model for a submarine ramp. The most significant feature of a submarine ramp is the lack of a dominant feeder system or submarine canyon. This prohibits the development of channelized inner fan and mid-fan deposits (Heller and Dickinson, 1985). Heller and Dickinson (1985) also state that bedding thicknesses are generally random, and that asymmetric cycles occur only rarely. Submarine ramps are composed of "relatively monotonous and laterally continuous sheets of sandstone, the average thickness of which gradually diminishes downramp as the sandstone to shale ratio gradually increases" (Heller and Dickinson, 1985). Ramp development occurs in basins that are of moderate depth, and have subdued margins.

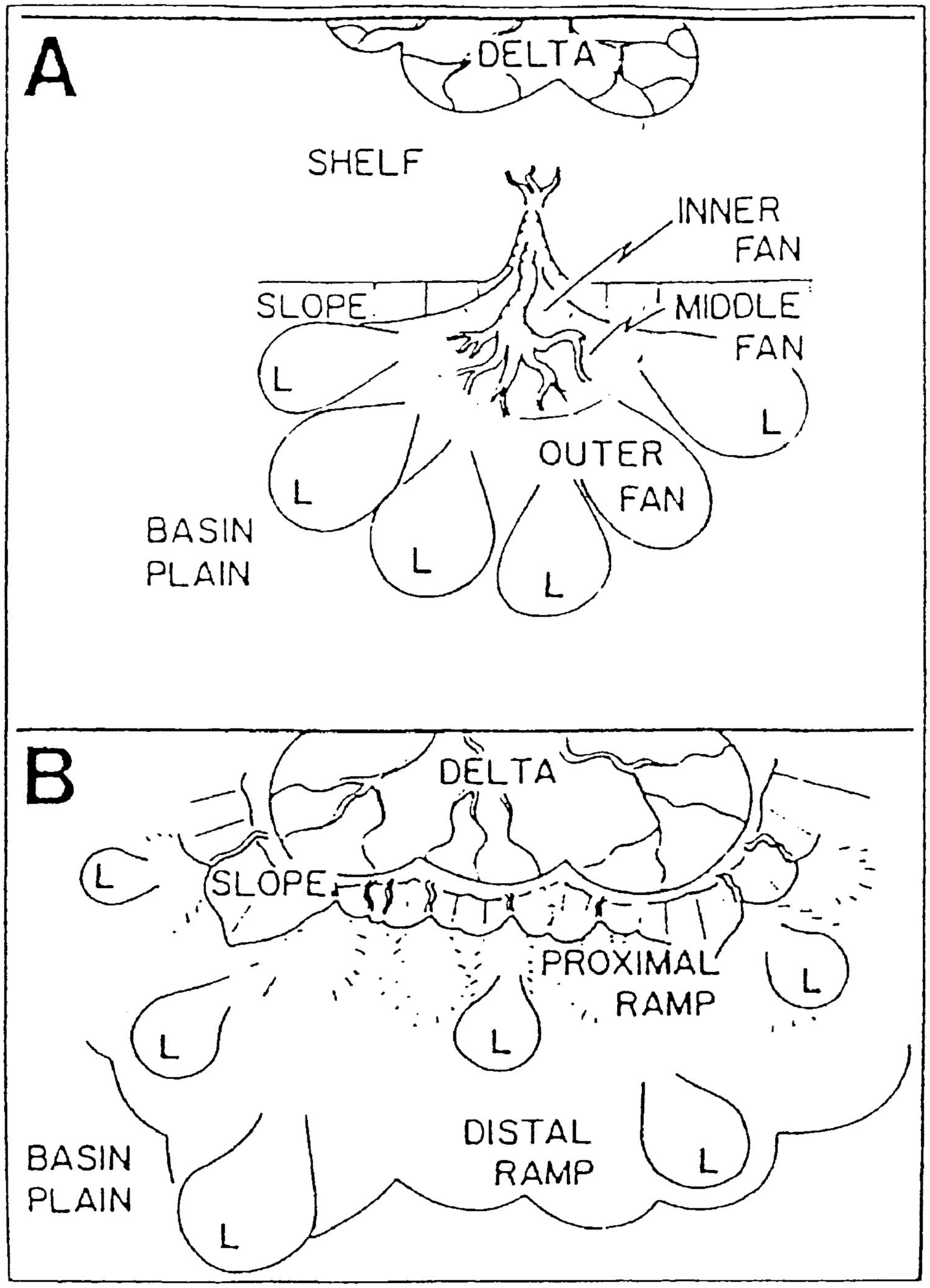


FIGURE 16: Comparison between fan (A) and ramp (B) depositional systems (Heller and Dickinson, 1985).

Another requirement is a high sedimentation rate that allows the shelf and slope break to be swamped with material, preventing the formation of canyons and channelized deposits (Heller and Dickinson, 1985). The ramp environment has also been described as a mass flow apron (Aitchison and Landis, 1990) and a slope apron (Ineson, 1989). Aitchison and Landis (1990) describe strata from the Triassic Stepehens Subgroup of Southland New Zealand as having characteristics consistent with deposition in a mid-fan area. However, Aitchison and Landis (1990) note that the depositional cycles are generally smaller in scale than those expected in submarine fan environments, but are reluctant to conclude that this alone indicates a ramp environment. They suggest that the lack of structure may be due to migratory feeder channels resulting from intra-basinal tectonic activity. Regardless of the cause, the Stephens Subgroup lacks a dominant feeder channel or channel system, and the resulting facies that such features produce. A ramp environment can be inferred when there is no evidence of point sources, or large-scale channels. The presence of structureless sand bodies with dewatering features suggests rapid deposition into deep water in these environments. Aitchison and Landis prefer to use the term "mass flow apron" to describe the ramp environment, but the main features are the same as the submarine ramp described by Heller and Dickinson (1985). Mass flow aprons have also been described by Ineson (1989) in Cretaceous rocks from Antarctica. The rocks described in Ineson's work appear to locally exhibit more structure (levee facies, channel facies, etc.) than that described by Heller and Dickinson (1985) and Aitchison and Landis (1990). This difference in morphology is attributed to the development of relatively small fans due to localized input of coarse arc-derived sediment. The localized input in Ineson's model results from variations in basin tectonics, or local increases in volcanic activity.

Where unchannelized, the environment and resulting sedimentary features (the slope apron deposits described by Ineson (1989)) resemble those of the submarine ramp of Heller and Dickinson (1985). It is clear therefore, that a relatively narrow shelf with no channelization is necessary for the development of a true submarine ramp environment. The lack of channelized sediment delivery results in little or no facies segregation into the channel facies typical of submarine fans and fan-deltas. Literature review suggests that there is a spectrum of depositional environments with the relatively unstructured, unchannelized submarine ramps of Heller and Dickinson (1985) at one end, and the highly structured fans generated by incised feeder channels in the shelf modelled by Walker (1978) and Mutti and Ricchi-Lucchi (1978) at the other end. This concept has been discussed by Barrett and Fralick (1989).

The features of a submarine ramp environment are easily recognized in the McKellar Harbour Sequence. The Sequence is dominated by sandy turbidites that show only obscure vertical bed thickness and grainsize trends, with the boundaries between Subsequences mostly transitional. In over 850m of section there is no evidence of channelized deposits, with the possible exception of the conglomeratic unit and associated thick and coarser-grained sandstone units that occur about 150m from the base of the Sequence. The sandstone units of the McKellar Harbour Sequence are also quite laterally continuous, with some units traced for over 1 km along strike. Overall, the lack of facies typical of the mid-fan and suprafan lobes, combined with the lateral continuity of the units indicates that the McKellar Harbour Sequence was deposited as a submarine ramp.

The Subsequences defined in the McKellar Harbour Sequence represent subtle changes in the processes at work during the deposition of the Sequence. Type 2 Subsequences (most common in the McKellar Harbour Sequence) are typical of the distal ramp facies of Heller and Dickinson (1985). As the units become thicker and show more sedimentary features (i.e. Type 1 Subsequence), a more proximal ramp environment can be interpreted. The thick, relatively ungraded units of the Type 3 Subsequences capped by black shale are indicative of proximal ramp facies (Heller and Dickinson, 1985). The Type 4 Subsequence (silty shale separated by thin sand units) is a bit of anomaly, as it does not fit the pattern of deposition usually encountered with a submarine ramp. It is possible that, during the transition from Type 2 (distal) to Type 3 (proximal) facies that occurs 641 m from the base of the section, a portion of the ramp was starved for coarser sediment, and only silt and minimal sand was deposited. Overall, it appears that the McKellar Harbour Sequence shows an upward transition from distal to proximal ramp facies, indicating progradation of the ramp onto the basin floor.

At the Steel River Schnieders' work (1987) shows the sedimentary rocks to possess more structuring/ordering than in the McKellar Harbour Area. The facies present have been interpreted as mid fan facies of Walker's (1978) submarine fan model. It is possible to develop minor lobes on a submarine ramp (Heller and Dickinson, 1985), and these would give the appearance of lobe deposits of Walker's (1978) mid-fan region. When put into a more regional context, and given their association with the relatively unstructured McKellar Harbour Sequence, it can be concluded that the structuring observed by Schnieders (1987) is the result of minor lobe development on a submarine ramp. These units may also reflect a change in basin tectonics that caused local channelization of the sediment supply as described by Ineson, (1989), resulting in a minor fan developing as part of the ramp.

## 5.3 Possible Source Areas

### 5.3.1 Schreiber-Winston Lake Region

To the north of Schreiber, in the Winston Lake area, volcaniclastic rocks are found in association with what has been interpreted as pillowed mafic flows (Balint et al. 1990) and gabbroic to peridotitic intrusive rocks. These relationships are illustrated in the Winston Lake Section (Figure 11). Thinly bedded units of volcaniclastic material lie intercalated with several units of biotite schist that have been interpreted as mafic flows (Balint et al., 1990). Bedding parallel layers of gabbroic rocks are thought to represent sub-volcanic intrusions (Balint et al, 1990).

Due to the alteration and metamorphism that has affected these rocks it is difficult to determine their mode of deposition. The association of the tuffaceous sedimentary and pyroclastic rocks with pillowed mafic volcanics indicates deposition either subaqueously, or near a body of water. It is quite possible that deposition of the bedded tuffaceous units occurred as airfall onto a standing body of water. It is also possible for the tuffaceous material to be transported through sedimentary processes to their site of deposition.

5.3.2 Lake Superior Area

The sedimentary rocks of this area are thicker and coarser than those of the McKellar Harbour Sequence, and do not show the same rhythmic development of turbidites. AA, AC, and CE turbidites dominate at this location. The sandstone to shale ratio is higher, with only occasional beds of shale. Features indicative of slumping are common, size grading is less apparent, and some units contain abundant lithic fragments. Slumping of sedimentary units occurs in areas of high slope and/or rapid deposition. Units in this area also tend to thicken and coarsen upwards. Exact interpretation of the depositional environment is difficult, but some general conclusions are possible. The lack of shallow water (i.e. wave-generated and beach facies) combined with the turbiditic nature of these rocks indicates deposition in a relatively deep marine (below storm wave depth) setting with a moderate to high slope, and fairly rapid sedimentation rates. The occurrence of two rhyolitic units within the section indicates a region close to a volcanic source, where felsic tuffs could fall on the water's surface, sink and become incorporated into the sedimentary sequence. The sedimentary rocks in this portion of the study area occur as a relatively thin wedge within the much thicker, intermediate to felsic pyroclastic rocks of the Heron Bay Group (Muir, 1982a). These volcanic rocks could represent the source for the sedimentary rocks of this area.

The incorporation of volcaniclastic units into sedimentary sequences in volcanic island settings has been documented by several workers (i.e. Aitchison and Landis, 1990, Ineson, 1989). This usually occurs in a depositional system that disperses material derived from a volcanic arc (both through airfall and through erosion) into a marine setting. Dispersal systems in these environments have been described as: mass flow aprons (Aitchison and Landis, 1990); fan/slope aprons (Ineson, 1989); marine volcaniclastic aprons (Busby-Spera, 1988); fan-deltas (Nocita and Lowe, 1990); and submarine ramps (Heller and Dickinson, 1985).

5.3.3 Pukaskwa Area

Sedimentary rocks of the Pukaskwa Area are characterised by sandstone units up to 4m thick that grade upwards to thin (cm) DE or BE turbidites. Some units (particularly the thicker ones) contain lithic fragments, and others consist of pebbly sandstone. Several units contain trough cross-stratification, and only two beds contain slump features. The pebbly sandstones below units of trough cross-stratified sandstone could represent deposition in distributary channels in a fluvial dominated delta (Reading, 1986, pp 140-141). Synsedimentary deformation in this environment is common and tends to disrupt the facies pattern (ibid), but a general pattern for the progradation of a fluvial dominated delta front has been developed. This sequence has silty mudstones with occasional turbidites passing upwards to parallel laminated siltstones, which are in turn overlain by conglomerate and massive to cross-bedded sandstones. The conglomerate units overlie erosional surfaces and represent lag deposits. Features of this type of sequence can be interpreted in the Pukaskwa Area. Pukaskwa Section 2 (Figure 12) in particular has the features common to a fluvial-distributary channel in a fluvial- dominated delta, with trough cross-stratified sandstones overlying conglomerates. The slump features that occur near the top of this section could be the result of bank slumping, and the pebbly sandstone lenses in silt at the top could represent overbank deposition into low lying areas adjacent to the channels.

### 5.3.4 Hemlo Area

The Hemlo Area is characterised by relatively fined-grained and thin-bedded sedimentary rocks closely associated with intermediate to felsic pyroclastic and volcanic rocks. Conglomerate units are also present, including an intraformational breccia that may have been produced by synsedimentary deformation. The close association of the turbiditic sandstone units with tuffaceous pyroclastic units indicates that the pyroclastic rocks were deposited as airfall into water, beneath which turbiditic sandstones and conglomerates were being deposited. The conglomerates may be the result of debris flows and are interbedded with turbidites. Volcaniclastic material delivered to the system at this point would fall on the water's surface, sink and become interstratified with the sedimentary units. A possible environment of deposition for these units would be subaqueous with at least a gentle slope to enable slump-generated debrites (Walker, 1984). Slumping likely resulted in the intraformational breccia (described above, Chapter 3) as a debrite. Delivery of coarse material resulting in the conglomerates could have occurred through channels near a delta front, or at the base of an alluvial fan. The lack of size grading in the conglomerate units is typical of disorganized bedded sub-aqueous mass-flows, and the association with turbidites further suggests sub-aqueous deposition.

### 5.3.5 Amwri Lake Area

The Amwri Lake Area is dominated by conglomerate units ranging from a few centimetres to a few metres in thickness, and where present, grading is crude at best. These conglomerates are generally in clast support, and some of these units are separated by relatively thin sandstone layers that only rarely show rough grading. Units of clast supported conglomerate showing crude reverse to normal grading have been shown to be deposited by sediment gravity flows (Lowe, 1982). Unorganized (ungraded) units likely represent deposition by "cohesive debris flows" (ibid), and the transition from reversely graded to normally graded units corresponds to the transition from debris flows (cohesive and grain flows) to high density turbidity currents. Lowe (1982) does not speculate on the determination of subaereal versus sub-aqueous deposition in sediment gravity flows. The lack of stream reworked pebbly units above conglomerate units, combined with a lack of well developed grading, and a mud free matrix in conglomerate units has been interpreted as indicating a sub-aqueous environment (Higgs, 1990). This description closely matches that of the Amwri Lake conglomerates, and it is therefore possible that they were also deposited sub-aqueously. Sandstone units that overtop the conglomerate units are then likely the result of turbidity currents as part of the same series of events as the underlying conglomerate, or as a separate, later, event.

# 6.0 DEPOSITIONAL SYSTEMS

## 6.1 Introduction

The depositional environments discussed in the previous chapter can now be placed in a more regional context and the depositional systems operating over a larger area can be interpreted.

## 6.2 Winston Lake Area

This portion of the study area lies immediately to the south of the Quetico Subprovince, which has been postulated as a south-facing accretionary wedge (Devaney and Williams, 1988, Williams, 1989) active at approximately 2700 Ma (D. Davis, ROM, pers. comm). Other workers have concluded that the Quetico Subprovince is a north facing accretionary wedge (i.e. Card, 1990). This conclusion fits well with the depositional environments for the Onaman-Tashota and Beardmore-Geraldton areas described by Barrett and Fralick (1985, 1989), Devaney (1987), Devaney and Fralick (1985), and Fralick (1987) which also favour northwards subduction. The Schreiber-Winston Lake area would then represent a volcanic arc on the trailing edge of the plate being subducted to the north under the Beardmore-Geraldton Terrane, with the Quetico accretionary complex lying between (Fralick and Barrett, 1991; Eriksson et al, 1994, in press).

The presence of pillowed mafic flows suggests a subaqueous environment for the deposition of units in the Winston Lake area. If the thin bedding of the volcaniclastic rocks associated with the pillowed mafic flows is taken to be primary, the tuffaceous units could have a turbiditic association. These rocks were probably deposited on the flanks of a volcanic edifice. Volcanism would have been active during deposition, as the flows and clastic rocks are interbedded. The isolated occurrences of carbonaceous sedimentary rocks with minor sand and siltstone would have been deposited within minor basins located on the flanks of the arc. Another possibility is that sediments from the Beardmore-Geraldton terrane to the north filled the Quetico trench, and were transported to the south through gaps in the Schreiber volcanic terrain. A submarine ramp has been interpreted as the depositional system operating in the Beardmore-Geraldton area (Barret and Fralick, 1989), and the Quetico Trench (Fralick et al, 1992). This environment is thought to occur where the sedimentation rates are high (Heller and Dickinson, 1985). Sediments carried over the trench by the submarine ramp would then have a distal ramp affinity, and would pond in small basins associated with the Schreiber volcanic terrain.

### 6.3 McKellar Harbour Area

This area shows a thick sequence of turbiditic sedimentary rocks. Schnieders (1987) interpreted rocks to the west as representing the mid-fan area in the submarine fan model (Walker, 1978), as these rocks show structuring similar to fan lobes. However, it is more likely that the McKellar Harbour sequence is representative of a submarine ramp environment (Heller and Dickinson, 1985; Barrett and Fralick, 1989). This interpretation is favoured due to the lateral and vertical consistency of thickness and bed type over the sequence as a whole, and a general lack of channel and depositional lobe facies. Schnieders' (1987) work indicates that some structuring of the ramp took place to the west of the McKellar Harbour Sequence, and this could represent lobe facies that can occur locally within both proximal and distal ramp environments (Heller and Dickinson, 1985). The lobe facies in a ramp environment should bear close resemblance to mid-fan facies (Walker, 1984), as both represent deposition at channel mouths.

6.4 Heron Bay - Hemlo Area

Sedimentary rocks in the vicinity of Randle Point and Pukaskwa National Park show more proximal affinities than those in McKellar Harbour. The sandstone units are generally coarser, and often contain lithic fragments. Some units are conglomeratic with pebbles in a sandy matrix. There is evidence of shallow water deposition in the presence of trough cross-stratification, which indicates possible channelization of these units (Figures 11 and 12 and photo 5). Moving from west to east (from Lake Superior to Amwri Lake) through the area, the nature of the sedimentary rocks changes. The units become thicker, and conglomeratic rocks appear more frequently. The rocks are clast-rich (usually in clast support) indicating a source proximal location. There are also associated felsic pyroclastic units, and mafic volcanic flows. Deposition of these units likely occurred sub-aqueously on the flanks of an active volcanic island system, and they do not have the sedimentary characteristics of a submarine ramp. It is therefore unlikely that they are genetically related to the McKellar Harbour Sequence, and are the result of deposition in a separate basin. There is currently insufficient stratigraphic information to ascertain the depositional system for these rocks.

# 7.0 PROVENANCE

## 7.1 Introduction

This chapter will interpret the provenance of some of the units in each region of the study area. Provenance determination of coarse-grained lithologies (i.e. conglomerates) is based mainly on the rock types of the clasts present in each unit. In some cases the relative abundances of the clast types was determined using a point counting method, but in other areas a visual estimation of the relative clast lithologies was made. The provenance of the finer grained lithologies (metasandstone and slate) occurring in each respective region was investigated using immobile elements in a geochemical data set. Unfortunately, only two samples of sandstone were collected from the Amwri Lake region, and hence provenance of the unit was not evaluated using geochemical data. More detailed information regarding the clast abundances was collected from this region, and this should compensate for the lack of geochemical data from the finer units.

## 7.2 Conglomerate Provenance

There was only one conglomeratic unit located in the McKellar Harbour Sequence. This thin unit contained clasts of only intermediate volcanic composition.

Clast lithologies present in the Amwri Lake Area conglomerate were counted, and the data indicate that the majority were of granitic and/or dioritic composition. It is likely that the conglomerates resulted from the unroofing of felsic to intermediate plutonic rocks. These plutons may have served as possible feeders for the extensive volcanic sequences in the region.

The conglomerates observed on the shore of Lake Superior in Pukaskwa National Park are dominated by clasts of granitic and dioritic origin, with slightly lesser quantities of clasts with a volcanic and/or sedimentary origin (the schistose clasts previously described). The clast lithologies indicate that the conglomerates evolved from a intrusive/extrusive terrane.

Conglomerate examined in the Hemlo region consists mainly of granitic feldspar-quartz porphyry clasts, with slightly less dominant proportions of biotite-hornblende schist clasts. The biotite-hornblende schist clasts probably represent fragments of metamorphosed fine-grained sediment. The two clast types are found supported by a matrix of sand. The origin of these units may be similar to that of the Amwri Lake conglomerates. However, the Hemlo conglomerate is matrix- as opposed to clast-supported, and the relative proportion of clasts of a sedimentary origin is greater in the Hemlo units. Unfortunately, these rocks were so poorly exposed that no meaningful stratigraphic information could be collected to place them in context.

A second type of conglomerate observed in the Hemlo area occurs on the Page Williams property. This unit is likely an intraformational breccia generated by slumping during deposition, or as a tectonic breccia produced during folding. The clasts appear to consist of material similar to that of the surrounding thinly laminated pelitic beds.

## 7.3 Sandstone Provenance

### 7.3.1 Introduction

Petrographic examination of rocks from the study area revealed only that they were derived from intermediate to felsic igneous sources (as evidenced by the presence of granitic and intermediate/felsic lithic fragments in the sandstone units). These data did not, however yield any information as to the actual source regions, and therefore a more precise technique for determining provenance was necessary. Whole rock geochemistry was selected as the tool for provenance determination. Samples were collected from the various regions within the study area, as indicated on the relevant maps and sections. Appendix B presents the methodology used for the determination of the oxide chemistry, and the data set itself. A discussion of the geochemical techniques used for the determination of sandstone provenance is presented below.

### 7.3.2 Sandstone Provenance - Geochemical Techniques

Sandstone provenance has been given much attention over the years. Roser and Korsch (1986, 1988), Bhatia and Crook (1986), and Bhatia (1983) have developed processes for provenance determination based on major element oxides and REE's. These workers tend to ignore the fact that some major elements (Na K, Ca, etc.) are highly mobile, and that the composition of sandstones is not necessarily reflective of their original composition. This original composition will begin to change as the rock breaks down both physically and chemically. The process continues through soil development, diagenesis, subsequent metamorphism, and possibly hydrothermal alteration. The combination of these processes results in a composition that can be quite different from that of the original rock. The mobility of a given element in a rock varies depending on the specific set of erosional, depositional, metamorphic and hydrothermal conditions that the rock has been subjected to. These factors become more important than the initial source rock composition (Heins, 1993, Palomares and Arribas, 1993, Melfi et al, 1983, Sastri and Sastry, 1982). Thus, when addressing the problem of provenance determination using sediment geochemistry, the physical and chemical mobility of the elements used in the determination must be addressed.

Fralick and Kronberg (in press) have developed a procedure for first testing the mobility of various elements, concentrating on the less mobile elements (as determined by a screening process) and using the immobile elements to infer sedimentary provenance. The key to this determination is to find elements in the data set that have a composition reflecting that of the parent material, and have been affected by quantifiable processes. As other elements are depleted/enriched, the concentration of immobile elements will be concentrated or diluted, and this "constant sum" (Fralick and Kronberg, in press) relationship can be used to determine if a given element has been immobile.

Immobile elements will increase or decrease in concentration as mobile elements are lost or gained by the rock. When plotted against one another, the points will move towards or away from the origin as mobile elements are added to or depleted from the rock. The amount of any immobile element (i.e. the number of atoms of that element) will stay relatively constant, it is the addition and/or depletion of the mobile elements that changes the relative proportions (i.e. mass of the rock), resulting in changes in the concentrations of the immobile elements in the rock. Physical weathering (hydraulic sorting) will cause elements that concentrate in finer fractions to give higher concentrations in the clays, and likewise elements that concentrate in the coarse fractions will give higher concentrations in sands. This physical fractionation will create a line connecting the origin and the two end members of the size gradation. This relationship is shown in Figure 17.

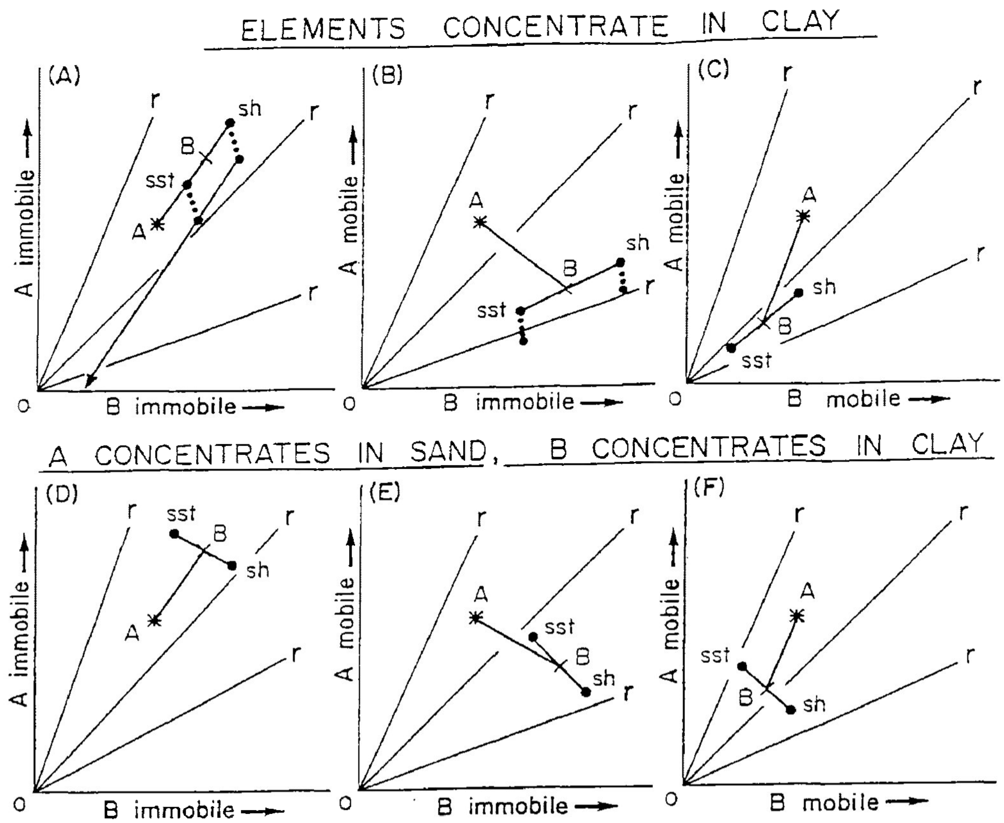


FIGURE 17: Theoretical sketches illustrating the use of scattergrams in determining element mobility.

(A): For immobile-immobile pairs the starting composition A moves to B as a result of loss of other consituents from the system. Composition B splits into sh (clay) and sst (sand) due to hydraulic fractionaltion (elements A and B enriched in clay). If the elements remain immobile during postdepositional alteration processes the points sh and sst will move along the A-B vector but will not move off it. If the elements were mobile during a phase of alteration, they will move off the A-B vector (one possible path is shown by the dotted lines). Plotting of immobile pairs from a number so samples will result in a linear array of points along radians (r) extending through the origin.

(B-F): Other possible scenarios involving mobile-immobile combinations: Plotting of multiple samples for any of these scenarios results in a scatter of points.

When a mobile element is plotted against an immobile element, the pattern is different. As the concentration of the mobile element decreases, the line connecting the coarse fraction and fine fraction will no longer pass through the origin. This relationship is illustrated in Figure 17.

This technique for mobility determination is most useful for data collected from multiple samples of sediment from the same source area. If both the plotted elements are immobile, and have behaved in a similar manner hydrodynamically, the data will form a linear trend which, when extended, passes through the origin. The data will appear scattered under any other circumstances. The chemistry of the source area must remain constant in order for this technique to work, and care must be taken to avoid plotting mobile elements that behave in a similar manner (i.e. REE's) against one another, as they may display a false linear trend that is not indicative of their mobility.

A second method developed by Fralick and Kronberg (in press) that is useful in the determination of the mobility of elements employs the premise that chemical and physical weathering break down all major mineral phases with the exception of quartz. The widely held belief that quartz-rich sands are more mature supports this assumption. $SiO_2$ must be relatively immobile in the given rocks for this technique to work. Figure 18 illustrates the following discussion. Sediment undergoing physical and chemical breakdown will split into two endpoints (sand and clay). For elements which are hydrodynamically concentrated in the fine-grained component. the points will lie on a line that connects 100 % $SiO_2$ with the original composition. Immobile elements that concentrate in the coarse fraction will form a linear trend that passes through the original composition and the origin. These linear trends will appear with the plotting of multiple data points, as long as the starting composition of the sediment did not change (i.e. the source rock composition did not change, nor did the provenance of the sediment).

A concern with reconstructing source area composition with geochemical data is that the concentrations of chemically immobile elements may not be similar to the starting compositions due to mass change during chemical and physical weathering (Floyd et. al, 1991). This problem can be avoided by examining the ratios of chemically immobile elements that have major mineral phases which concentrate in the same size fraction, which will not change significantly during chemical alteration and hydrodynamic sorting, and will reflect the ratios present in the source rocks, assisting in the determination of provenance.

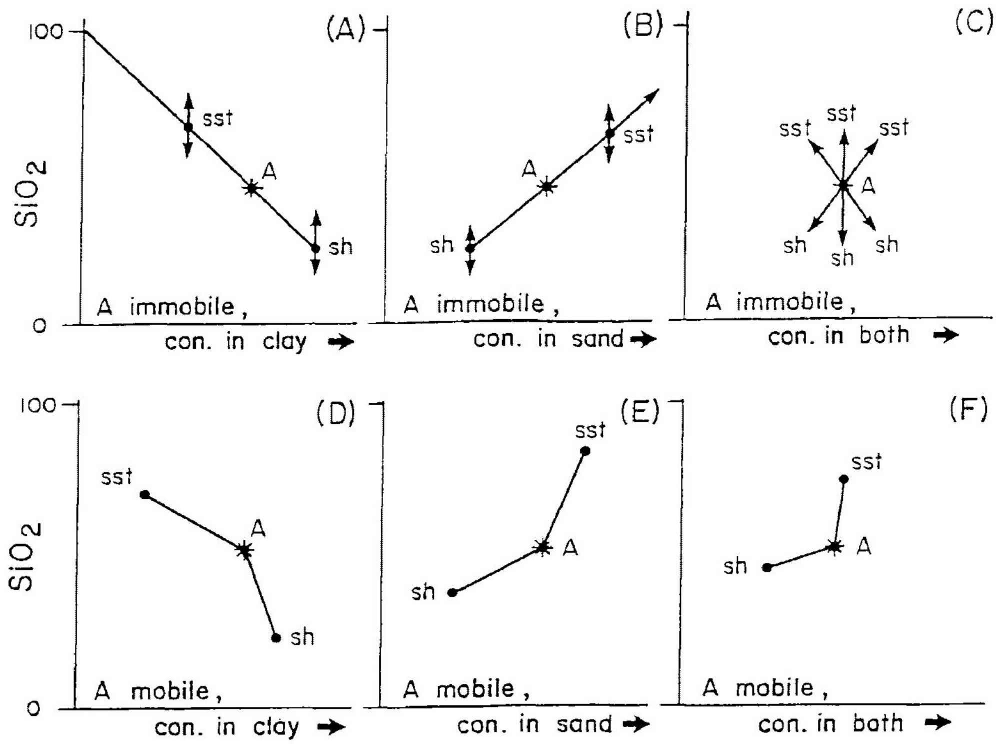


FIGURE 18: Theoretical sketches illustrating the use of $SiO_2$ plots in determining element mobility.

Starting composition splits into fine (sh) and coarse (sst) subpopulations due to chemical weathering and hydrodynamic sorting. Changes in $SiO_2$ content proceed at the same rate as changes in concentration of the immobile element resulting in a vector extending to 100% $SiO_2$ for an immobile element which concentrates in clay (A) and 0% $SiO_2$ for an immobile element which concentrates in sand (B).

Arrows denote movement of points if element A becomes mobile during a later phase of alteration.

Plotting of numerous data points will result in linear trends extending to either 100 or 0% $SiO_2$ for scenarios (A) and (B). Other scenarios: (C), (D), (E), (F), will result in a scatter of points when multiple samples are plotted.

### 7.3.3 Application of the Technique to the Study Area

The suspected immobile elements in sandstone and shales were plotted against one another in order to determine their respective mobilities, and the plots are included as Appendix D. This process was applied to rocks from each of the study regions: Winston Lake, Schreiber, McKellar Harbour, Lake Superior, Pukaskwa, and Hemlo. A linear trend towards the origin indicates that the elements in question have remained chemically immobile, and have hydrodynamically fractionated in a similar manner (Fralick and Kronberg, in press). The plots of Nb vs $TiO_2$ and $Al_2O_3$ show that data from the Winston Lake area are scattered, and thus these elements have not remained immobile. This is true as well for data from Hemlo and Lake Superior. The data from the Schreiber area indicate that the elements have remained immobile, and have been hydraulically fractionated in a similar manner. The data from McKellar Harbour show a linear trend towards the origin. The data appear to be oddly clustered, but this is due to the fact that the analyses were given to the nearest 1 ppm Nb, causing the data to "string out" on single incremental values of Nb. The data indicate that the elements are immobile and have behaved in a hydrodynamically similar manner. Data from the Pukaskwa Area show a linear trend towards the origin, indicating that the elements are immobile. Y produces a wide scatter when plotted with other elements, indicating that throughout the study area, it has been relatively mobile, limiting it's use in this technique. Zr plotted with $TiO_2$ shows a linear trend to the origin only for the Pukaskwa region, all others show scattering. Plots of Zr vs $Al_2O_3$ indicate that Schreiber and Hemlo have linear trends towards the origin, but data from the other regions are scattered.

Further information concerning the chemical and hydrodynamic behaviour of an element can be obtained by plotting the element against $SiO_2$. Elements that concentrate in the coarser fractions (i.e. sand) will show an increase with increasing $SiO_2$, resulting in a linear trend (positive slope). If the element concentrates in the finer fraction (i.e. shale), the trend will show decreasing values with increasing $SiO_2$ content (negative slope).

Zr data from McKellar Harbour, Pukaskwa, and Hemlo show a linear trend with a negative slope, indicating that Zr has concentrated in the finer fractions, but these linear trends are not well developed. Lake Superior data were scattered, as were data from Winston Lake and Schreiber.

Y data from all the study areas are scattered, as are Rb data.

The plot of $SiO_2$ vs $Al_2O_3$ shows a rough negatively sloped linear trend for data from the Lake Superior region, but data from McKellar Harbour, Pukaskwa, and Hemlo are scattered. Winston Lake shows a poorly developed negative slope, as does that from Schreiber.

### 7.3.4 Geochemical Interpretation

The data indicate that with the exception of the Winston Lake and Hemlo areas, $TiO_2$, Nb, and $Al_2O_3$ were relatively immobile and behaved in a hydrodynamically similar manner. The $SiO_2$ scattergrams indicate that for the McKellar, Schreiber and Hemlo areas these elements were concentrated in the fine fraction, while the Pukaskwa depositional processes concentrated these elements in the coarse fraction. Ratios of the Ti, Al, Zr and Nb from each region will be strongly related to the average ratios of the source rocks for these regions.

Plots of these ratios for the McKellar Harbour and Schreiber areas compared to the ratios of rocks from potential source areas provides a great deal of information on provenance. Figure 19 plots the average Ti/Al ratio vs the average Ti/Nb ratio for sedimentary rocks from the study area with data from the Quetico Subprovince and Beardmore-Geraldton greenstone belt (Fralick et al. 1992, data set included in Appendix C). The plot clearly shows that data from McKellar Harbour, Schreiber, and Quetico are tightly clustered. The Pukaskwa, Beardmore-Geraldton, and Western Quetico data lie close to this cluster. Data from Winston Lake, Amwri Lake, Hemlo, and Lake Superior are separate from the cluster. This indicates that rocks from the Schreiber, McKellar Harbour, and Quetico were derived from source rocks with similar Ti/Al and Ti/Nb ratios, and metasediments from Pukaskwa and the Beardmore-Geraldton area also have similar ratios.

This interpretation is reinforced by plotting Zr/Al vs Ti/Zr for the same rocks (Figure 20). The scatter plot shows the data from McKellar Harbour, Schreiber, Quetico (south of Geraldton) and the Beardmore-Geraldton areas lying in a tight linear arrangement. The composition of rocks from these areas follow a trend from Beardmore-Geraldton, Quetico south of Geraldton, Schreiber, then McKellar Harbour. The Lake Superior area plots below but further along the trend. This trend combined with the Ti/Al -Ti/Nb plot indicates that rocks from the Beardmore-Geraldton, Quetico, Schreiber, and McKellar Harbour areas are derived from a very similar source. That the data form a linear trend further reinforces this concept, as Ti tends to accumulate in the finer (e.g. clay) fraction, and Ti becomes concentrated relative to Zr with distance from source. Thus more distal turbidites have slightly different Ti/Zr ratios due to an increase in fine-grained matrix content. This trend is predictable and similar to the tight linear trend apparent in the data. It can therefore be concluded that the McKellar Harbour Sequence was probably derived from material produced in the Beardmore-Geraldton terrane.

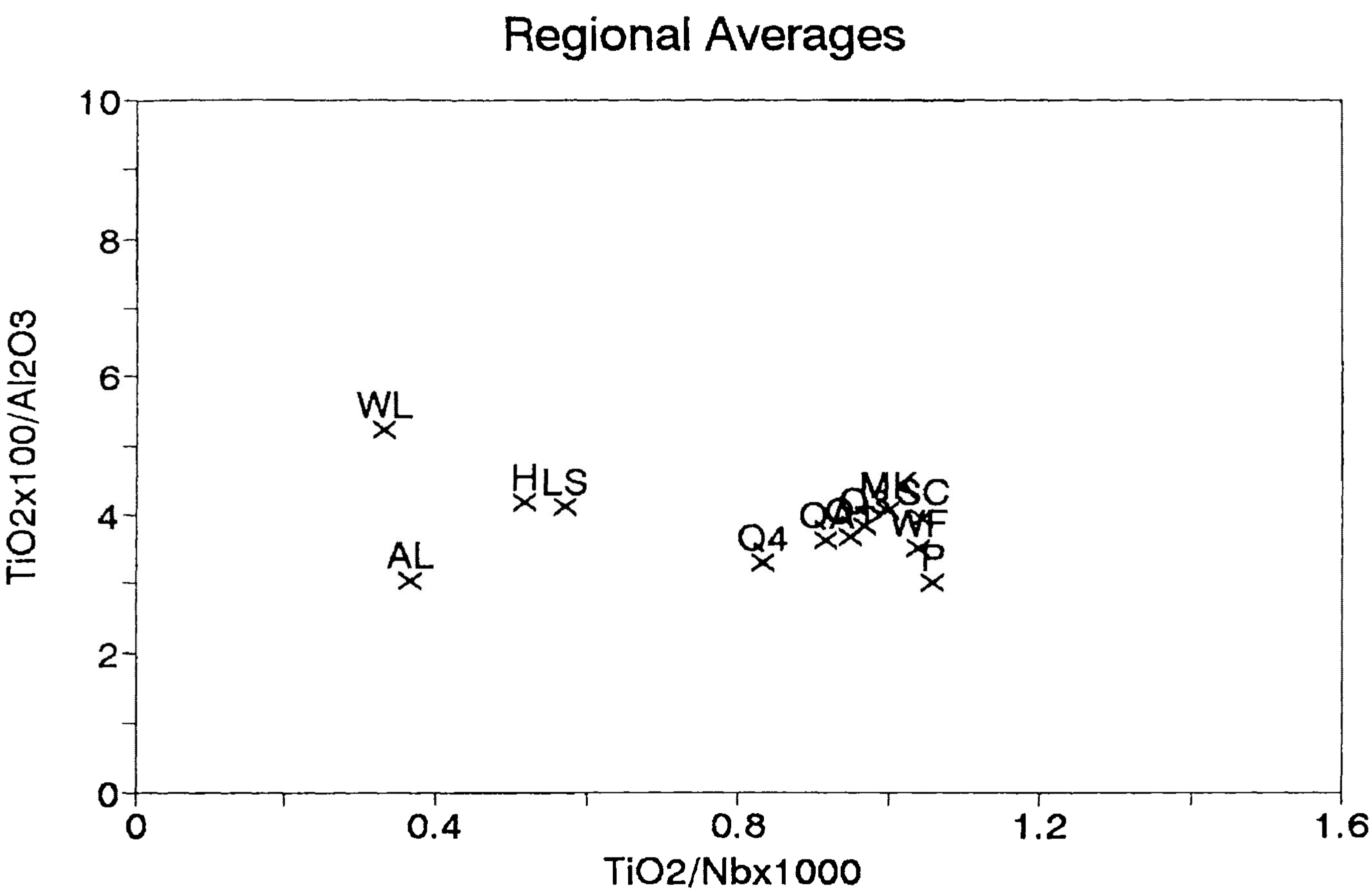


FIGURE 19: Immobile Element Ratios for: Amwri Lake (AL), Hemlo (H), Lake Superior (LS), McKellar Harbour (MK), Pukaskwa (P), Schreiber (SC), Quetico south of Geraldton (Q1), Quetico west of Thunder Bay (Q2-Q4), Average Quetico (QA), and Beardmore-Geraldton (Wabigoon Intermontane) (WI).

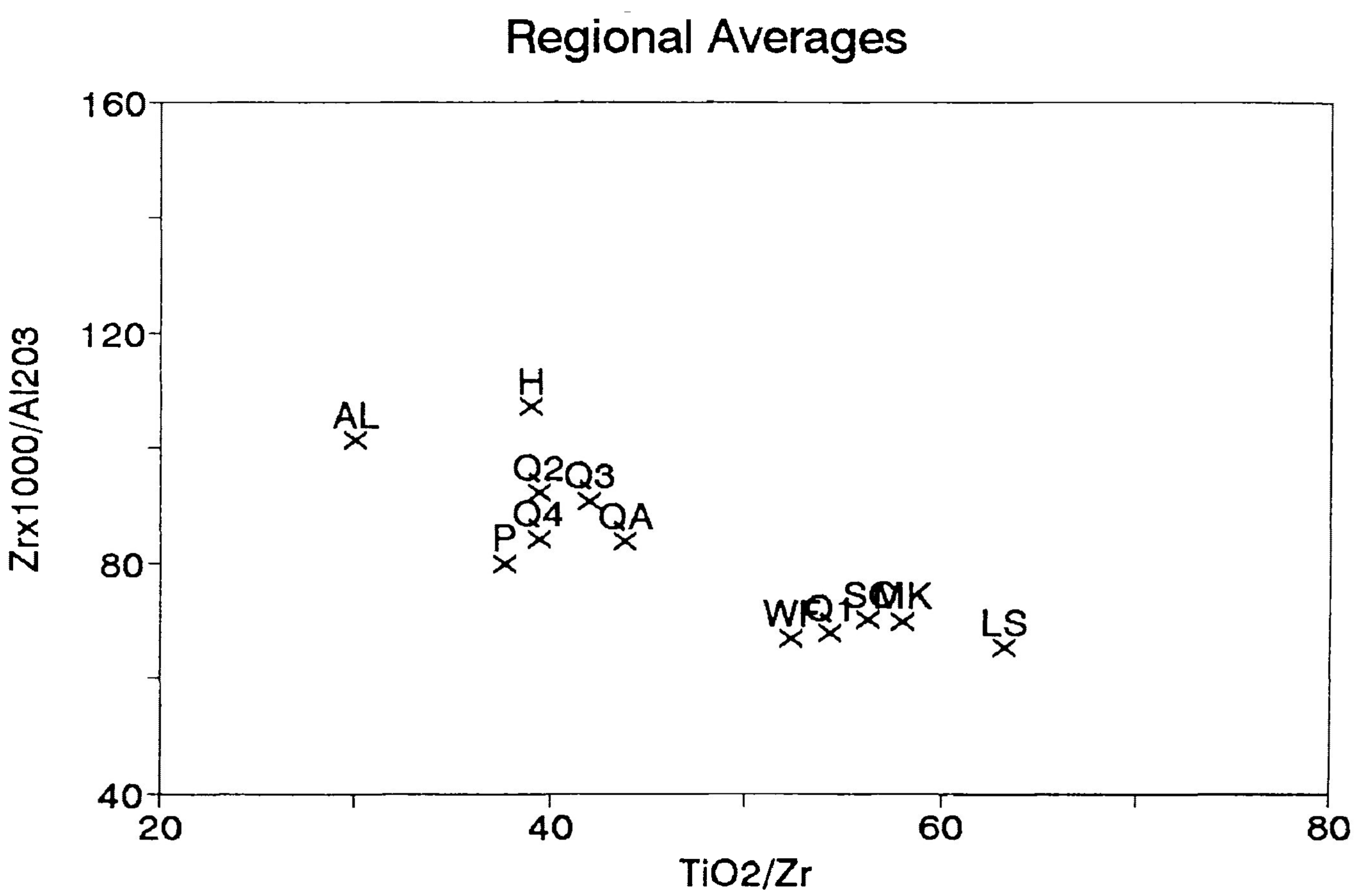


FIGURE 20: Immobile Element Ratios for: Amwri Lake (AL), Hemlo (H), Lake Superior (LS), McKellar Harbour (MK), Pukaskwa (P), Schreiber (SC), Quetico south of Geraldton (Q1), Quetico west of Thunder Bay (Q2-Q4), Average Quetico (QA), and Beardmore-Geraldton (Wabigoon Intermontane) (WI).

# 8.0 DISCUSSION AND CONCLUSIONS

The stratigraphic and geochemical evidence suggest that the McKellar Harbour Sequence was deposited on the distal portion of a submarine ramp being fed by sediment from the Beardmore-Geraldton terrane. It thus forms the distal portion of the proximal submarine ramp (Fralick et al., 1992) present in the Quetico metasedimentary belt. Other possible sediment feed areas are shown to have been deposited in other environments, and to have been derived from source areas with quite different immobile-element geochemistry. Figure 21 is a geological model illustrating the interpreted configuration of the area at the time of deposition of the McKellar Harbour Sequence. Sediment from the Onaman-Tashota and Beardmore-Geraldton terranes is carried across the trench, through gaps in the Schreiber volcanic island system. It collects in basins associated with the volcanic islands. The mechanism for this transport is a submarine ramp that has developed due to the rapid sedimentation rate on a narrow shelf in the Beardmore-Geraldton terrane. Sediments carried to the Schreiber volcanic system are distal portions of the Beardmore-Geraldton submarine ramp, and are preserved as the McKellar Harbour Sequence. Sediments in the Amwri, Hemlo, and Pukaskwa regions were deposited in basins not linked to the Schreiber - McKellar Harbour basin. Sediment in these three other areas was deposited by processes that are quite different from that of a submarine ramp, and the volcanic assemblage in the Hemlo area is quite different geochemically than that of the Onaman-Tashota/Beardmore-Geraldton terrane. This difference in chemistry is illustrated by the immobile element chemistry. Sediments in the Heron Bay - Hemlo area require further investigation.

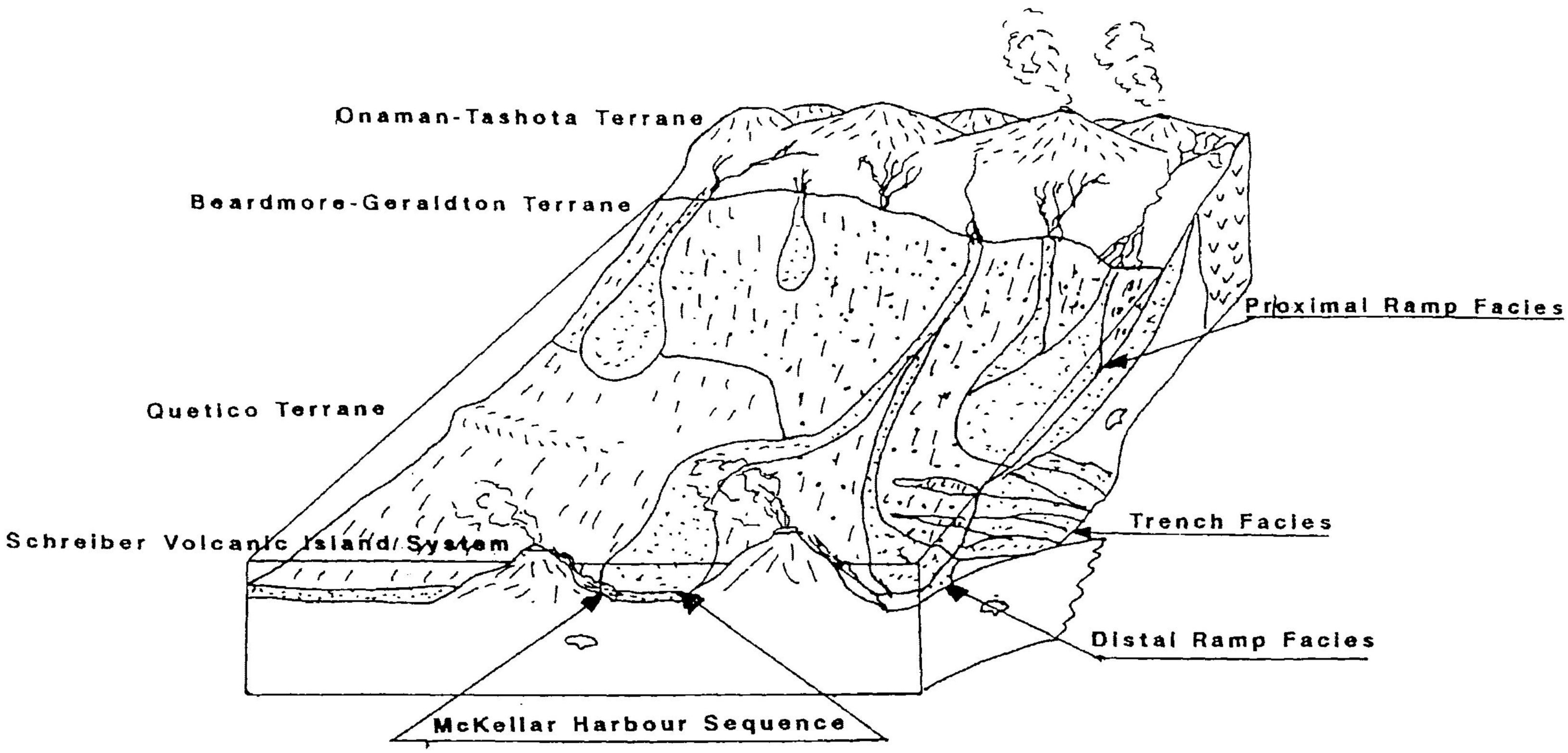


FIGURE 21: Paleoenvironmental Reconstruction (after Fralick, 1992).

This investigation has shown that geological subprovince boundaries are not barriers to geological processes. There is a continuum of depositional systems that has been shown to start in the Wabigoon Subprovince, cross the Quetico Subprovince, and result in deposition in the Wawa-Abitibi Subprovince. If cross-boundary deposition can happen in one area, it is reasonable to conclude that it can also take place in other regions (see Zaleski et al, 1994).

## REFERENCES

Aitchison, J.C. and Landis, C.A. 1990. Sedimentology and tectonic setting of the Late Permian-early Triassic Stephens Subgroup, Southland, New Zealand: an arc-derived mass flow apron; Sedimentary Geology, v. 68, p. 55-74.

Balint, F., Sim, R.C., and Morrison, I.R. 1990. The Winston Lake Massive Sulphide Deposit; unpublished field trip guide, Minnova Inc.

Barrett, T.J., and Fralick, P.W., 1985. Sediment redeposition in Archean iron formation: examples from the Bearmore-Geraldton greenstone belt, Ontario, Journal of Sedimentary Petrology, v. 55, p. 205-212.

Barrett, T.J., and Fralick, P.W., 1989, Turbidites and iron formations, Beardmore-Geraldton, Ontario: application of a combined ramp fan model to Archean clastic and chemical sedimentation; Sedimentology, v 36, p. 221-234.

Bartley, M.W., and Page, T.W. 1958. A geological report on the Hemlo Area; Western Miner and Oil Review, v. 31, no. 8.

Bartley, M.W., and Page, T.W., 1957. A geological report on the Hemlo area, Thunder Bay District; unpublished report, Canadian Pacific Railway, Resident Geologist's Files, Schreiber-Hemlo District, Thunder Bay, 20p.

Bhatia, M.R. 1983. Plate tectonics and geochemical composition of sandstones; Journal of Geology, v. 91, p. 611-627

Bhatia, M.R., and Crook, K.A.W. 1986. Trace element characteristics of greywackes and tectonic setting discrimination of sedimentary basins; Contributions to Mineralogy and Petrology, v. 92, p. 181-193.

Bouma, A.H. 1962. Sedimentology of some flysch deposits: a graphic approach to facies interpretation. Elsevier, Amsterdam, 168 p.

Brown, P., et. al. 1985. Golden Giant joint venture properties-Hemlo; in Gold and copper-zinc metallogeny within metamorphosed greenstone terrain: Hemlo-Manitouwadge-Winston Lake, Ontario, Canada; joint publication, Geological Association of Canada and Canadian Institute of Mining and Metallurgy, p. 58-65.

Busby-Spera, C.J. 1988. Evolution of a Middle Jurassic back-arc basin, Cedros Island, Baja, California: evidence from a marine volcaniclastic apron; Geological Society of America Bulletin, v. 100, p. 218-233.

Card K.D 1990. A review of the Superior Province of the Canadian Shield, a product of Archean accretion; Precambrian Research v. 48, p. 99-156.

Carter, M.W. 1988. Geology of Schreiber-Terrace Bay Area, District of Thunder Bay; Ontario Geological Survey Open File Report 5692.

Church, S.E. 1981. Multielement analysis of fifty-four geochemical reference samples using inductivly coupled plasma-atomic emission spectroscopy; Geostandards Newsletter, v. 2, p. 133-160.

Corfu, F. and Muir, T.L., 1989a. The Hemlo-Heron Bay greenstone belt and Hemlo Au-Mo deposit, Superior Province, Ontario, Canada 1. Sequence of igneous activity determined by zircon U-Pb geochronology; Chemical Geology, v. 79, p. 183-200.

Corfu, F. and Muir, T.L., 1989b. The Hemlo-Heron Bay greenstone belt and Hemlo Au-Mo deposit, Superior Province, Ontario, Canada 2. Timing of metamorphism, alteration and Au mineralisation from titanite, rutile and monzanite U-Pb geochronology; Chemical Geology (Isotope Geology Section) v. 79, p. 201-223.

Devaney, J.R. 1987. Sedimentology and stratigraphy of the northern and central metasedimentary belts in the Beardmor-Geraldton area of norhtern Ontario; unpublished M.Sc. thesis, Lakehead University, Thunder Bay, Ontario.

Devaney, J.R. and Fralick, P. 1985. Regional sedimentology of the Namewaminikan Group, northern Ontario: Archean fluvial fans, braided rivers, deltas and an aquabasin; in Current Research, Part B, Geological Survey of Canada, Paper 85-1B, p. 2-31.

Devaney, J.R., and Williams, H.R. 1989. Evolution of an Archean subprovince boundary: A sedimentological and structural study of part of the Wabigoon-Quetico boundary in northern Ontario; Canadian Journal of Earth Sciences, v. 26, p. 1013-1026.

Eriksson K.A., Krapez, B., and Fralick, P.W. 1994. Sedimentology of Greenstone Belts: Signature of Tectonic Evolution: (in press).

Floyd, P.A. et. al. 1991. Geochemistry and provenance of Rhenohercynian synorogenic sandstones: implications for tectonic environment discrimination; in A.C. Morton, S.P. Todd, and P.D.W. Haughton (eds), Developments in Sedimentary Provenance Studies, Geological Society Special Publication No. 57, p. 173-188.

Fralick, P., 1987. Depositional environment of Archean iron formation: inferences from layering in sediment and volcanic hosted end members; in Precambrian Iron-Formations, P. Appel and G. LaBerge, editors, Theophrastus Publications, S.A., Athens, Greece, p. 251-266.

Fralick, P., Barret, T.J., Jarvis, K.E., Schnieders, B.R., and VandeKemp, R. 1989. Sulphide-facies iron formation at the Archean Morley occurrence, northwestern Ontario: contrasts with oceanic hydrothermal deposits; Canadian Mineralogist, v 27, p 601-616.

Fralick, P., and Barret, T.J., 1991. Precambrian Depositional Systems along the Southwestern Edge of the Superior Craton; Geological Association of Canada, Mineralogical Association of Canada, Society of Economical Geologists, Joint Annual Meeting, Toronto '91, Field Trip A3: Guidebook, 54p.

Fralick, P., Wu, J., and Williams, H.R. 1992. Trench and slope basin deposits in and Archean metasedimentary belt, Superior Province, Canadian Shield; Canadian Journal of Earth Sciences, v. 29, p. 2551-2557.

Fralick, P., and Kronberg, B.I. 1995 (in press). The geochemistry of clastic sedimentary rocks: Seeing through the haze. Geological Society of America Bulletin.

Ghibaudo, G. 1992. Subaqueous sediment gravity flow deposits: practical criteria for their field description and classification; Sedimentology, v. 39, p. 423-454.

Gliddon, D.J. 1985. The mineralogy and genesis of the Late Archean Hemlo barite occurrences in northern Ontario; unpublished H.B.Sc. thesis, Lakehead University, Thunder Bay, Ontario, 208 p.

Heins, W.A. 1993. Source rock texture versus climate and topography as controls on the composition of modern plutonoclastic sand; in, M.J. Johnsson and A.Basu (eds) Processes Controlling the Composition of Clastic Sediments, Geological Society of America Special Paper 284, p. 135-146.

Heller, P.L., and Dickinson, W.R. 1985. Submarine ramp facies model for delta-fed sand-rich turbidite systems; AAPG Bulletin, v. 69 no. 6 (June, 1985), p. 960-976. 60, 66

Higgs, R. 1990. Sedimentology and tectonic implications of Cretaceous fan-delta conglomerates, Queen Charlotte Islands, Canada; Sedimentology, v. 37, p. 83-103.

Ineson, J.R. 1989. Coarse-grained submarine fan and slope apron deposits in a Cretaceous back-arc basin, Antarctica; Sedimentology, v. 36, p. 793-819.

Lowe, D.R. 1982. Sediment gravity flows: II. Depositional models with special reference to the deposits of high density turbidity currents; Journal of Sedimentary Petrology, v. 52, no. 1, p. 279-297.

Mann, W.D. 1986. Lithostratigraphy of a section of the Moose Lake Formation, Golden Sceptre and Interlake properties, Hemlo gold camp; unpublished M.Sc. paper, Queen's University, Kingston, Ontario, 43p.

Melfi, A.K., et al. 1983. Granitic weathering: A Brazilian study; Journal of Soil Science, v. 34, 841-851.

Milne, V.G., 1967. Geology of the Cirrus Lake-Bamoos Lake Area, District of Thunder Bay; Ontario Department of Mines, Geological Report 43, 63 p.

1968. Geology of the Black River area, District of Thunder Bay, Ontario Department of Mines, Geological Report 72.

Muir, T.L., 1982a. Geology of the Heron Bay Area, District of Thunder Bay; Ontario Geological Survey, Geological Report 218, 89p.

1982b. Geology of the Hemlo Area, District of Thunder Bay, Ontario Geological Survey, Geological Report 217, 65p.

1984. Hemlo Stratigraphic study; in Summary of Field Work 1984, Ontario Geological Survey, Miscellaneous Paper 119, p. 49-50.

Mutti, E., and Ricci-Lucchi, F. 1978. Turbidites of the northern Apennines: introduction to facies analysis; International Geology Review, v. 20, p. 126-166.

Nocita, B.W., and Lowe, D.R. 1990. Fan-delta sequence in the Archean Fig Tree Group, Barberton Greenstone Belt, South Africa; Precambrian Research, v. 48, p. 375-393.

Page, T.W., 1947. A report on the Ollmann-Williams group of claims, Hemlo, Ontario; unpublished report, assessment files, Resident Geologist's Office, Schreiber-Hemlo District, Thunder Bay, 8p.

Palomares, M., and Arribas, J. 1993. Modern stream sands from compound crystalline sources: composition and sand generation index; in M.J. Johnsson and A. Basu (eds) Processes Controlling the Composition of Clastic Sediments, Geological Society of America Special Paper 284, p. 313-322.

Pan, Y. and Fleet, M.E. 1989. Metamorphic petrology and gold mineralisation of the White River gold prospect, Hemlo area; in Geoscience Research Program, Summary of Research 1988-1989, Ontario Geological Survey, Miscellaneous Paper 143.

Pan, Y., and Fleet, M.E., 1989. Metamorphic petrology and gold mineralization of the White River Gold Prospect, Hemlo area; in Geoscience Research Grant Program, Summary of Research 1989-1990, Ontario Geological Survey, Miscellaneous Paper 150, p. 13-26.

Pan, Y., 1990. Metamorphic petrology and gold mineralization of the White River gold prospect, Hemlo area, Ontario; unpublished Ph.D. thesis, University of Western Ontario, London, Ontario, 256p.

Pan, Y., Fleet, M.E., and Stone, W.E., 1991. Calc-silicate alteration in the Hemlo gold deposit, Ontario: Mineral assemblages, P-T-X constraints and association with gold mineralization; Geological Association of Canada-Mineralogical Association of Canada-Society of Economic Geologists, Joint Annual Meeting, Program with Abstracts, Toronto, Ontario, p. A94.

Patterson, G.C. 1984. Field Trip Guidebook to the Hemlo Area; Ontario Geological Survey Miscellaneous Paper 118, p. 1-33.

Percival, J.A. 1989. A regional perspective of the Quetico metasedimentary belt, Superior Province, Canada; Canadian Journal of Earth Sciences v. 23, p 158-171.

Pye, E.G., 1964. Mineral deposits of the Big Duck Lake area, District of Thunder Bay; Ontario Department of Mines, Geological Report 27, 47p.

Quartermane, R.A. 1985. Road guide to the geology of the Teck-Corona Mine at Hemlo, Ontario; in Gold and copper-zinc metallogeny within metamorphosed greenstone terrain, Hemlo-Manitouwadge-Winston Lake, Ontario, Canada, joint publication of the Geological Association of Canada and the Canadian Institute of Mining and Metallurgy, p. 39-46.

Reading, H.G. 1986. Sedimentary Environments and Facies; Blackwell Scientific Publications, Boston, 615p.

Roser, B.P. and Korsch, R.J. 1986. Determination of tectonic setting of sandstone mudstone suites using SiO2 content and K2O/Na2O ratio; Journal of Geology, v. 94, p.635-650

1988. Provenance signatures of sandstone-mudstone suites determined using discriminant function analysis of major element data; Chemical Geology, v. 67, p. 119-139.

Sastri, G.G.K., and Sastry, G.S. 1982. Chemical characteristics and evolution of the laterite profile in Hazaridadar Bauxite Plateau, Madhya Pradesh, India; Economic Geology, v. 77, p. 154-161.

Schandl, E.S., Davis, D.W., Gorton, M.P., and Wasteneys, H.A. 1991. Geochronology of hydrothermal alteration around volcanic-hosted massive sulphide deposits in the Superior Province; Ontario Geological Survey, Miscellaneous Paper 156, p. 105-120.

Schnieders, B.R.S. 1987. The Geology of Sulphide-Facies Iron Formation and Associated Rocks in the Lower Steel River-Little Steel Lake Area, Terrace Bay, Ontario; unpublished M.Sc. Thesis, Lakehead University, Thunder Bay, Ontario.

Siragussa, G.M., 1984a. Precambrian geology, White Lake area, western part, District of Thunder Bay; Ontario Geological Survey, Preliminary Map P. 2701.

1984b. Precambrian geology, White Lake area, eastern part, District of Thunder Bay; Ontario Geological Survey, Preliminary Map P.2702.

1985a. Precambrian geology, White Lake area, Animons Lake section, District of Thunder Bay; Ontario Geological Survey, Preliminary Map P.2739.

Siragussa, G.M.,1985b. Precambrian geology, White Lake area, Theresa Lake section, District of Thunder Bay; Ontario Geological Survey, Preliminary Map P.2738.

Stow, D.A.V. 1985. Fine grained sediments in deep water: an overview of processes and facies models; Geo-Mar. Lett., v. 5 p. 17-23.

Thomson, J. E., 1931. Geology of the Heron Bay area, District of Thunder Bay; Ontario Department of Mines, Annual Report, v. 41, pt. 6, p. 34-52.

Thomson, J.E. 1931. Geology of the Heron Bay Area, District of Thunder Bay; Ontario Department of Mines, Annual Report, v. 40.

Thomson, J.E., 1933. Geology of the Heron Bay-White Lake Area, District of Thunder Bay; Ontario Department of Mines, Annual Report, v 41.

Thomson, K., 1985. Sedimentology of the Hemlo Area; uncompleted M.Sc. thesis, Lakehead University, Thunder Bay, Ontario.

Thomson, M. and Walsh, J.N. 1989. Inductivly coupled plasma spectrometry. Chapman and Hill, New York, p. 315.

Valliant, R.I. 1985. The LAC discoveries: The geology of the Hemlo pyritic gold deposit in light of the Bousquet and Doyon examples; Canadian Mining Journal, v. 106, no. 5 p. 39-47.

Valliant, R.I. et al. 1985. Field guide to geological setting of LAC Minerals Ltd. Pyritic gold orebodies, Hemlo, Ontario; in Gold and copper-zinc metallogeny within metamorphosed greenstone terrain; Hemlo-Manitouwadge-Winston Lake, Ontario, Canada; Joint Publication of the Geological Association of Canada and the Canadian Institute of Mining and Metallurgy, p. 47-57.

Walker, J.W.R., 1967. Geology of the Jackfish-Middleton area, District of Thunder Bay; Ontario Department of Mines, Geological Report 50, 41p.

Walker, R.G. 1978. Deepwater sandatone facies and ancient submarine fans: models for exploration for stratigraphic traps; AAPG Bulletin, v. 62, p 932-966.

Williams, H.R. 1987. Structural studies in the Wabigoon and Quetico Subprovinces; Ontario Geological Survey, Open File Report 5668, 163p.

Williams, H.R. 1989. Geological Studies in the Wabigoon, Quetico and Abitibi-Wawa Suprovinces, Superior Province of Ontario, with emphasis on the structural development of the Beardmore-Geraldton Belt; Ontario Geological Survey Open File Report 5724.

1990. Subprovince accretion tectonics in the south-central Superior Province; Canadian Journal of Earth Science, v 27.

Zaleski, , E., Peterson, V.L., and van Breeman, O. 1995. Geological and age relationships of the margins of the Manitouwadge greenstone belt and the Wawa-Quetico subprovince boundary, northwestern Ontario; in Current Research, 1995-C, Geological Survey of Canada, p.35-44.

# APPENDIX A - GHIBAUDO'S FACIES CLASSIFICATION

Table 2. The names and letter-codes used for the facies and subfacies distinguished in the present review.

| | |
|---|---|
| Facies G (gravel beds) | |
| mG: | massive gravel |
| xG: | cross-stratified gravel |
| sG: | plane-stratified gravel |
| gG: | graded gravel |
| gsG: | graded to plane-stratified gravel |
| Facies GS (gravel–sand couplets) | |
| gGS: | graded gravel–sand couplet |
| gxGS: | graded to cross-stratified gravel–sand couplet |
| gsGS: | graded to plane-stratified gravel–sand couplet |
| glGS: | graded to laminated gravel–sand couplet |
| gsxGS: | graded to plane-stratified to cross-stratified gravel–sand couplet |
| gslGS: | graded to plane-stratified to laminated gravel–sand couplet |
| Facies GyS (gravelly sand beds) | |
| mGyS: | massive gravelly sand |
| xGyS: | cross-stratified gravelly sand |
| gGyS: | graded gravelly sand |
| gxGyS: | graded to cross-stratified gravelly sand |
| gsGyS: | graded to plane-stratified gravelly sand |
| glGyS: | graded to laminated gravelly sand |
| gsxGyS: | graded to plane-stratified to cross-stratified gravelly sand |
| gslGyS: | graded to plane-stratified to laminated gravelly sand |
| sGyS: | plane-stratified gravelly sand |
| sxGyS: | plane-stratified to cross-stratified gravelly sand |
| slGyS: | plane-stratified to laminated gravelly sand |
| Facies S (sand beds) | |
| mS: | massive sand |
| xS: | cross-stratified sand |
| gS: | graded sand |
| gxS: | graded to cross-stratified sand |
| gsS: | graded to plane-stratified sand |
| glS: | graded to laminated sand |
| gsxS: | graded to plane-stratified to cross-stratified sand |
| gslS: | graded to plane-stratified to laminated sand |
| sS: | plane-stratified sand |
| sxS: | plane-stratified to cross-stratified sand |
| slS: | plane-stratified to laminated sand |
| Facies SM (sand–mud couplets) | |
| gSM: | graded sand–mud couplet |
| glSM: | graded to laminated sand–mud couplet |
| lSM: | laminated sand–mud couplet |
| xSM: | cross-stratified sand–mud couplet |
| tgSM: | thin-bedded, graded sand–mud couplet |
| trSM: | thin-bedded, rippled sand–mud couplet |
| Facies MS (mud–sand couplets) | |
| glMS: | graded to laminated mud–sand couplet |
| lMS: | laminated mud–sand couplet |
| Facies TM (silt–mud couplets) | |
| lTM: | laminated silt–mud couplet |
| gTM: | graded silt–mud couplet |
| Facies MT (mud–silt couplets) | |
| lMT: | laminated mud–silt couplet |
| gMT: | graded mud–silt couplet |
| Facies M (mud beds) | |
| lgM: | laminated to graded mud |
| gM: | graded mud |
| Facies MyS (muddy sand beds) | |
| mMyS: | massive muddy sand |
| gMyS: | graded muddy sands |
| Facies SyM (sandy mud beds) | |
| mSyM: | massive sandy mud |
| gSyM: | graded sandy mud |
| Facies MyG (muddy gravel beds) | |
| mMyG: | massive muddy gravel |
| gMyG: | graded muddy gravel |
| Facies GyM (gravelly mud beds) | |
| mGyM: | massive gravelly mud |
| gGyM: | graded gravelly mud |

**(Ghibaudo, 1992)**

# APPENDIX B - McKELLAR HARBOUR SECTION

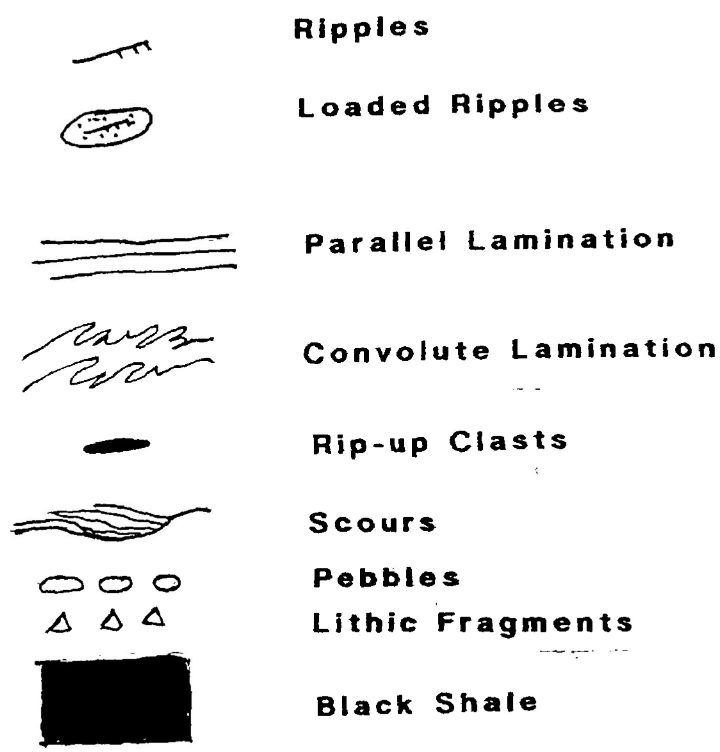


FIGURE B-1: Legend for Stratigraphic Sections

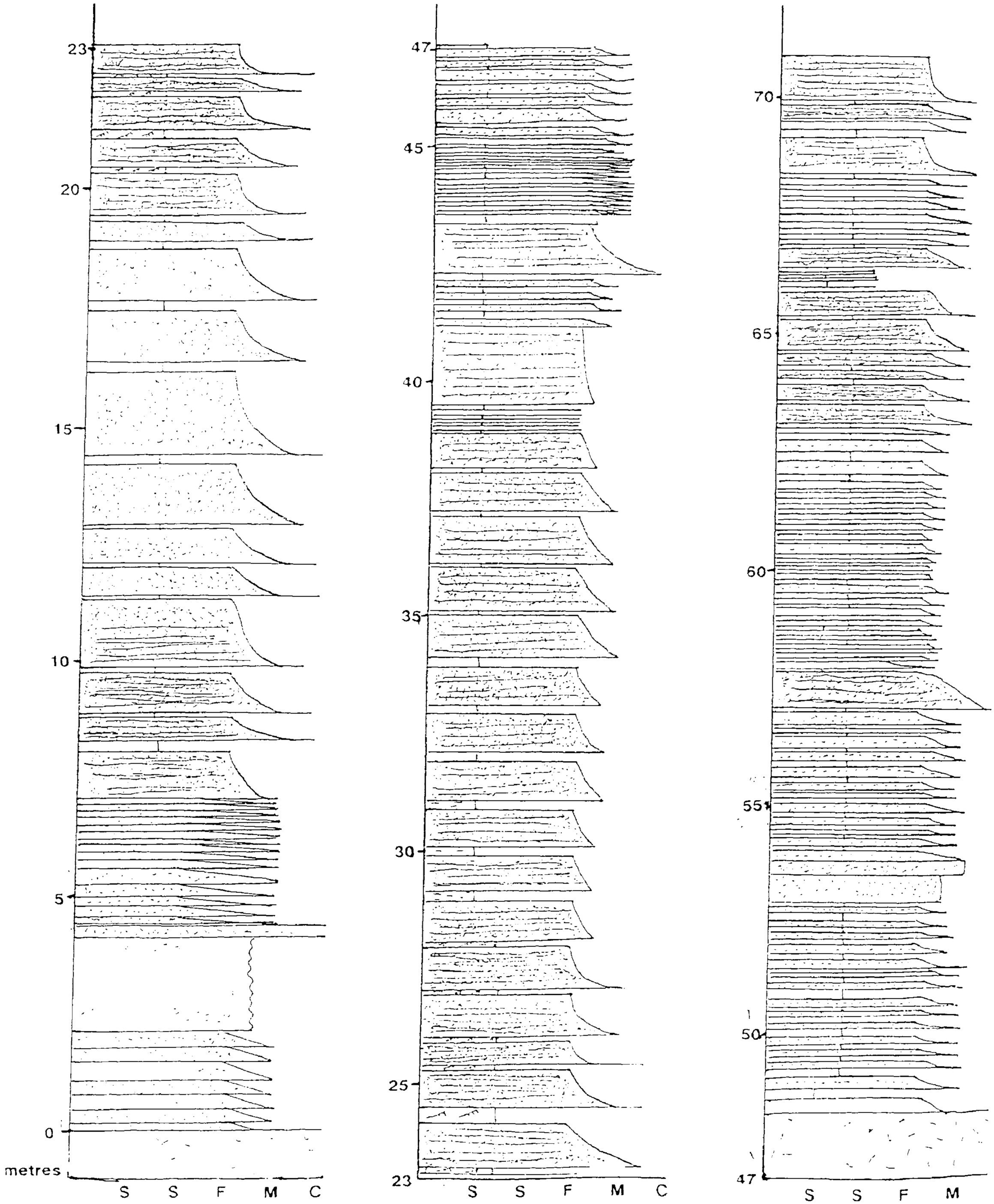
metres
0
5
10
15
20
23
25
30
35
40
45
47
50
55
60
65
70
S S F M C
S S F M C
S S F M

# McKELLAR HARBOUR SECTION

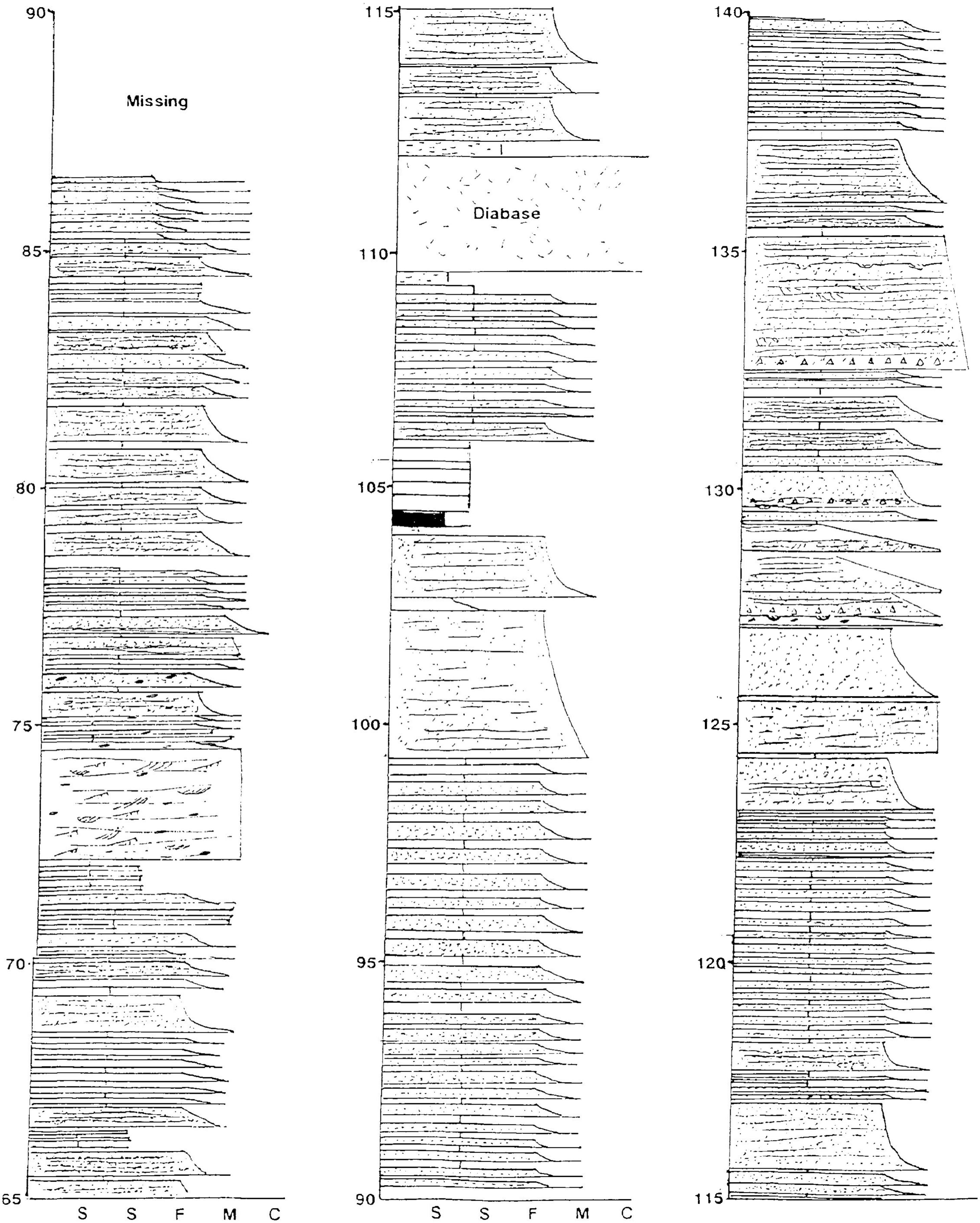

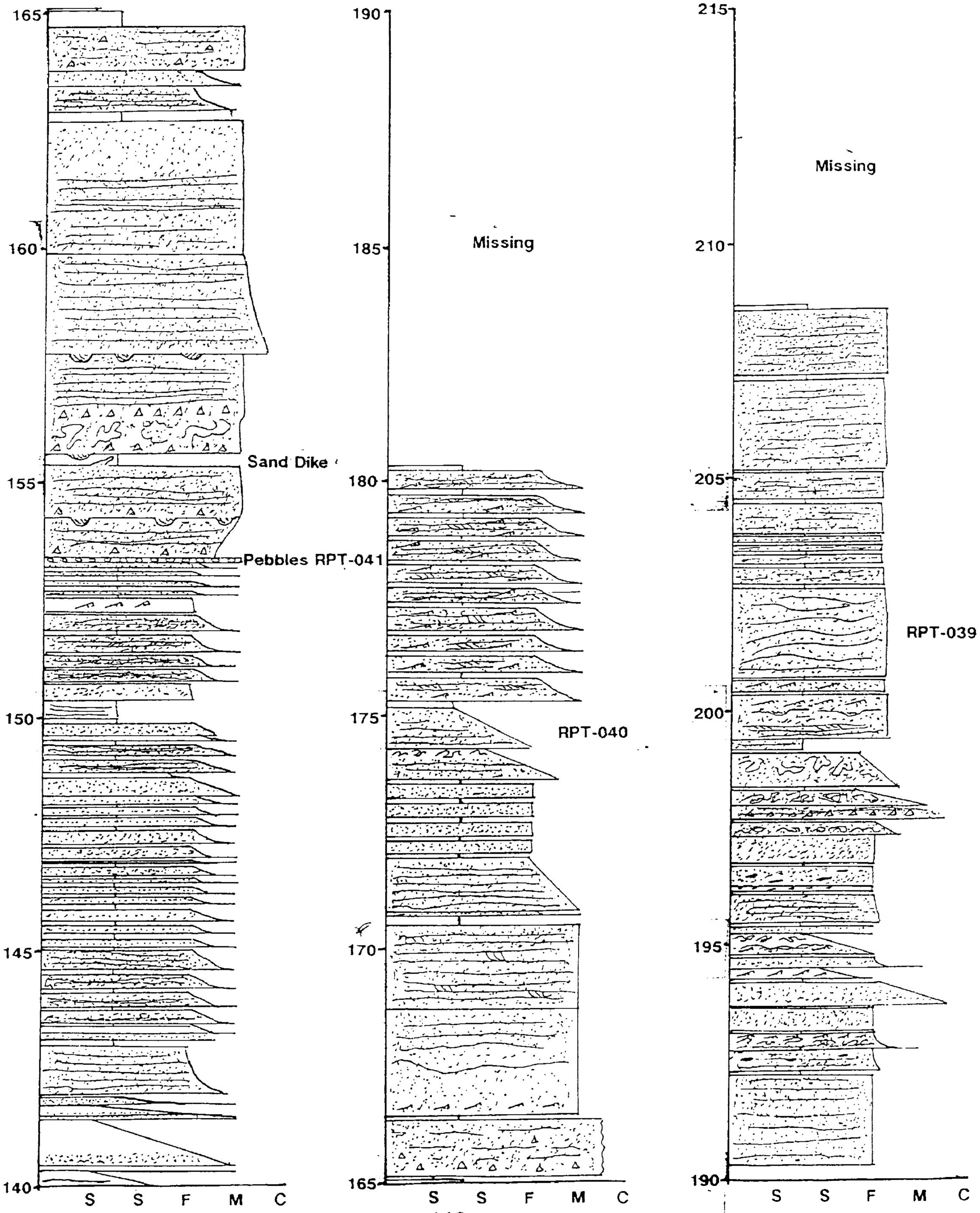
165
160
155
150
145
140
Sand Dike
Pebbles RPT-041
S S F M C
190
185
180
175
170
165
Missing
RPT-040
S S F M C
215
210
205
200
195
190
Missing
RPT-039
S S F M C

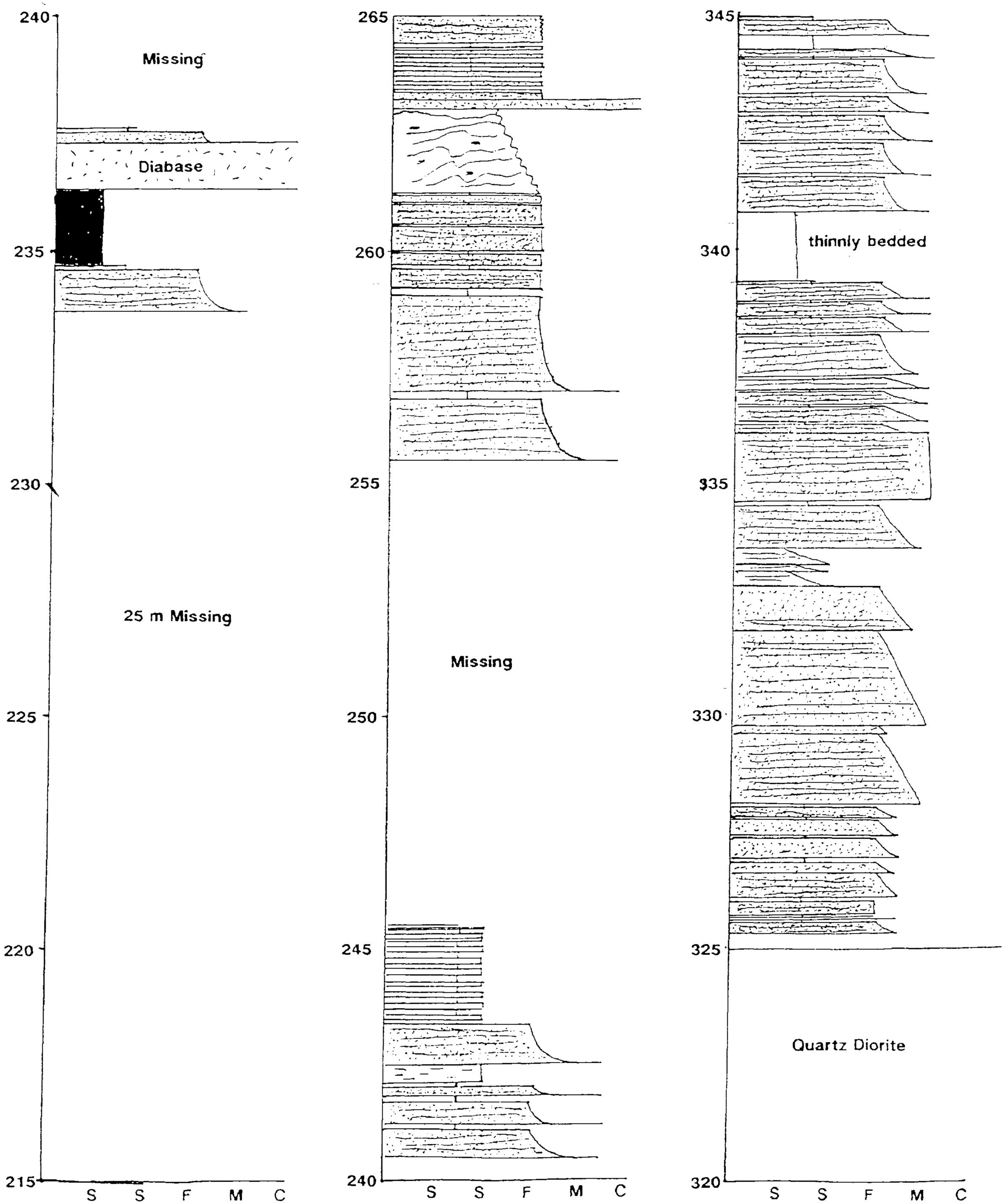
240
Missing
Diabase
235
230
25 m Missing
225
220
215
S S F M C
265
260
255
Missing
250
245
240
S S F M C
345
340
thinnly bedded
335
330
325
Quartz Diorite
320
S S F M C

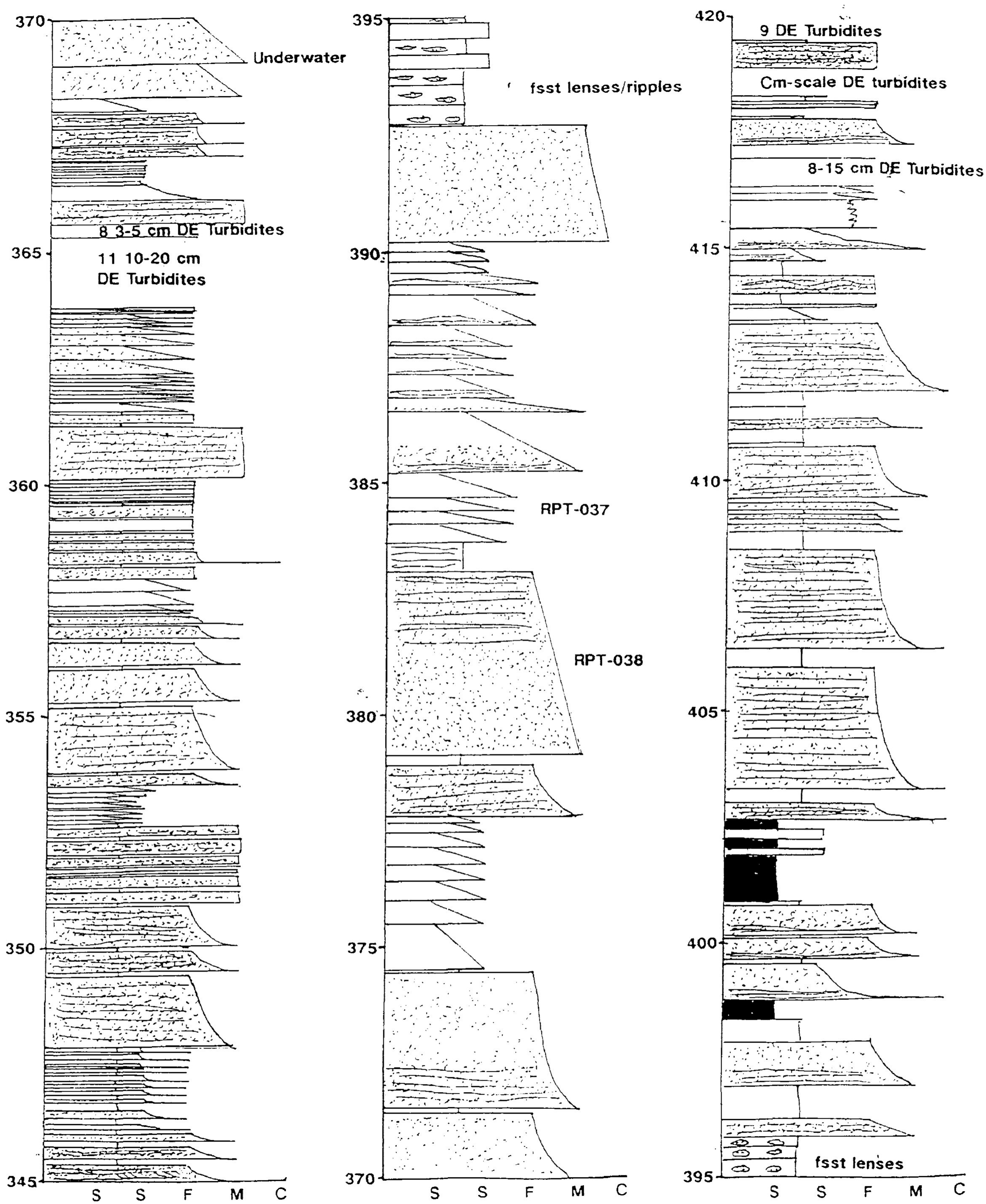
370
Underwater
8 3-5 cm DE Turbidites
365
11 10-20 cm
DE Turbidites
360
355
350
345
S S F M C
395
fsst lenses/ripples
390
385
RPT-037
RPT-038
380
375
370
S S F M C
420
9 DE Turbidites
Cm-scale DE turbidites
8-15 cm DE Turbidites
415
410
405
400
fsst lenses
395
S S F M C

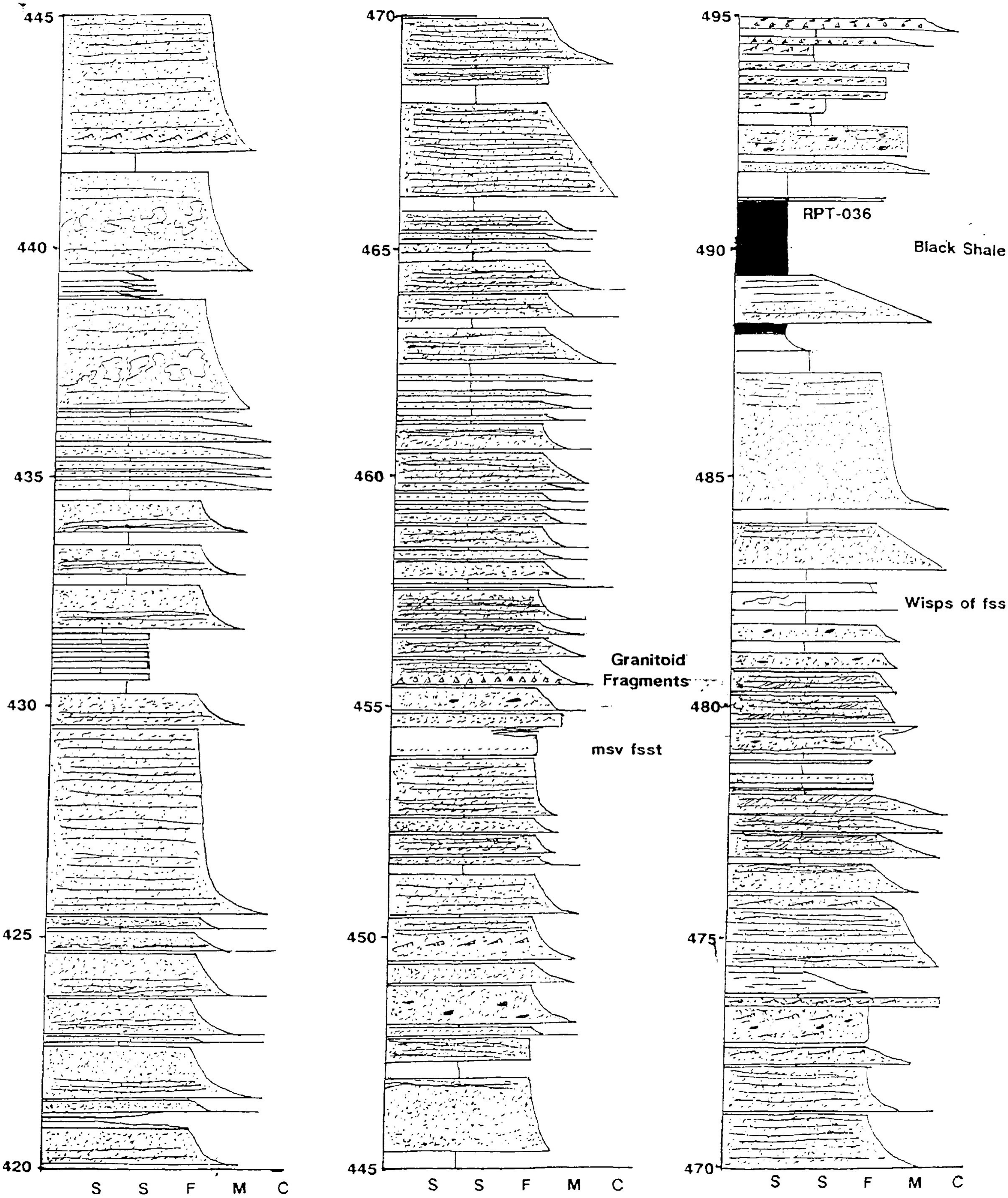
445
440
435
430
425
420
S S F M C
470
465
460
455
450
445
Granitoid Fragments
msv fsst
S S F M C
495
490
485
480
475
470
RPT-036
Black Shale
Wisps of fss
S S F M C

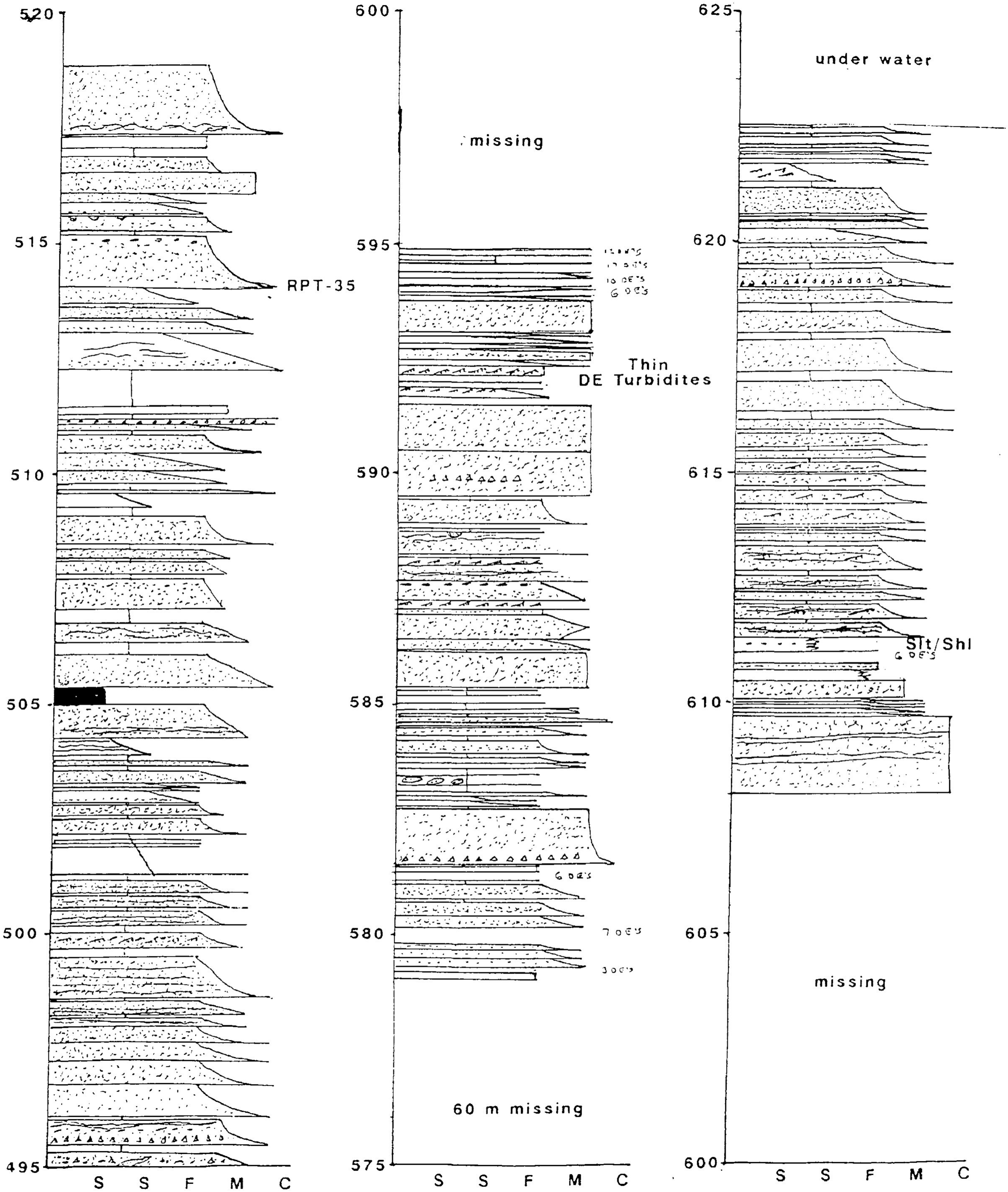
520
515
510
505
500
495
RPT-35
S S F M C
600
595
590
585
580
575
missing
Thin
DE Turbidites
60 m missing
S S F M C
625
620
615
610
605
600
under water
Slt/Shl
missing
S S F M C

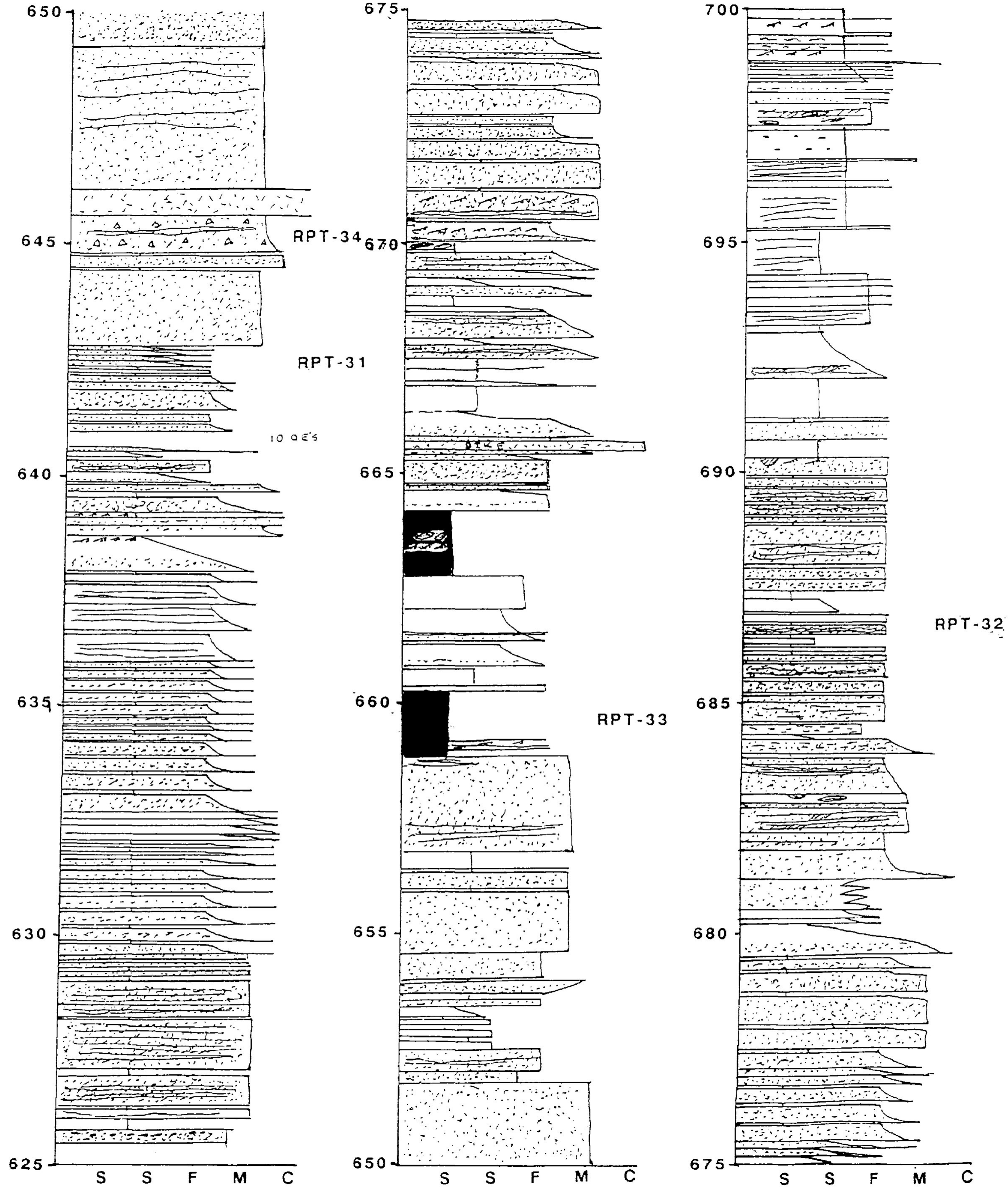
650
645
RPT-34
RPT-31
10 QE's
640
635
630
625
S S F M C
675
670
665
DIKE
660
RPT-33
655
650
S S F M C
700
695
690
RPT-32
685
680
675
S S F M C

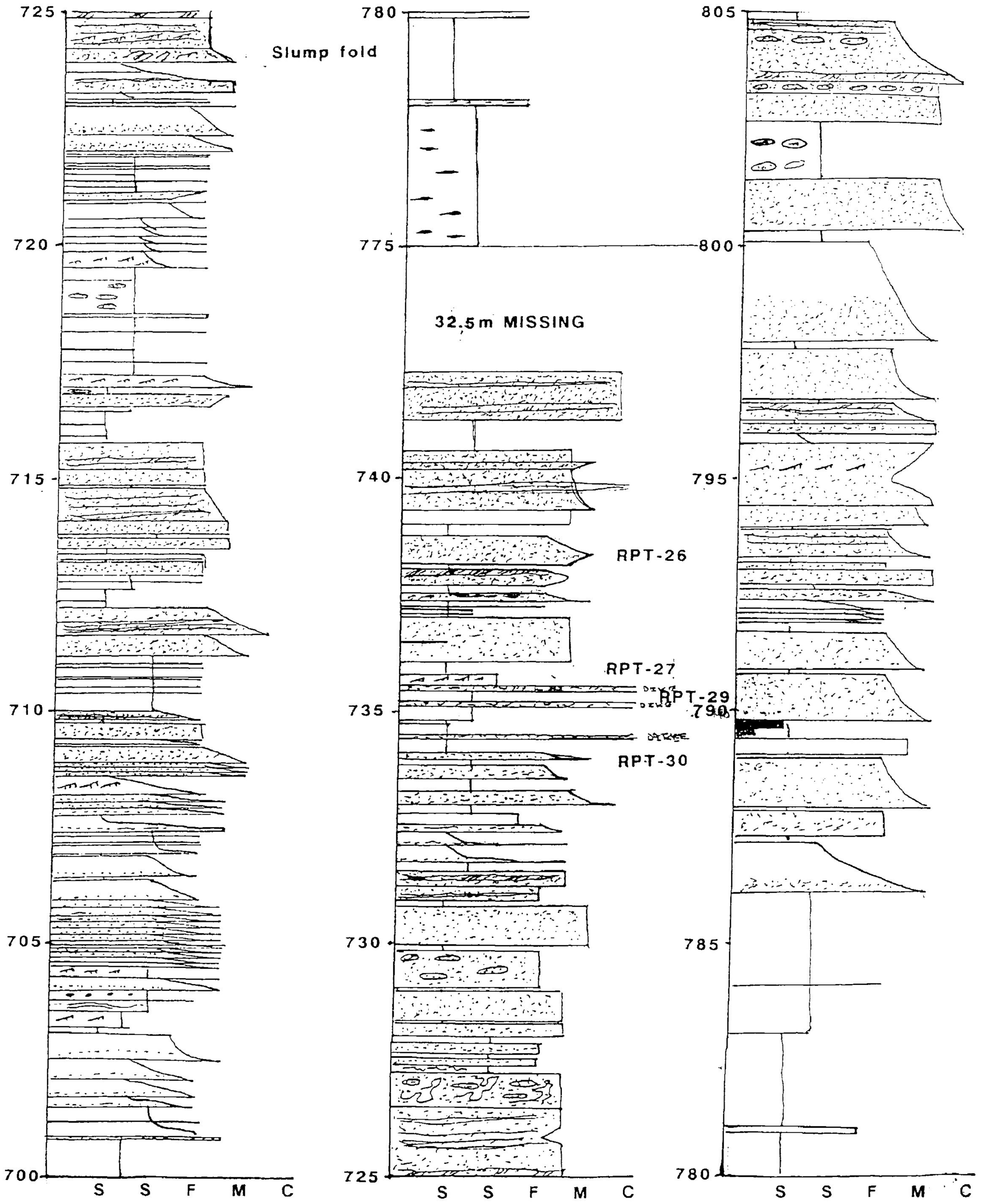
725
720
715
710
705
700
Slump fold
780
775
32.5m MISSING
740
735
730
725
RPT-26
RPT-27
RPT-29
RPT-30
805
800
795
790
785
780
S S F M C
S S F M C
S S F M C

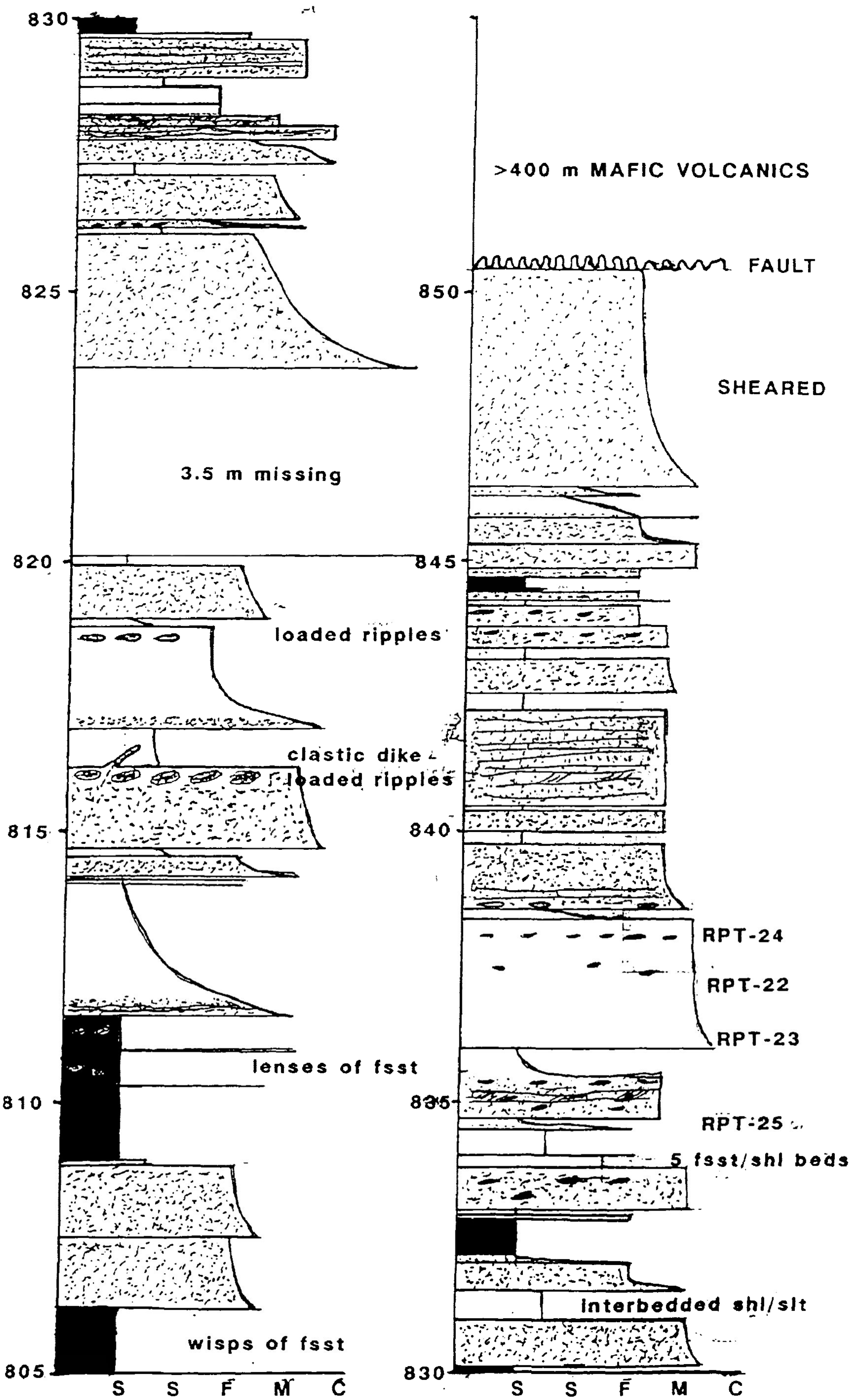
830
825
3.5 m missing
820
loaded ripples
clastic dike
loaded ripples
815
lenses of fsst
810
wisps of fsst
805
S S F M C
>400 m MAFIC VOLCANICS
FAULT
850
SHEARED
845
840
RPT-24
RPT-22
RPT-23
835
RPT-25
5 fsst/shl beds
interbedded shl/slt
830
S S F M C

# APPENDIX C - METHODOLOGIES AND DATA SET

The samples collected for this study were analysed in the Lakehead University Department of Chemistry Analytical Laboratory using inductively coupled plasma atomic emission spectrometry (ICP-AES). ICP-AES can be used for the determination of all elements except argon (Thompson and Walsh, 1989), however there are some limitations. Unstable elements require special facilities for handling the radioactive fume from the plasma, and the determination of fluorine, chlorine, and bromine requires special optics for the transmission of the very short wavelengths produced from these elements. Also a few elements such as nitrogen and rubidium have poor sensitivities in relation to other analytical techniques, and to the concentrations normally encountered (Thompson and Walsh, 1989). Despite these complexities, ICP-AES, when backed up with a dedicated computer and proper calibration, remains a powerful analytical technique for the geologist. The techniques used to prepare samples for analyses using ICP-AES are best outlined by Church (1981).

Table C-1 shows the data set of oxide chemistry and element ratios used to produce the graphs included as Appendix D. Table C-2 presents data from the Beardmore-Geraldton and Quetico terranes (Fralick and Kronberg, in press).

Figures C-1 and C-2 show the sample locations for the McKellar Harbour and Heron Bay - Hemlo Areas. Figure C-3 shows Fralick and Kronberg's sample locations.

# TABLE C-1: GEOCHEMICAL DATA

| | OXIDE | | SiO2 | TiO2 | Al2O3 | Fe2O3 | MnO | MgO | CaO | Na2O | K2O | P2O5 | CO2 * | H2O | TOTAL | Rb | Sr | Y | Zr | Nb | Ba | TiO2X100/ | TiO2/NbX100 | ZrX100,000/ | TiO2/Zr | YX10,000/Al2O3 |
|---|---|---|---|---|---|---|---|---|---|---|---|---|---|---|---|---|---|---|---|---|---|---|---|---|---|---|
| SAMPLE NO. | ROCK TYPE | LOCATION | | | | | | | | | | | | | | | | | | | | | | | | |
| RPT 001 | sat | Schrieber | 72.86 | 0.48 | 14.27 | 3.69 | 0.08 | 1.64 | 2.11 | 5.32 | 0.82 | 0.09 | 0.73 | 1.26 | 103.36 | 16 | 356 | 6 | 70 | 4 | 221 | 3.36 | 1.20 | 53.26 | 83.16 | 3.50 |
| RPT 002 | shl | Schrieber | 73.58 | 0.13 | 12.58 | 1.60 | 0.02 | 0.69 | 0.17 | 1.39 | 5.73 | 0.06 | 12.80 | 1.71 | 110.45 | 109 | 113 | 11 | 126 | 3 | 645 | 1.03 | 0.43 | 100.16 | 10.32 | 8.74 |
| RPT 003 | sat | Schrieber | 56.11 | 1.30 | 15.75 | 10.53 | 0.23 | 5.83 | 4.07 | 3.36 | 1.04 | 0.14 | 1.21 | 1.82 | 100.19 | 24 | 193 | 18 | 114 | 11 | 238 | 8.25 | 1.18 | 72.38 | 114.04 | 11.43 |
| RPT 004 | shl | Schrieber | 59.42 | 0.71 | 16.64 | 7.42 | 0.13 | 3.86 | 1.41 | 2.76 | 2.82 | 0.16 | 0.70 | 3.42 | 99.43 | 84 | 216 | 15 | 120 | 7 | 709 | 4.27 | 1.01 | 72.12 | 59.17 | 9.01 |
| RPT 005 | sat | Schrieber | 61.86 | 0.54 | 14.94 | 4.84 | 0.06 | 3.01 | 2.11 | 4.42 | 1.77 | 0.16 | 0.51 | 2.25 | 96.40 | 41 | 444 | 11 | 106 | 5 | 560 | 3.61 | 1.08 | 70.96 | 50.94 | 7.36 |
| RPT 006 | sat | Schrieber | 60.87 | 0.59 | 14.84 | 5.38 | 0.09 | 2.85 | 4.62 | 3.87 | 1.89 | 0.17 | 2.27 | 2.16 | 99.90 | 41 | 538 | 12 | 121 | 6 | 696 | 3.96 | 0.98 | 80.99 | 48.76 | 8.03 |
| RPT 008 | sat | Schrieber | 71.61 | 0.32 | 13.87 | 3.13 | 0.06 | 1.40 | 3.94 | 1.70 | 2.30 | 0.09 | 0.44 | 1.20 | 100.01 | 59 | 182 | 5 | 50 | 3 | 537 | 2.31 | 1.07 | 42.64 | 64.24 | 3.60 |
| RPT 010 | sat | Hwy 17 | 60.66 | 0.57 | 16.45 | 6.32 | 0.06 | 3.65 | 1.56 | 3.74 | 2.11 | 0.17 | 1.17 | 2.97 | 99.45 | 58 | 255 | 12 | 118 | 5 | 572 | 3.47 | 1.14 | 71.73 | 48.31 | 7.29 |
| RPT 011 | sat | Hwy 17 | 62.74 | 0.57 | 14.79 | 5.10 | 0.07 | 3.25 | 2.99 | 4.27 | 1.37 | 0.21 | 2.20 | 2.34 | 99.90 | 24 | 328 | 11 | 105 | 5 | 450 | 3.86 | 1.14 | 70.99 | 54.29 | 7.44 |
| RPT 012 | sat | Hwy 17 | 61.78 | 0.54 | 15.62 | 4.92 | 0.08 | 2.25 | 3.86 | 3.72 | 2.32 | 0.20 | 3.12 | 1.82 | 100.03 | 67 | 203 | 13 | 113 | 5 | 609 | 3.46 | 1.08 | 72.34 | 47.79 | 8.32 |
| RPT 013 | shl | Hwy 17 | 63.36 | 0.60 | 15.04 | 5.19 | 0.08 | 3.26 | 2.16 | 5.47 | 0.94 | 0.17 | 1.39 | 2.43 | 100.09 | | 372 | 12 | 110 | 6 | 344 | 3.99 | 1.00 | 73.14 | 54.55 | 7.98 |
| RPT 014 | sat | Hwy 17 | 63.28 | 0.60 | 14.60 | 5.70 | 0.08 | 3.36 | 2.48 | 4.68 | 1.57 | 0.17 | 1.32 | 2.07 | 100.17 | 50 | 420 | 11 | 119 | 5 | 464 | 4.05 | 1.20 | 80.41 | 50.42 | 7.43 |
| RPT 015 | shl | Hwy 17 | 62.14 | 0.72 | 18.02 | 6.43 | 0.08 | 3.83 | 0.94 | 3.53 | 3.47 | 0.19 | 0.11 | 3.24 | 102.70 | 101 | 240 | 13 | 130 | 6 | 1174 | 4.00 | 1.20 | 72.14 | 56.38 | 7.21 |
| RPT 022 | sat | Hwy 17 | 60.79 | 0.61 | 14.10 | 5.92 | 0.09 | 2.70 | 4.33 | 3.91 | 1.90 | 0.16 | 2.57 | 1.89 | 98.97 | 56 | 203 | 10 | 105 | 7 | 439 | 4.33 | 0.87 | 74.47 | 58.10 | 11.35 |
| RPT 023 | sat | Hwy 17 | 61.14 | 0.67 | 15.02 | 6.79 | 0.10 | 3.36 | 2.07 | 3.75 | 1.63 | 0.17 | 0.77 | 2.34 | 97.81 | 45 | 303 | 13 | 116 | 7 | 430 | 4.46 | 0.96 | 78.56 | 56.78 | 8.60 |
| RPT 024 | sit | McKellar | 56.06 | 0.72 | 17.80 | 7.32 | 0.09 | 3.73 | 1.96 | 2.60 | 3.30 | 0.20 | 0.62 | 3.06 | 98.10 | 89 | 270 | 10 | 128 | 8 | 1063 | 4.04 | 0.90 | 71.91 | 56.25 | 8.99 |
| RPT 025 | sat | McKellar | 56.20 | 0.68 | 16.39 | 5.78 | 0.11 | 2.91 | 5.21 | 3.34 | 2.63 | 0.18 | 2.03 | 2.16 | 96.52 | 78 | 308 | 18 | 118 | 8 | 648 | 4.15 | 0.85 | 72.00 | 57.63 | 10.98 |
| RPT 026 | sat | McKellar | 60.58 | 0.62 | 16.36 | 6.07 | 0.08 | 3.45 | 1.90 | 4.56 | 1.42 | 0.19 | | 2.16 | 97.68 | 34 | 478 | 13 | 108 | 6 | 433 | 3.79 | 1.03 | 66.06 | 57.41 | 7.95 |
| RPT 027 | shl | McKellar | 59.74 | 0.76 | 17.15 | 7.38 | 0.10 | 3.46 | 1.06 | 2.17 | 3.40 | 0.19 | 0.29 | 2.79 | 98.49 | 89 | 250 | 14 | 105 | 7 | 853 | 4.43 | 1.09 | 61.22 | 72.38 | 8.16 |
| RPT 030 | shl | McKellar | 59.61 | 0.72 | 16.92 | 7.51 | 0.08 | 3.63 | 0.96 | 2.97 | 2.72 | 0.16 | 1.69 | 2.70 | 99.67 | 78 | 203 | 13 | 102 | 7 | 684 | 4.26 | 1.03 | 60.28 | 70.59 | 7.68 |
| RPT 031 | sat | McKellar | 60.58 | 0.57 | 15.24 | 5.60 | 0.07 | 2.06 | 2.74 | 3.89 | 1.47 | 0.19 | 0.28 | 2.25 | 96.12 | 34 | 480 | 11 | 69 | 6 | 429 | 3.74 | 0.95 | 46.28 | 82.61 | 7.22 |
| RPT 032 | shl | McKellar | 59.12 | 0.77 | 17.70 | 7.94 | 0.09 | 3.81 | 1.46 | 2.70 | 3.00 | 0.26 | 0.26 | 3.06 | 100.23 | 78 | 105 | 17 | 201 | 8 | 755 | 4.35 | 0.90 | 113.56 | 38.31 | 9.60 |
| RPT 034 | sat | McKellar | 63.10 | 0.59 | 15.61 | 5.05 | 0.09 | 3.30 | 3.85 | 3.83 | 1.43 | 0.17 | 0.73 | 1.98 | 100.33 | 34 | 473 | 12 | 76 | 6 | 490 | 3.78 | 0.98 | 48.69 | 77.63 | 7.69 |
| RPT 035 | sat | McKellar | 61.84 | 0.57 | 15.05 | 5.59 | 0.09 | 3.36 | 3.04 | 4.24 | 1.32 | 0.29 | 1.03 | 2.25 | 98.67 | 34 | 382 | 13 | 82 | 6 | 491 | 3.79 | 0.95 | 54.49 | 69.51 | 8.64 |
| RPT 036 | shl | McKellar | 55.63 | 0.78 | 18.01 | 8.78 | 0.09 | 4.11 | 1.47 | 2.98 | 3.24 | 0.18 | 0.37 | 2.34 | 97.98 | 111 | 319 | 17 | 109 | 8 | 703 | 4.33 | 0.98 | 60.52 | 71.56 | 9.44 |
| RPT 037 | shl | McKellar | 48.23 | 0.94 | 21.87 | 10.24 | 0.10 | 5.33 | 1.04 | 1.01 | 5.14 | 0.22 | 0.37 | 4.77 | 99.20 | 155 | 68 | 22 | 161 | 10 | 969 | 4.30 | 0.94 | 73.62 | 58.39 | 10.06 |
| RPT 038 | sat | McKellar | 63.80 | 0.56 | 14.94 | 6.11 | 0.07 | 3.24 | 1.74 | 4.57 | 1.62 | 0.20 | 0.95 | 3.24 | 100.04 | 34 | 204 | 11 | 104 | 6 | 556 | 3.75 | 0.93 | 69.61 | 53.85 | 7.36 |
| RPT 039 | sat | McKellar | 62.72 | 0.62 | 15.51 | 1.99 | 0.09 | 2.99 | 2.34 | 4.13 | 1.90 | 0.18 | 0.77 | 2.07 | 95.40 | 45 | 372 | 13 | 112 | 6 | 585 | 4.00 | 1.03 | 72.21 | 55.30 | 8.38 |
| RPT 040 | shl | McKellar | 57.84 | 0.77 | 17.36 | 8.01 | 0.10 | 4.08 | 1.20 | 2.18 | 3.34 | 0.27 | 0.64 | 3.24 | 99.23 | 67 | 233 | 17 | 114 | 8 | 837 | 4.44 | 0.96 | 65.67 | 67.54 | 9.79 |
| RPT 041 | frag | McKellar | 67.10 | 0.53 | 14.04 | 4.83 | 0.07 | 2.92 | 1.58 | 3.73 | 2.39 | 0.19 | 0.07 | 1.60 | 99.26 | 56 | 424 | 11 | 80 | 5 | 600 | 3.77 | 1.00 | 56.98 | 66.25 | 7.83 |
| RPT 042 | sat | McKellar | 63.98 | 0.56 | 14.14 | 6.04 | 0.08 | 3.19 | 3.10 | 2.94 | 1.92 | 0.18 | 1.83 | 1.96 | 99.92 | 45 | 187 | 18 | 114 | 5 | 422 | 3.90 | 1.12 | 80.62 | 49.12 | 12.73 |
| RPT 043 | shl | McKellar | 56.20 | 0.69 | 17.98 | 8.54 | 0.04 | 3.69 | 1.62 | 1.46 | 4.08 | 0.17 | 1.54 | 3.15 | 99.16 | 111 | 137 | 12 | 129 | 6 | 790 | 3.84 | 1.15 | 71.75 | 53.49 | 6.67 |
| RPT 045 | sat | McKellar | 60.70 | 0.58 | 14.44 | 5.73 | 0.04 | 2.60 | 4.09 | 2.88 | 2.62 | 0.21 | 3.23 | 1.89 | 99.19 | 78 | 232 | 11 | 124 | 5 | 628 | 3.88 | 1.12 | 85.87 | 45.16 | 7.62 |
| RPT 046 | shl | McKellar | 57.38 | 0.67 | 18.13 | 8.34 | 0.06 | 4.00 | 1.07 | 2.19 | 3.30 | 0.23 | 0.95 | 3.24 | 99.60 | 89 | 205 | 13 | 147 | 6 | 653 | 3.70 | 1.12 | 81.08 | 45.58 | 7.17 |
| RPT 047 | | McKellar | 62.55 | 0.50 | 14.52 | 5.71 | 0.07 | 3.41 | 2.41 | 3.62 | 3.41 | 0.20 | 1.39 | 2.25 | 100.04 | 45 | 431 | 12 | 107 | 5 | 647 | 3.44 | 1.00 | 73.69 | 46.73 | 8.26 |
| RPT 050 | sat | Pukaskwa | 67.30 | 0.48 | 14.85 | 2.16 | 0.04 | 1.26 | 3.38 | 5.45 | 1.35 | 0.29 | 3.01 | 0.63 | 100.20 | 24 | 634 | 10 | 140 | 4 | 506 | 3.23 | 1.20 | 94.28 | 34.29 | 6.73 |
| RPT 051 | sat | Pukaskwa | 61.72 | 0.53 | 15.72 | 5.00 | 0.04 | 2.32 | 4.78 | 4.43 | 1.93 | 0.35 | 1.94 | 0.81 | 99.57 | 36 | 979 | 11 | 120 | 5 | 503 | 3.37 | 1.06 | 76.34 | 44.17 | 7.00 |
| RPT 052 | sit | Pukaskwa | 66.16 | 0.42 | 13.41 | 4.08 | 0.05 | 2.30 | 4.38 | 2.65 | 2.10 | 0.38 | 3.56 | 1.44 | 101.51 | 36 | 575 | 10 | 137 | 4 | 542 | 3.13 | 1.05 | 102.16 | 30.66 | 7.46 |
| RPT 053 | sat | Pukaskwa | 72.04 | 0.31 | 15.66 | 1.75 | 0.01 | 0.42 | 1.34 | 5.37 | 1.46 | 0.11 | 0.04 | 0.36 | 98.89 | 36 | 502 | 5 | 84 | 3 | 425 | 2.11 | 1.10 | 40.87 | 51.50 | 3.19 |
| RPT 054 | sit | Pukaskwa | 65.44 | 0.44 | 16.71 | 4.44 | 0.03 | 2.19 | 1.60 | 4.60 | 2.04 | 0.39 | 0.22 | 0.90 | 99.29 | 48 | 503 | 12 | 130 | 5 | 741 | 2.83 | 0.88 | 77.80 | 33.85 | 7.18 |
| RPT 055 | sat | Pukaskwa | 60.93 | 0.63 | 16.22 | 5.24 | 0.06 | 2.21 | 4.48 | 4.59 | 1.82 | 0.37 | 2.27 | 0.54 | 99.30 | 48 | 854 | 13 | 120 | 6 | 1115 | 3.88 | 1.06 | 73.98 | 52.50 | 8.01 |
| RPT 056 | shl | Pukaskwa | 58.60 | 0.84 | 20.61 | 1.63 | 0.01 | 0.72 | 1.12 | 3.20 | 4.07 | 0.28 | 0.88 | 1.80 | 94.40 | 60 | 302 | 9 | 194 | 6 | 783 | 3.11 | 1.07 | 94.13 | 32.90 | 4.37 |
| RPT 057 | shl | Pukaskwa | 72.97 | 0.34 | 13.46 | 4.47 | 0.02 | 1.15 | 0.92 | 2.09 | 2.34 | 0.24 | 0.73 | 1.71 | 100.44 | 48 | 214 | 7 | 107 | 3 | 775 | 2.53 | 1.13 | 79.49 | 31.78 | 5.20 |
| RWL 001 | | W L | 82.69 | 0.15 | 8.50 | 2.45 | 0.01 | 0.73 | 0.87 | 3.94 | 0.71 | 0.01 | 0.73 | 0.99 | 102.78 | | 50 | 74 | 237 | 15 | 101 | 1.58 | 0.10 | 249.47 | 6.33 | 77.80 |
| RWL 002 | | W L | 64.56 | 0.67 | 4.21 | 20.12 | 0.31 | 6.41 | 0.20 | 0.58 | 0.03 | 0.06 | 0.11 | 1.60 | 99.06 | | 3 | 12 | 202 | 5 | 13 | 15.91 | 1.34 | 479.81 | 33.17 | 28.50 |
| RWL 003 | | W L | 63.54 | 1.52 | 13.72 | 12.33 | 0.23 | 4.40 | 6.94 | 3.00 | 1.04 | 0.09 | 0.81 | 2.07 | 99.78 | 12 | 151 | 23 | 71 | 13 | 192 | 11.08 | 1.17 | 51.75 | 214.08 | 16.76 |
| RWL 004 | | W L | 67.91 | 0.74 | 11.32 | 17.33 | 1.20 | 1.99 | 2.40 | 2.02 | 0.00 | 0.15 | 0.11 | 2.25 | 98.28 | 12 | 79 | 98 | 280 | 22 | 79 | 6.71 | 0.36 | 252.05 | 26.67 | 86.57 |
| RWL 005 | | W L | 57.87 | 1.34 | 14.19 | 11.77 | 0.18 | 4.19 | 5.09 | 3.34 | 1.50 | 0.09 | 0.04 | 1.89 | 101.35 | 49 | 205 | 24 | 73 | 12 | 333 | 9.44 | 1.12 | 51.44 | 183.56 | 16.91 |
| RWL 006 | | W L | 68.12 | 0.78 | 11.31 | 8.35 | 0.09 | 1.70 | 3.77 | 3.67 | 0.93 | 0.18 | 0.18 | 0.63 | 99.61 | 12 | 103 | 109 | 391 | 25 | 138 | 6.90 | 0.31 | 345.71 | 19.95 | 96.37 |
| RWL 007 | | W L | 79.87 | 0.43 | 11.35 | 1.63 | 0.02 | 0.61 | 2.32 | 5.23 | 0.38 | 0.05 | 0.11 | 0.36 | 102.20 | | 95 | 207 | 553 | 42 | 89 | 3.79 | 0.10 | 487.22 | 7.78 | 182.38 |
| RWL 008 | | W L | 74.86 | 0.34 | 10.94 | 3.50 | 0.01 | 4.15 | 1.20 | 3.23 | 1.91 | 0.02 | 0.07 | 0.90 | 101.13 | 25 | 107 | 42 | 657 | 16 | 162 | 3.11 | 0.21 | 600.55 | 5.18 | 38.39 |
| RWL 009 | | W L | 81.90 | 0.33 | 9.97 | 1.67 | 0.01 | 1.38 | 1.22 | 4.02 | 0.30 | 0.06 | 0.04 | 0.03 | 101.59 | | 113 | 6 | 90 | 3 | 55 | 3.31 | 1.10 | 90.27 | 36.67 | 6.02 |
| RWL 010 | | W L | 81.07 | 0.13 | 9.54 | 1.40 | 0.01 | 2.77 | 1.01 | 3.23 | 0.96 | 0.00 | 0.04 | 0.63 | 100.86 | | 89 | 84 | 262 | 17 | 80 | 1.36 | 0.08 | 274.63 | 4.96 | 88.05 |
| RWL 011 | | W L | 78.26 | 0.34 | 11.12 | 3.37 | 0.02 | 1.57 | 1.24 | 4.46 | 0.34 | 0.02 | 0.15 | 1.35 | 102.24 | | 127 | 84 | 590 | 14 | 58 | 3.06 | 0.24 | 530.58 | 5.76 | 57.55 |
| RWL 012 | | W L | 81.37 | 0.31 | 10.20 | 2.26 | 0.01 | 0.94 | 1.30 | 4.22 | 0.38 | 0.02 | 0.11 | 0.45 | 101.57 | | 124 | 74 | 564 | 16 | 64 | 3.04 | 0.19 | 552.94 | 5.50 | 72.55 |

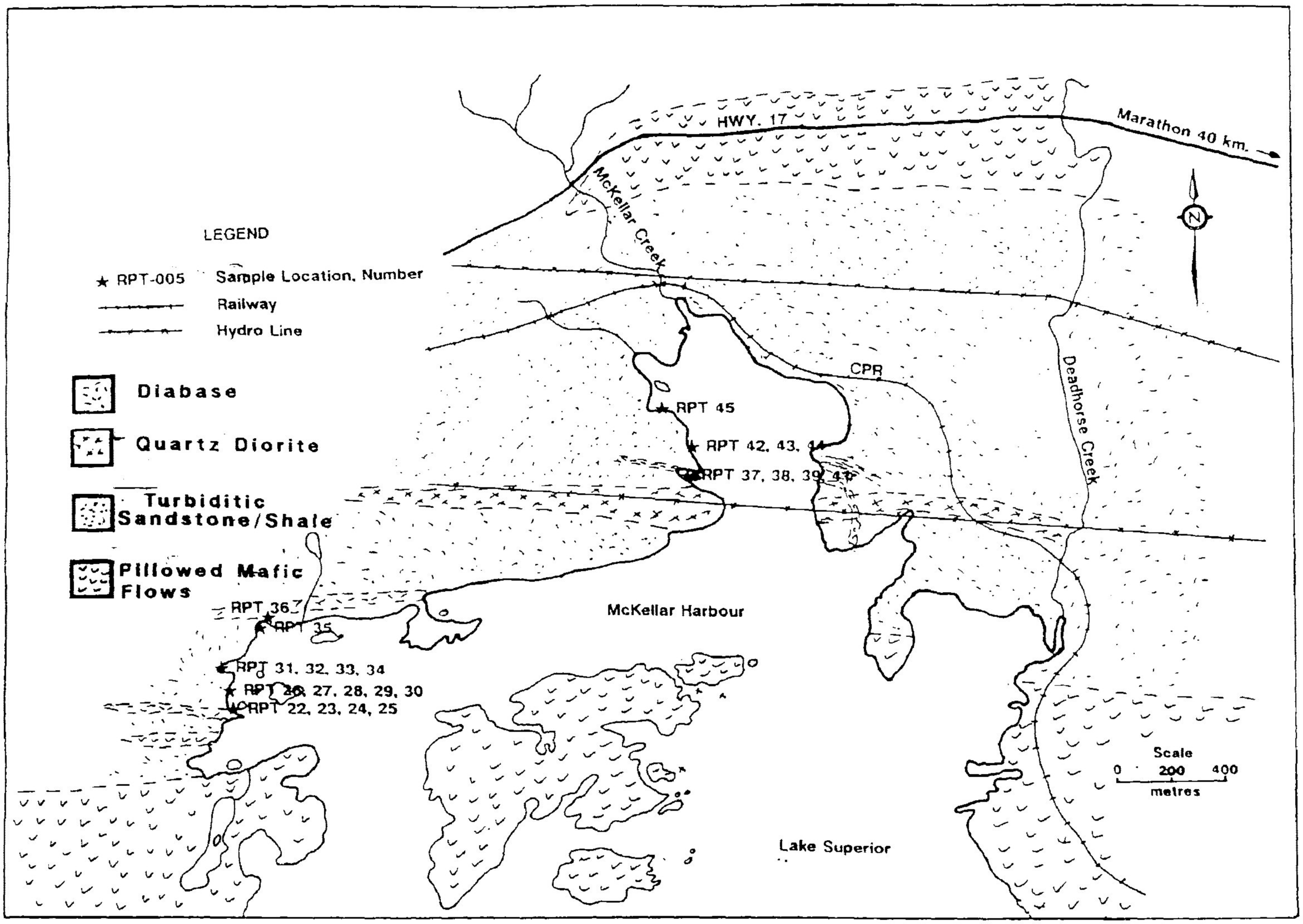


**General Geology and Sample Locations McKellar Harbour**

FIGURE C-1: General Geology and Sample Locations - McKellar Harbour.

# TABLE C-2: GEOCHEMICAL DATA.

| SAMPLE NO. | OXIDE ROCK TYPE | LOCATIO | SiO2 | TiO2 | Al2O3 | Fe2O3 | MnO | MgO | CaO | Na2O | K2O | P2O5 | CO2 * | H2O | TOTAL |
|---|---|---|---|---|---|---|---|---|---|---|---|---|---|---|---|
| H1 | shl | L. Sup | 56.59 | 0.86 | 18.31 | 4.42 | 0.14 | 4.72 | 4.58 | 6.00 | 1.10 | 0.13 | | 2.25 | 98.65 |
| H2 | slt | L. Sup | 66.06 | 0.63 | 18.70 | 5.60 | 0.09 | 2.31 | 1.96 | 2.66 | 0.06 | 0.16 | | 1.61 | 99.18 |
| H3 | sst | L. Sup | 64.70 | 0.79 | 16.88 | 8.60 | 0.18 | 4.92 | 7.38 | 3.46 | 0.30 | 0.12 | | 6.57 | 98.18 |
| H4 | sst | L. Sup | 53.15 | 0.73 | 17.68 | 8.01 | 0.14 | 4.13 | 7.46 | 3.78 | 0.82 | 0.17 | | 1.62 | 98.38 |
| H5 | sst | L. Sup | 60.14 | 0.79 | 17.20 | 6.54 | 0.10 | 3.00 | 4.18 | 5.21 | 0.36 | 0.10 | | 1.89 | 97.58 |
| H6 | sst | L. Sup | 68.54 | 0.42 | 16.65 | 3.83 | 0.08 | 1.17 | 2.10 | 5.85 | 0.85 | 0.11 | | 1.96 | 100.38 |
| H7 | sst | L. Sup | 66.33 | 0.54 | 16.54 | 5.66 | 0.10 | 2.51 | 4.06 | 5.43 | 0.18 | 0.11 | | 1.53 | 94.49 |
| H8 | sst | L. Sup | 52.38 | 0.74 | 16.90 | 8.86 | 0.08 | 4.42 | 8.72 | 5.63 | 0.15 | 0.13 | 0.07 | 1.80 | 97.87 |
| H9 | sst | L. Sup | 53.71 | 0.70 | 16.67 | 8.72 | 0.14 | 4.04 | 6.58 | 5.41 | 0.40 | 0.14 | | 2.07 | 95.49 |
| H10 | sst | L. Sup | 56.19 | 0.66 | 17.07 | 2.54 | 0.18 | 4.10 | 8.46 | 4.86 | 0.21 | 0.15 | | 1.71 | 94.40 |
| H11 | sst | L. Sup | 56.47 | 0.86 | 16.33 | 8.70 | 0.15 | 4.18 | 8.08 | 4.60 | 0.15 | 0.14 | | 1.44 | 96.63 |
| H12 | sst | L. Sup | 54.57 | 0.81 | 16.60 | 8.81 | 0.18 | 6.21 | 5.96 | 5.67 | 0.15 | 0.16 | | 1.96 | 98.03 |
| H13 | sst | L. Sup | 53.93 | 0.73 | 16.23 | 10.27 | 0.17 | 6.01 | 5.90 | 5.32 | 0.33 | 0.14 | | 2.25 | 98.05 |
| H14 | sst | L. Sup | 56.63 | 0.73 | 16.56 | 8.05 | 0.10 | 4.75 | 7.13 | 5.41 | 0.48 | 0.14 | | 1.89 | 98.92 |
| H15 | sst | L. Sup | 56.54 | 0.75 | 16.26 | 8.36 | 0.15 | 3.87 | 7.48 | 4.37 | 0.26 | 0.15 | | 1.96 | 98.20 |
| H18 | slt | L. Sup | 61.64 | 0.62 | 16.61 | 4.53 | 0.08 | 1.98 | 4.92 | 3.06 | 1.36 | 0.14 | 0.33 | 1.71 | 94.73 |
| H20 | slt | L. Sup | 68.64 | 0.46 | 14.48 | 2.39 | 0.02 | 0.84 | 1.17 | 4.30 | 2.21 | 0.12 | 0.40 | 1.44 | 96.13 |
| H21 | slt | L. Sup | 56.07 | 0.36 | 14.78 | 4.50 | 0.07 | 2.51 | 12.77 | 3.96 | 2.24 | 0.12 | 0.40 | 1.08 | 96.37 |
| H22 | slt | L. Sup | 57.60 | 0.68 | 17.06 | 8.14 | 0.08 | 2.08 | 4.67 | 3.66 | 2.50 | 0.27 | 0.30 | 2.79 | 97.14 |
| H24 | slt | L. Sup | 56.67 | 0.78 | 18.12 | 7.62 | 0.11 | 3.32 | 2.67 | 4.08 | 2.67 | 0.24 | 0.15 | 2.34 | 96.09 |
| H25 | slt | L. Sup | 49.06 | 1.06 | 18.14 | 11.93 | 0.13 | 4.71 | 3.87 | 3.06 | 3.01 | 0.30 | | 0.90 | 96.29 |
| H28 | slt | L. Sup | 56.26 | 0.82 | 17.18 | 3.74 | 0.15 | 4.13 | 6.68 | 2.67 | 2.21 | 0.26 | 0.12 | 4.05 | 94.10 |
| H31 | slt | Puk | 67.54 | 0.41 | 17.48 | 2.68 | 0.01 | 0.97 | 6.66 | 2.77 | 2.86 | 0.13 | 0.76 | 1.53 | 96.67 |
| H33 | slt | Puk | 70.60 | 0.40 | 17.04 | 3.30 | 0.03 | 1.29 | 2.13 | 2.81 | 2.08 | 0.15 | | 1.53 | 99.82 |
| H38 | gm | | 71.14 | 0.66 | 10.90 | 8.88 | 0.14 | 1.19 | 0.03 | 0.66 | 2.43 | 0.07 | | 2.81 | 96.90 |
| H41 | slt | | 60.64 | 0.60 | 16.44 | 5.44 | 0.01 | 0.64 | 2.39 | 3.95 | 1.43 | 0.13 | 0.42 | 0.90 | 100.47 |
| H53 | sst | Amwn | 66.42 | 0.54 | 17.37 | 4.06 | 0.04 | 1.80 | 3.89 | 4.91 | 1.49 | 0.19 | | 0.63 | 100.77 |
| H54 | sst | Amwn | 67.32 | 0.48 | 16.17 | 3.64 | 0.06 | 2.36 | 3.28 | 6.01 | 1.64 | 0.17 | | 1.28 | 100.70 |
| H57 | shl | Hendo | 56.18 | 0.90 | 16.99 | 10.80 | 0.26 | 2.10 | 1.06 | 2.75 | 1.14 | 0.14 | | 2.79 | 101.13 |
| H58 | shl | Hendo | 62.41 | 1.09 | 18.30 | 4.15 | 0.22 | 1.63 | 2.87 | 3.86 | 1.72 | 0.14 | | 2.70 | 101.18 |
| H59 | slt | Hendo | 64.02 | 0.61 | 17.78 | 5.06 | 0.06 | 1.80 | 2.19 | 5.06 | 2.11 | 0.28 | | 1.53 | 99.82 |
| H60 | sst | Hendo | 64.68 | 0.47 | 15.38 | 3.48 | 0.11 | 1.20 | 5.67 | 6.00 | 1.02 | 0.17 | 0.05 | 1.35 | 97.71 |
| H61 | sst | Hendo | 64.74 | 0.68 | 16.00 | 4.74 | 0.06 | 2.06 | 3.87 | 4.66 | 2.63 | 0.26 | 0.02 | 0.81 | 98.71 |
| H62 | slt | Hendo | 61.82 | 0.76 | 17.41 | 6.46 | 0.08 | 3.26 | 1.84 | 2.99 | 0.84 | 0.17 | | 1.08 | 95.42 |
| H63 | shl | Hendo | 58.06 | 0.82 | 17.76 | 8.79 | 0.06 | 4.17 | 1.61 | 2.01 | 2.04 | 0.11 | | 1.71 | 97.21 |
| H68 | shl | Hendo | 68.04 | 0.77 | 18.64 | 6.21 | 0.04 | 4.40 | 3.02 | 3.46 | 2.97 | 0.14 | | 1.63 | 100.70 |
| H71 | sst | Hendo | 73.17 | 0.61 | 14.93 | 4.43 | 0.04 | 1.15 | 2.38 | 2.82 | 3.09 | 0.11 | | 1.06 | 101.45 |
| H73 | sst | Hendo | 64.83 | 0.66 | 17.15 | 4.63 | 0.04 | 2.03 | 3.18 | 4.47 | 2.42 | 0.27 | | 0.90 | 101.26 |
| H74 | sst | Hendo | 58.51 | 0.66 | 16.63 | 6.66 | 0.06 | 3.82 | 4.33 | 7.03 | 3.51 | 0.34 | | 0.81 | 101.25 |
| H75 | sst | Hendo | 63.36 | 0.73 | 17.12 | 6.44 | 0.09 | 2.80 | 3.62 | 3.86 | 3.07 | 0.29 | | 0.90 | 100.39 |

| SAMPLE NO. | Rb | Sr | Y | Zr | Nb | Ba | TiO2X100/ | TiO2/NbX1000 | ZrX100,000/Al2O3 | TiO2/Zr | YX10,000/Al2O3 |
|---|---|---|---|---|---|---|---|---|---|---|---|
| H1 | 24 | 323 | 14 | 96 | 9 | 437 | 3.99 | 0.72 | 58.85 | 86.42 | 8.59 |
| H2 | 23 | 494 | 23 | 133 | 13 | 393 | 3.77 | 0.48 | 78.64 | 47.37 | 13.77 |
| H3 | 1 | 402 | 28 | 83 | 7 | 634 | 4.68 | 1.13 | 49.17 | 96.15 | 16.60 |
| H4 | 8 | 462 | 18 | 85 | 10 | 203 | 4.15 | 0.73 | 48.36 | 86.88 | 10.24 |
| H5 | 5 | 365 | 15 | 114 | 13 | 283 | 4.07 | 0.54 | 66.28 | 61.40 | 8.72 |
| H6 | 13 | 209 | 12 | 115 | 15 | | 2.52 | 0.28 | 69.07 | 36.52 | 7.21 |
| H7 | 11 | 265 | 22 | 115 | 9 | | 3.28 | 0.60 | 70.13 | 46.56 | 13.30 |
| H8 | 53 | 309 | 12 | 115 | 13 | 90 | 4.39 | 0.67 | 68.28 | 63.79 | 7.09 |
| H9 | 12 | 243 | 27 | 108 | 12 | | 4.47 | 0.58 | 67.66 | 66.04 | 17.23 |
| H10 | 3 | 325 | 26 | 88 | 9 | 239 | 3.96 | 0.78 | 50.38 | 79.07 | 15.23 |
| H11 | 13 | 378 | 27 | 117 | 13 | 107 | 4.23 | 0.63 | 71.66 | 68.07 | 16.53 |
| H12 | 1 | 244 | 18 | 98 | 8 | 54 | 4.88 | 1.01 | 63.01 | 92.06 | 11.46 |
| H13 | 6 | 314 | 28 | 114 | 12 | | 4.50 | 0.61 | 70.24 | 64.04 | 17.87 |
| H14 | 10 | 326 | 20 | 111 | 12 | 176 | 4.41 | 0.61 | 67.03 | 65.77 | 12.08 |
| H15 | 1 | 347 | 28 | 89 | 13 | 278 | 4.60 | 0.60 | 54.77 | 87.84 | 17.23 |
| H18 | 44 | 606 | 15 | 94 | 12 | 674 | 3.13 | 0.43 | 56.60 | 66.32 | 9.03 |
| H20 | 78 | 301 | 11 | 126 | 14 | 348 | 3.11 | 0.32 | 87.14 | 36.71 | 7.61 |
| H21 | 22 | 240 | 18 | 103 | 22 | 399 | 2.44 | 0.16 | 69.69 | 34.95 | 12.80 |
| H22 | 86 | 269 | 18 | 127 | 14 | 605 | 3.98 | 0.49 | 74.30 | 53.54 | 5.78 |
| H24 | 76 | 442 | 14 | 148 | 13 | 804 | 4.30 | 0.60 | 81.68 | 52.70 | 7.73 |
| H25 | 87 | 483 | 18 | 157 | 12 | 975 | 5.84 | 0.88 | 78.52 | 77.57 | 10.47 |
| H28 | 44 | 301 | 22 | 86 | 10 | 674 | 5.36 | 0.82 | 50.06 | 106.98 | 12.81 |
| H31 | 22 | 372 | 17 | 134 | 13 | 808 | 2.36 | 0.32 | 78.75 | 30.60 | 9.74 |
| H33 | 49 | 862 | 17 | 220 | 17 | 1120 | 2.36 | 0.24 | 129.11 | 18.18 | 9.98 |
| H38 | 35 | 72 | 7 | 44 | 13 | 22903 | 6.09 | 0.61 | 40.37 | 150.00 | 6.42 |
| H41 | 16 | 224 | 14 | 146 | 16 | 784 | 3.04 | 0.31 | 88.80 | 34.48 | 8.52 |
| H53 | 41 | 870 | 14 | 184 | 16 | 850 | 3.11 | 0.34 | 105.93 | 28.36 | 8.06 |
| H54 | 45 | 561 | 17 | 156 | 12 | 752 | 2.97 | 0.40 | 96.47 | 30.77 | 10.51 |
| H57 | 57 | 466 | 20 | 137 | 13 | 534 | 6.01 | 0.62 | 85.84 | 65.30 | 12.53 |
| H58 | 68 | 609 | 21 | 176 | 17 | 686 | 6.98 | 0.64 | 96.17 | 61.93 | 11.48 |
| H59 | 51 | 951 | 14 | 248 | 15 | 1040 | 3.43 | 0.41 | 140.20 | 24.60 | 7.88 |
| H60 | 37 | 1010 | 21 | 200 | 16 | 675 | 3.06 | 0.25 | 130.04 | 23.50 | 13.66 |
| H61 | 66 | 1223 | 21 | 240 | 16 | 1569 | 3.72 | 0.38 | 153.86 | 24.17 | 13.48 |
| H62 | 11 | 259 | 15 | 127 | 10 | 293 | 4.37 | 0.76 | 72.96 | 59.84 | 8.62 |
| H63 | 95 | 311 | 16 | 111 | 9 | 654 | 4.62 | 0.91 | 62.50 | 73.87 | 9.01 |
| H68 | 84 | 391 | 11 | 138 | 12 | 860 | 4.13 | 0.64 | 74.57 | 56.40 | 5.90 |
| H71 | 98 | 479 | 10 | 178 | 13 | 807 | 3.42 | 0.39 | 117.98 | 28.98 | 6.70 |
| H73 | 60 | 613 | 13 | 172 | 11 | 1356 | 3.79 | 0.59 | 100.29 | 37.79 | 7.58 |
| H74 | 106 | 963 | 12 | 234 | 16 | 901 | 4.14 | 0.41 | 140.99 | 28.21 | 7.53 |
| H75 | 109 | 796 | 12 | 203 | 14 | 111 | 4.26 | 0.52 | 118.57 | 36.98 | 7.01 |

HERON BAY - HEMLO SAMPLE LOCATIONS

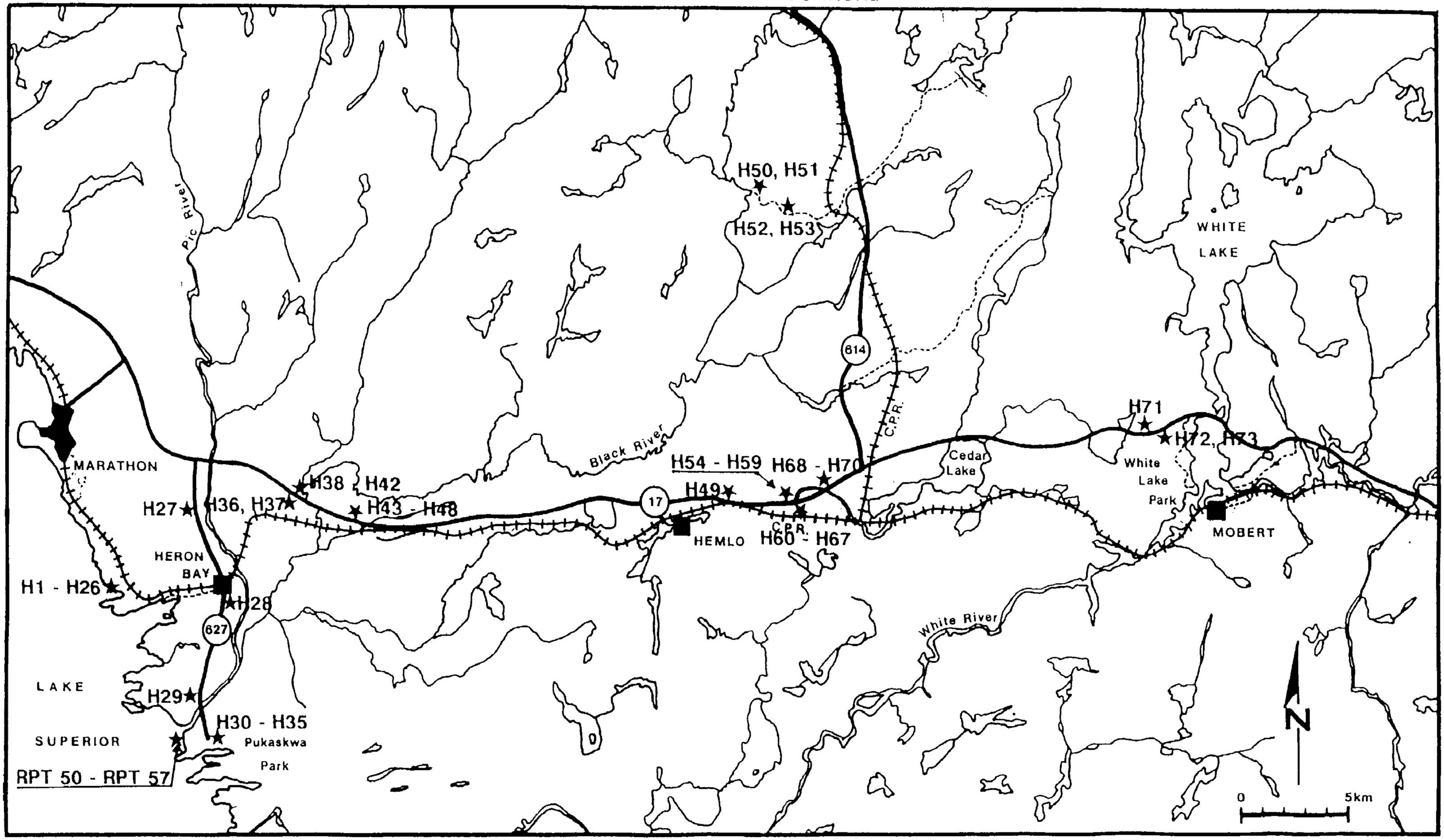


★ H34 Sample collected by Thomson, 1989.

★ RPT 53 Sample collected by Purdon, this study.

FIGURE C-2: Hemlo area sample locations.

TABLE C-3: Geochemical data from Fralick and Kronberg (in press).

Analysis of metasediments from the Beardmore-Geraldton Region

| | Forearc Fluvial | | | Forearc Turbidites | | | | Trench Turbidites | | | | | | | |
|---|---|---|---|---|---|---|---|---|---|---|---|---|---|---|---|
| | 1 | 2 | 3 | 4 | 5 | 6 | 7 | 8 | 9 | 10 | 11 | 12 | 13 | 14 | 15 |
| $SiO_2$ | 69.8 | 66.6 | 66.4 | 64.7 | 64.4 | 65.7 | 61.5 | 64.3 | 63.6 | 64.8 | 65.5 | 62.2 | 64.8 | 60.9 | 67.1 |
| $TiO_2$ | 0.43 | 0.57 | 0.42 | 0.56 | 0.57 | 0.44 | 0.59 | 0.54 | 0.55 | 0.56 | 0.55 | 0.59 | 0.68 | 0.60 | 0.51 |
| $Al_2O_3$ | 12.7 | 14.6 | 12.7 | 15.3 | 15.2 | 14.0 | 17.2 | 15.7 | 15.7 | 16.0 | 15.6 | 16.6 | 13.5 | 16.5 | 14.4 |
| $Fe_2O_3$ | 5.17 | 4.31 | 4.52 | 5.60 | 5.78 | 4.75 | 5.87 | 5.44 | 5.88 | 5.48 | 5.47 | 6.42 | 7.16 | 6.48 | 4.85 |
| MnO | .09 | .08 | .10 | .08 | .09 | .10 | .08 | .09 | .08 | .08 | .07 | .10 | .12 | .10 | .09 |
| MgO | 1.65 | 1.71 | 2.18 | 2.63 | 3.00 | 2.03 | 3.26 | 3.54 | 3.23 | 2.54 | 2.97 | 3.74 | 3.15 | 3.73 | 2.69 |
| CaO | 2.73 | 2.30 | 2.91 | 2.37 | 2.79 | 4.76 | 2.30 | 2.44 | 2.66 | 2.25 | 2.41 | 2.05 | 3.84 | 2.90 | 3.93 |
| $Na_2O$ | 3.40 | 4.77 | 5.21 | 3.98 | 3.57 | 4.03 | 3.50 | 3.80 | 3.92 | 4.94 | 3.79 | 4.19 | 3.37 | 4.39 | 3.82 |
| $K_2O$ | 1.41 | 1.54 | 0.68 | 1.98 | 1.93 | 1.62 | 2.78 | 2.13 | 2.30 | 1.53 | 2.17 | 1.87 | 1.09 | 1.32 | 1.50 |
| $P_2O_5$ | 0.09 | 0.12 | 0.10 | 0.15 | 0.15 | 0.11 | 0.16 | 0.15 | 0.15 | 0.15 | 0.15 | 1.15 | 0.12 | 1.17 | 0.14 |
| LOI | 1.93 | 3.00 | 5.23 | 2.08 | 2.00 | 1.93 | 2.39 | 1.85 | 1.08 | 1.70 | 1.62 | 2.31 | 1.39 | 2.54 | 1.08 |
| Total | 99.5 | 99.7 | 100.5 | 99.6 | 99.7 | 99.6 | 99.8 | 100.2 | 99.3 | 100.2 | 100.5 | 100.4 | 99.4 | 99.8 | 100.3 |
| Ba | 440 | 430 | 260 | 710 | 660 | 560 | 880 | 670 | 660 | 490 | 680 | 520 | 390 | 410 | 420 |
| Co | 21 | 29 | 20 | 29 | 18 | 21 | 26 | 24 | 21 | 20 | 21 | 24 | 42 | 20 | 23 |
| Cr | 74 | 110 | 70 | 130 | 150 | 89 | 120 | 220 | 180 | 110 | 200 | 110 | 170 | 190 | 160 |
| Cu | 27 | 40 | 13 | 49 | 55 | 24 | 32 | 10 | 35 | 15 | 20 | 33 | 57 | 47 | 34 |
| Mo | 1.0 | 1.7 | .1 | 2.6 | .1 | 2.3 | .1 | 3.0 | .1 | .9 | .7 | .3 | .4 | 1.7 | 2.0 |
| Nb | 4.4 | 4.0 | 4.0 | 6.3 | 6.2 | 5.0 | 6.5 | 5.6 | 5.4 | 6.1 | 5.3 | 6.1 | 7.5 | 6.1 | 5.0 |
| Pb | 70 | 87 | 73 | 98 | 80 | 86 | 100 | 100 | 97 | 110 | 100 | 72 | 86 | 100 | 88 |
| Rb | 57 | 65 | 37 | 68 | 85 | 58 | 104 | 86 | 99 | 74 | 96 | 48 | 44 | 60 | 76 |
| Se | 300 | 310 | 290 | 360 | 370 | 320 | 400 | 380 | 370 | 370 | 370 | 280 | 350 | 350 | 320 |
| Sr | 100 | 150 | 170 | 370 | 350 | 420 | 350 | 410 | 400 | 510 | 410 | 280 | 330 | 360 | 440 |
| V | 86 | 100 | 70 | 100 | 100 | 70 | 96 | 97 | 100 | 90 | 100 | 80 | 130 | 100 | 82 |
| Y | 9 | 8 | 7 | 12 | 12 | 11 | 11 | 8 | 8 | 11 | 7 | 14 | 14 | 10 | 8 |
| Zn | 54 | 41 | 45 | 69 | 73 | 60 | 78 | 60 | 61 | 48 | 61 | 48 | 83 | 55 | 54 |
| Zr | 74 | 154 | 100 | 100 | 92 | 70 | 133 | 92 | 104 | 136 | 93 | 88 | 120 | 116 | 73 |

TABLE C-3 Geochemical data - Beardmore-Geraldton

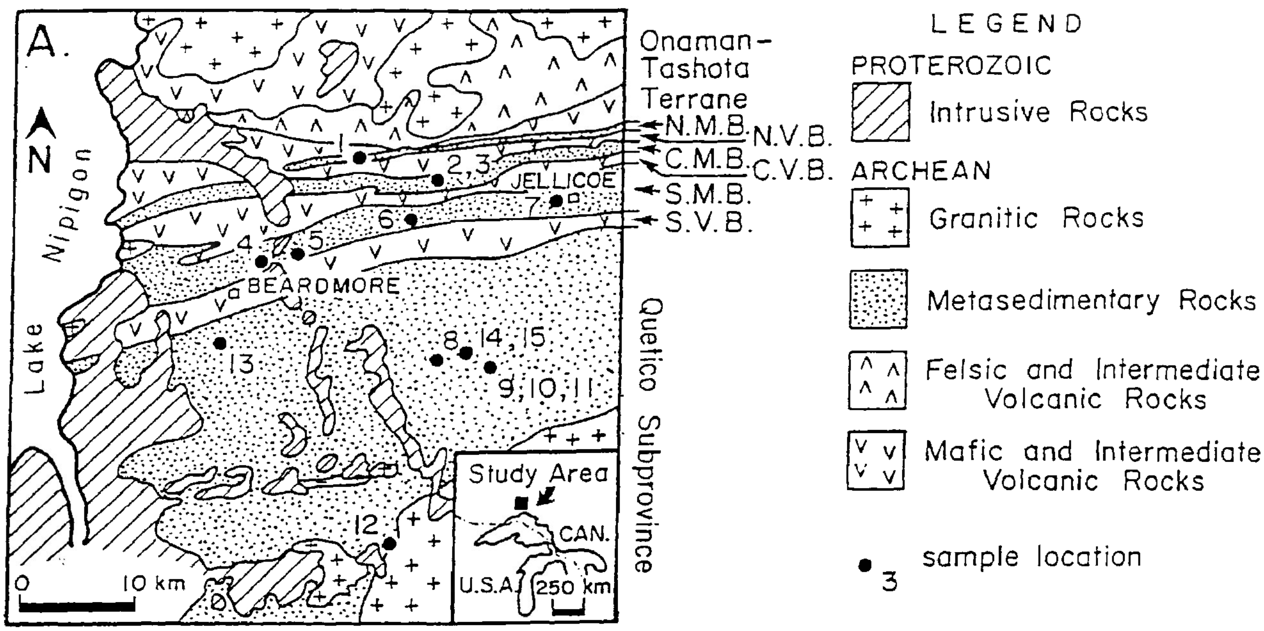


FIGURE C-3: Sample Locations - Beardmore-Geraldton.

# APPENDIX D - DETERMINATION OF ELEMENT MOBILITY

# Nb vs Al2O3

## Winston Lake

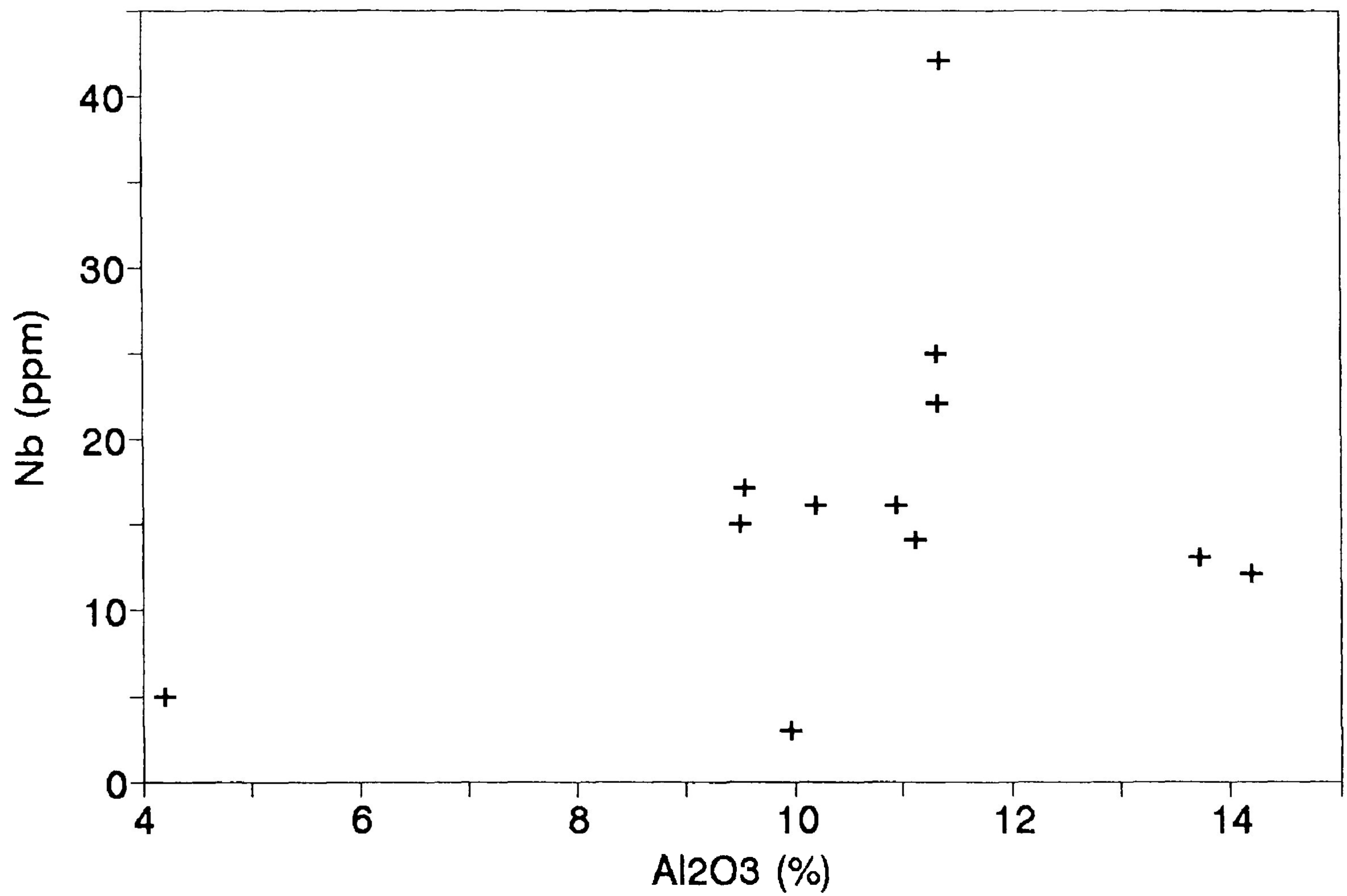

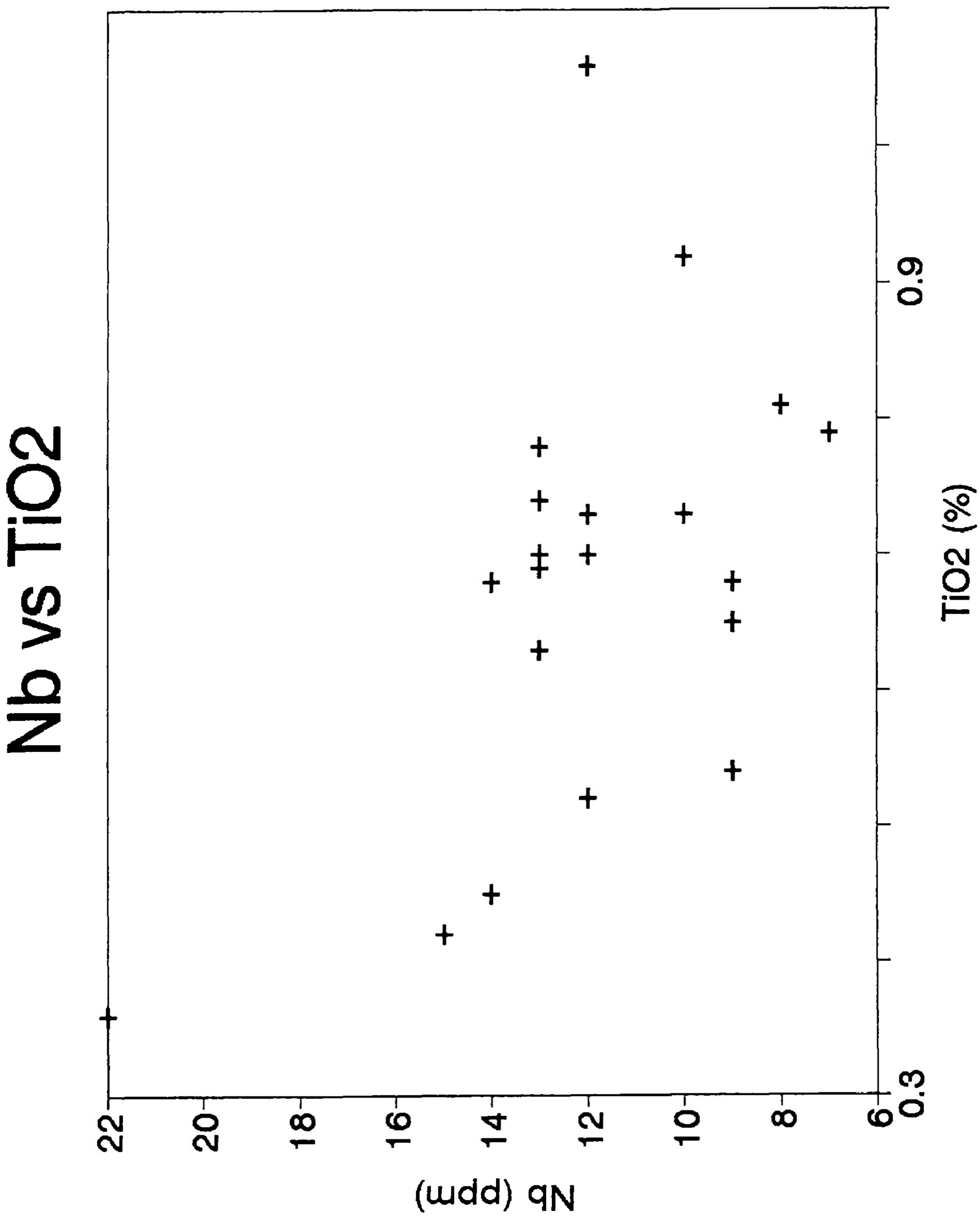
Nb vs TiO2
Nb (ppm)
22
20
18
16
14
12
10
8
6
0.3
0.9
TiO2 (%)

# Nb vs TiO2
## McKellar

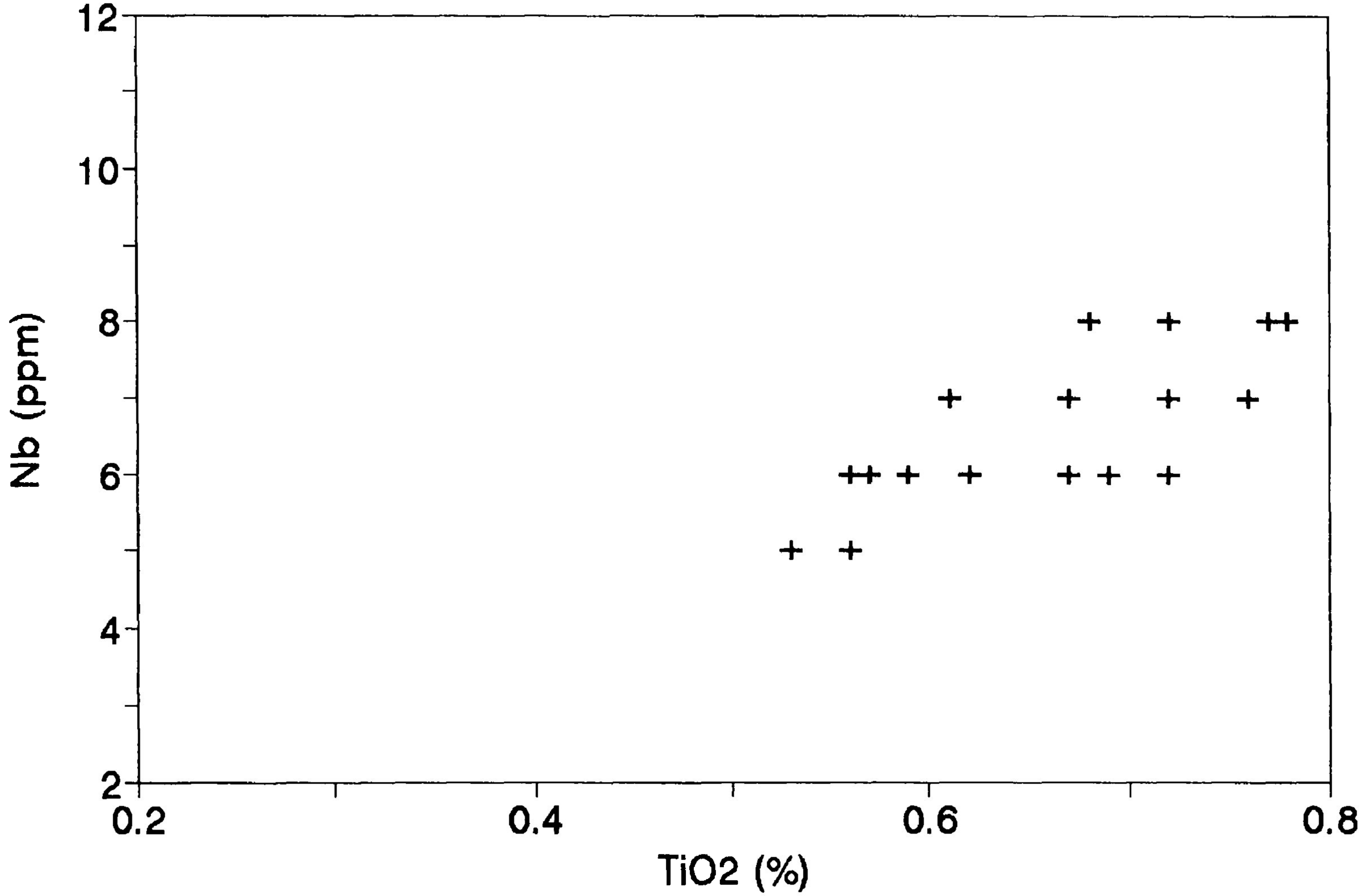

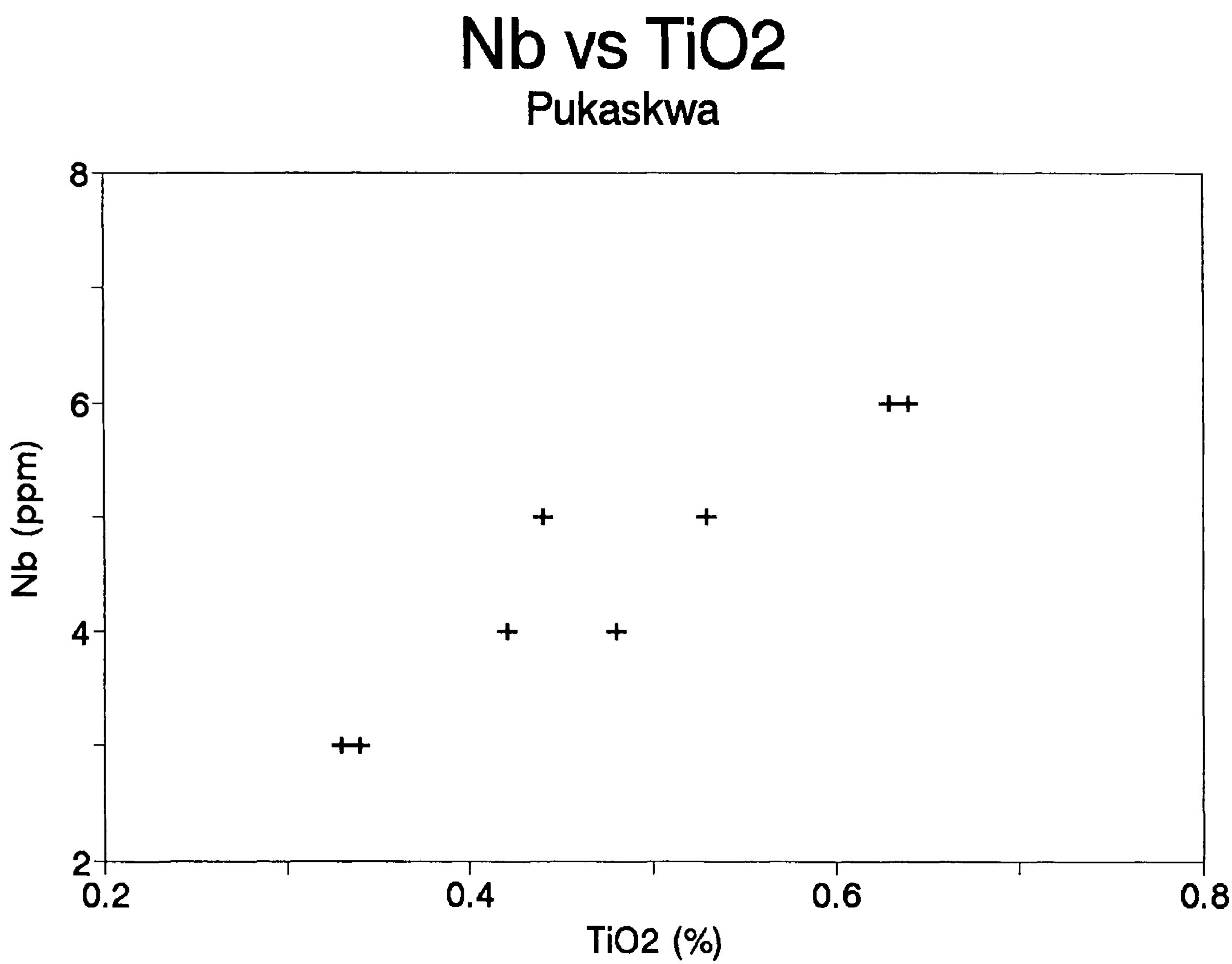
Nb vs TiO2
Pukaskwa
Nb (ppm)
8
6
4
2
0.2
0.4
0.6
0.8
TiO2 (%)

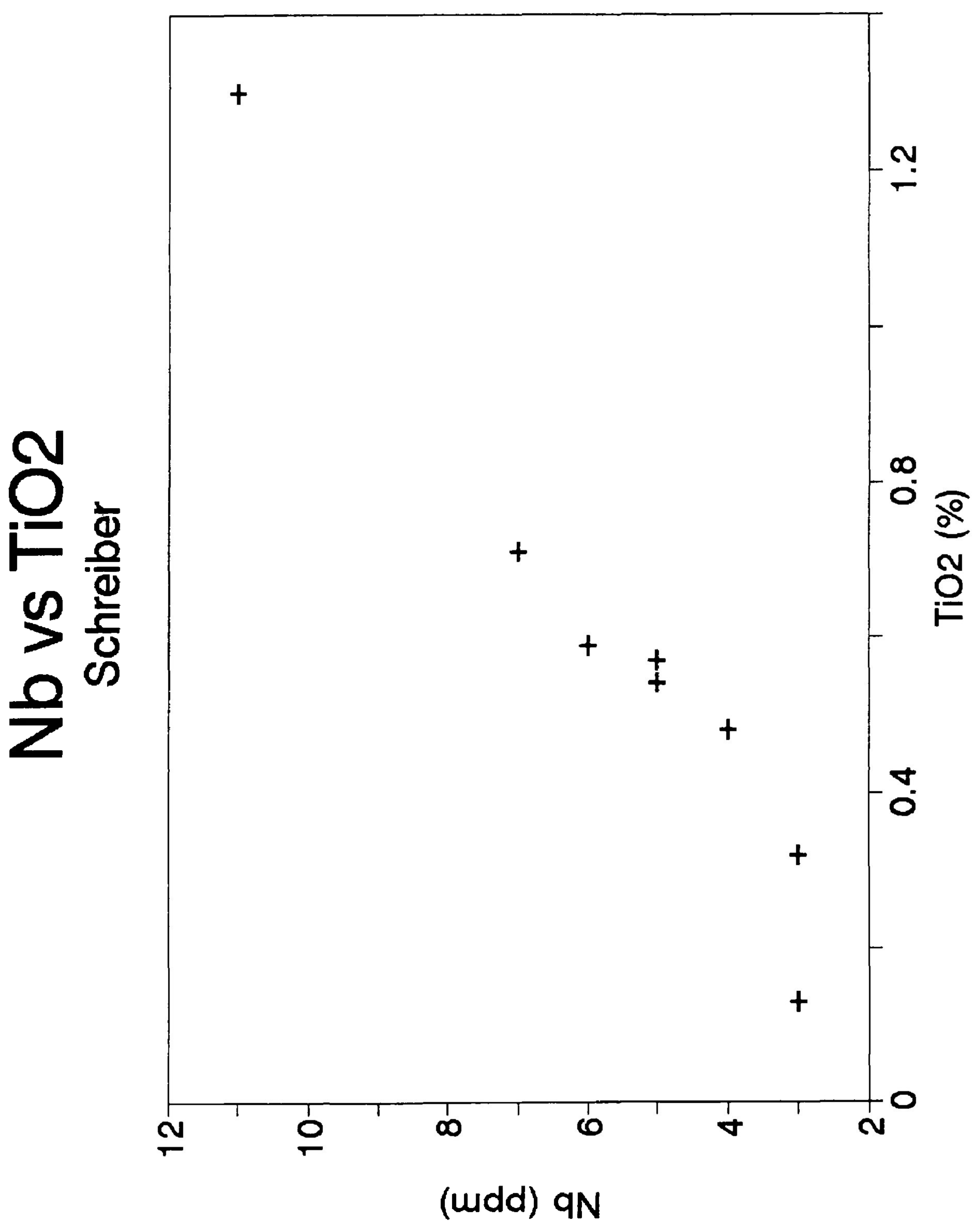
Nb vs TiO2
Schreiber
Nb (ppm)
TiO2 (%)
2
4
6
8
10
12
0
0.4
0.8
1.2

# Nb vs TiO2
## Winston Lake

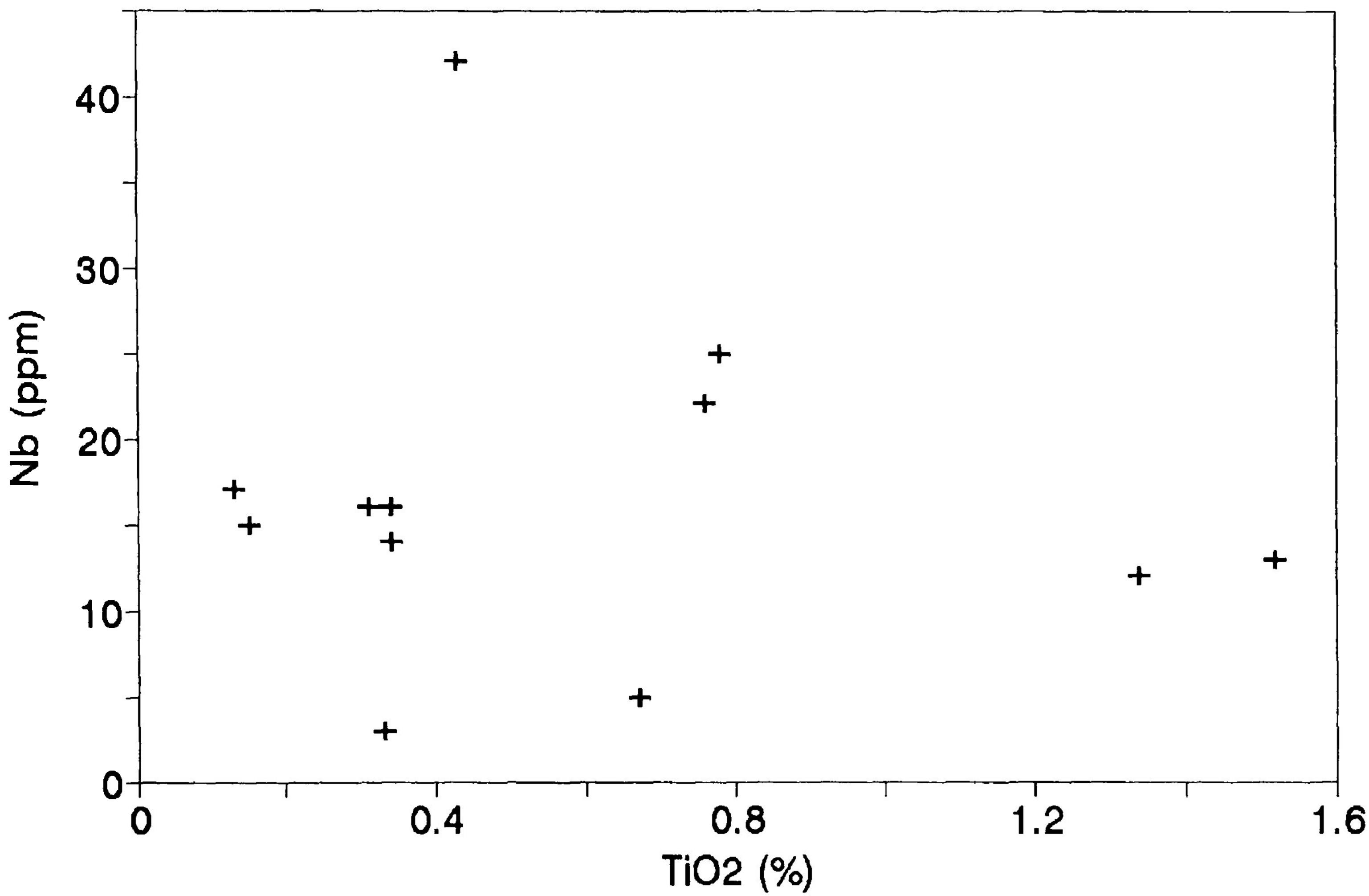

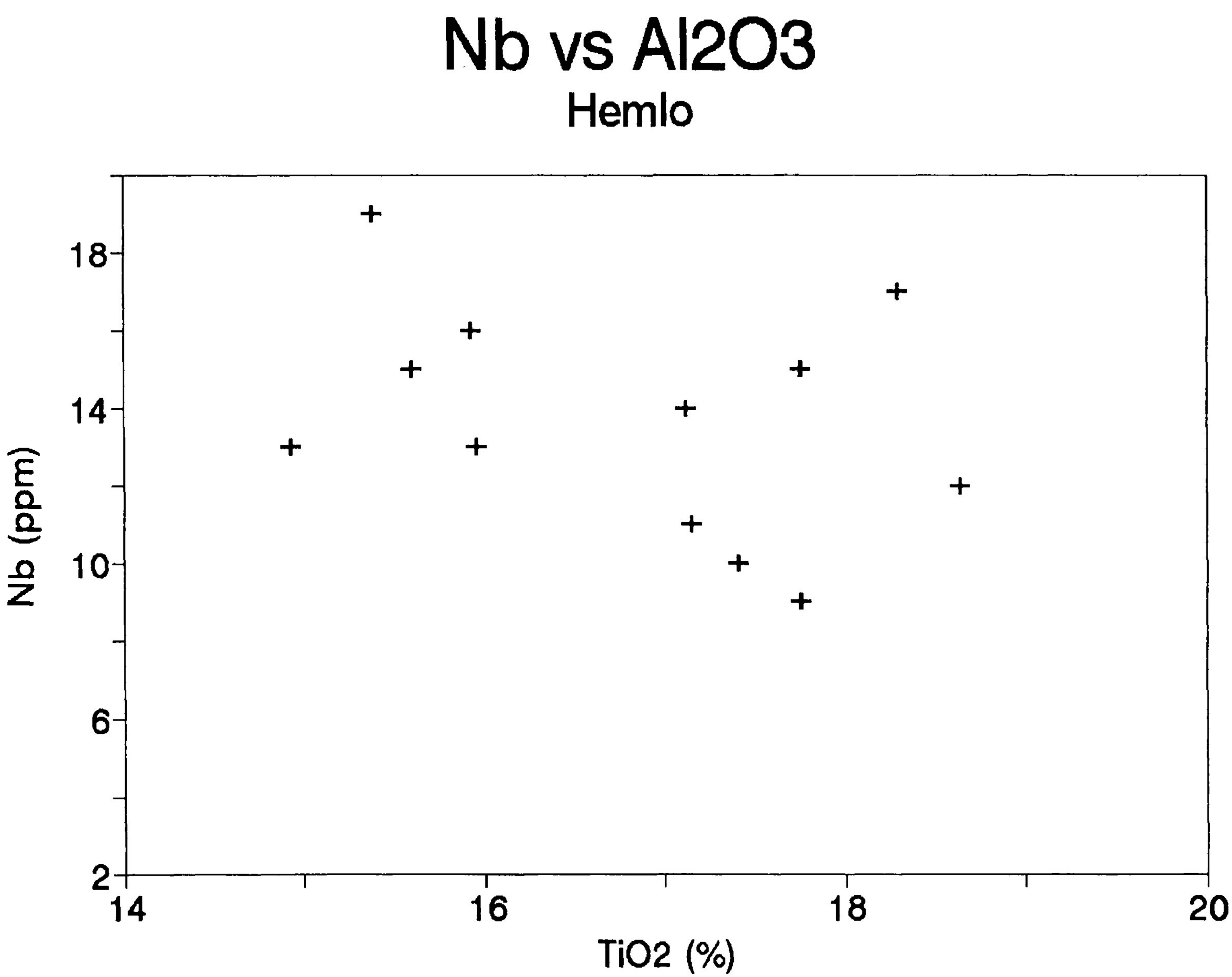
Nb vs Al2O3
Hemlo
Nb (ppm)
18
14
10
6
2
14
16
18
20
TiO2 (%)

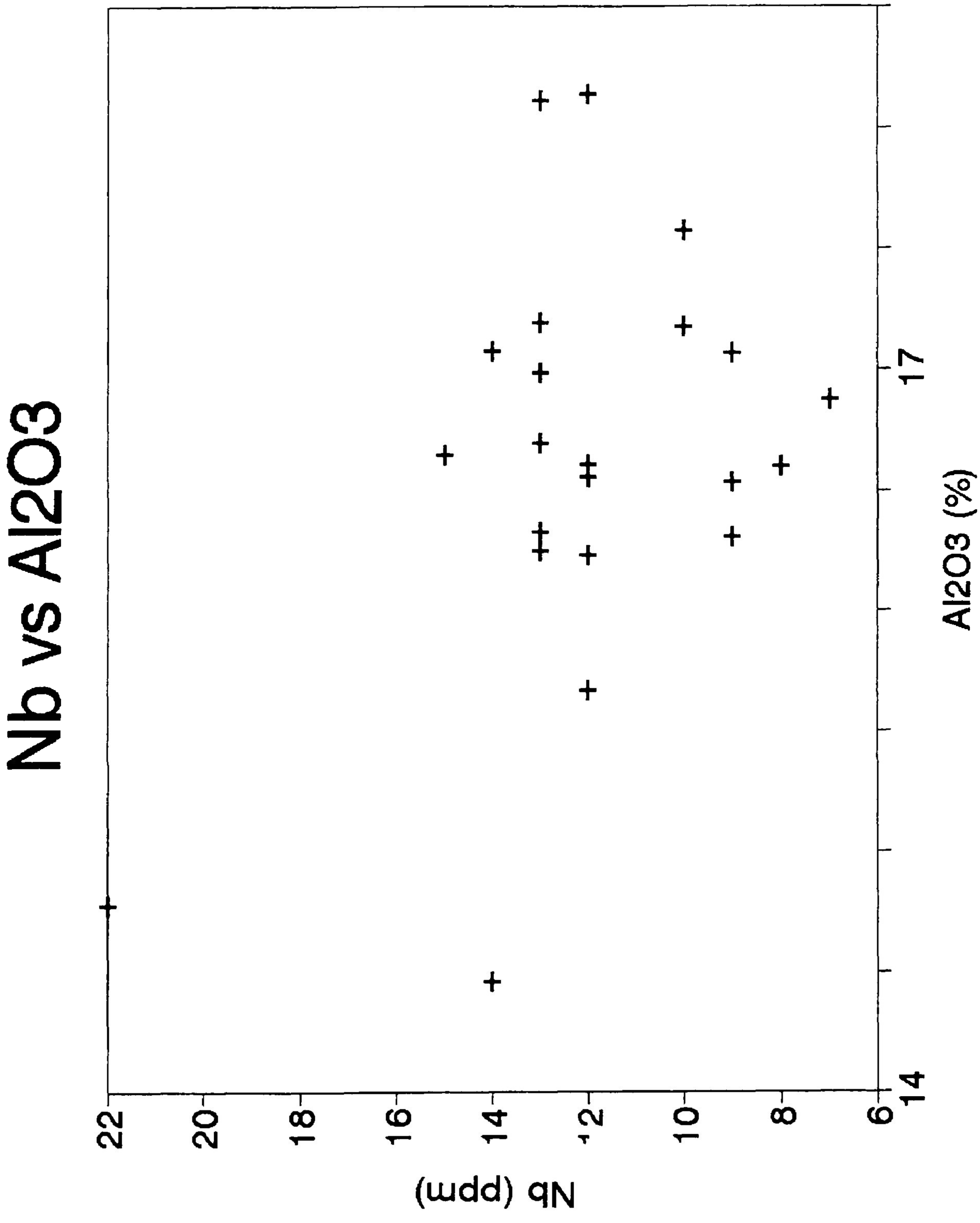
Nb vs Al2O3
Nb (ppm)
22
20
18
16
14
12
10
8
6
14
17
Al2O3 (%)

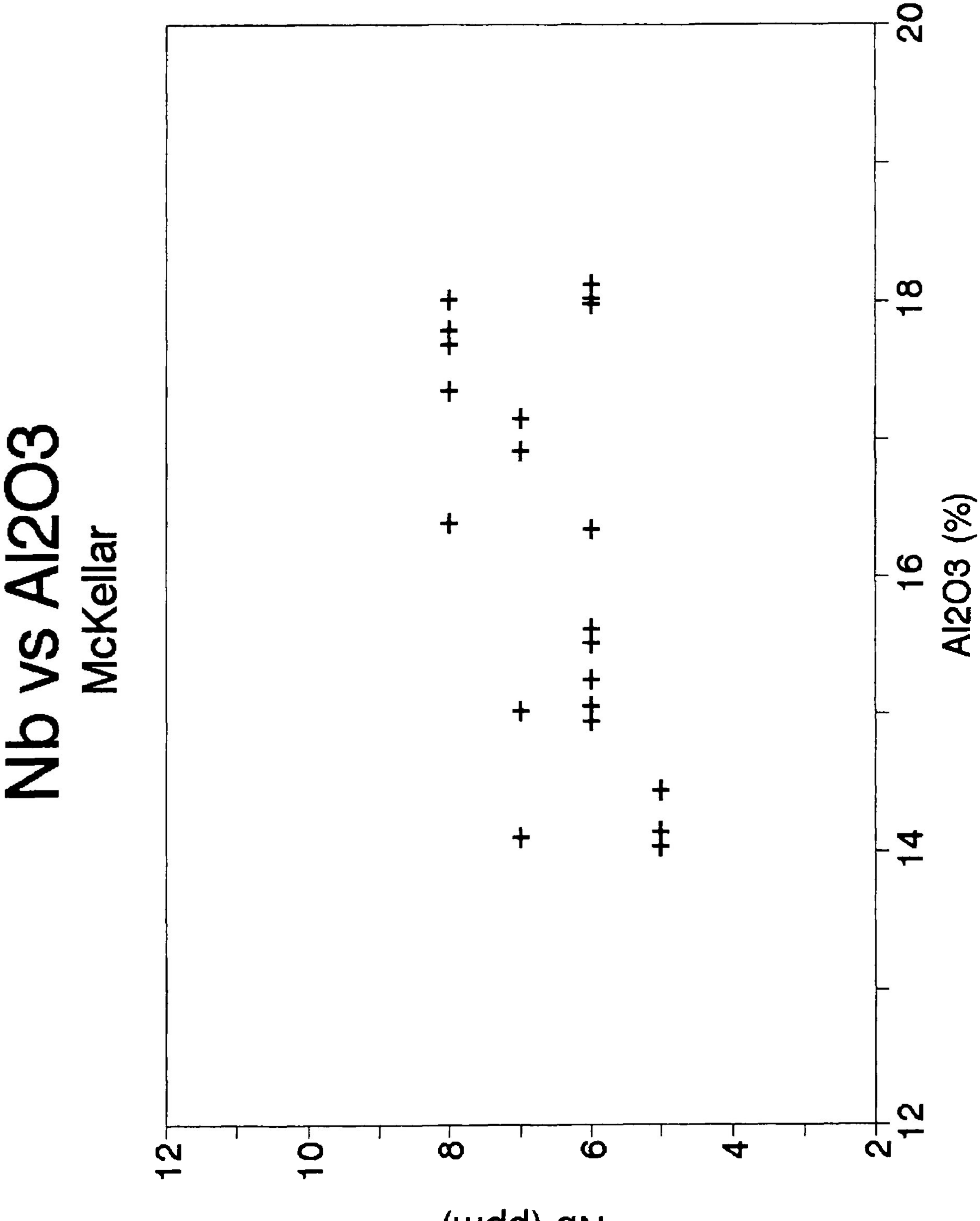
Nb vs Al2O3
McKellar
Nb (ppm)
Al2O3 (%)
2
4
6
8
10
12
12
14
16
18
20

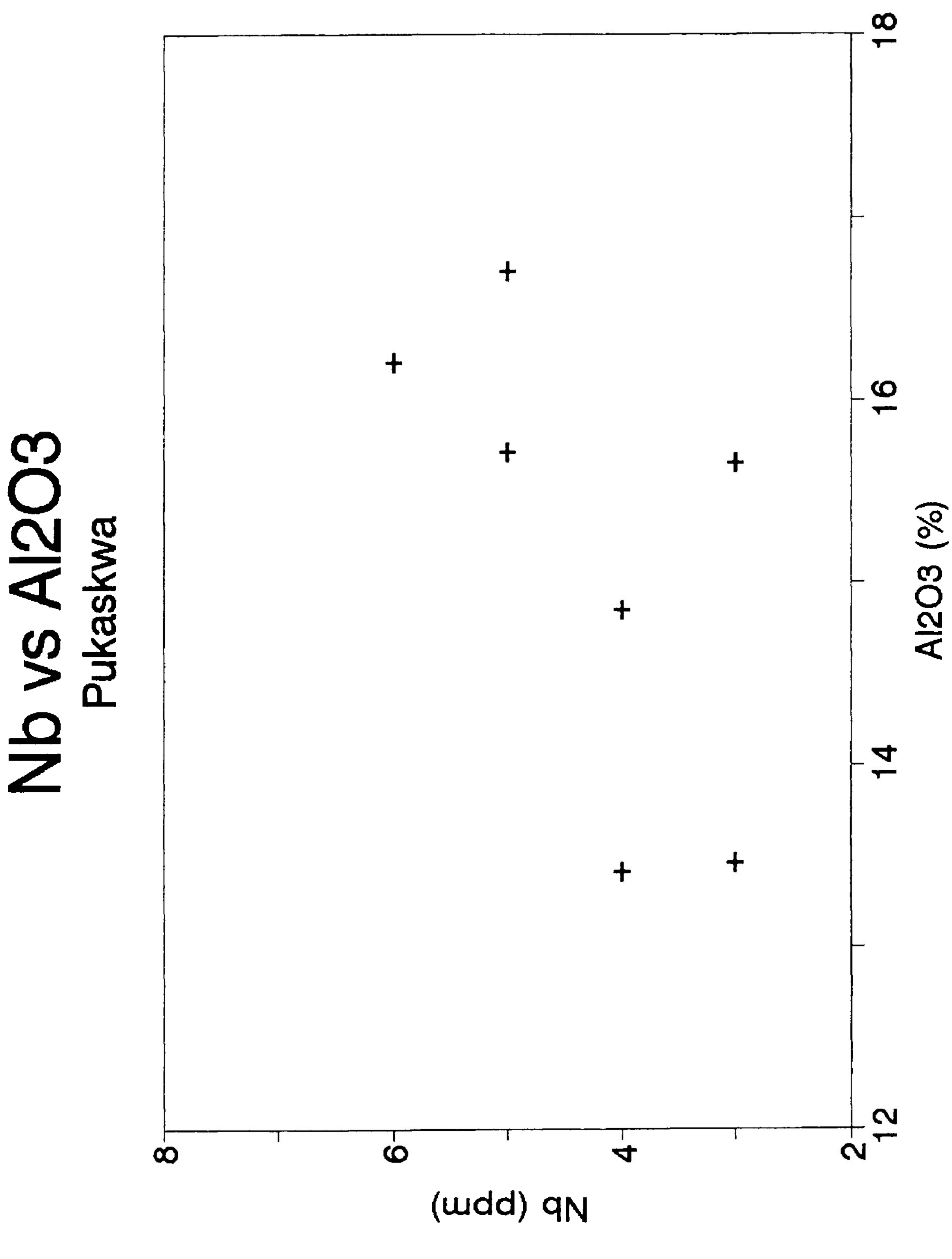
Nb vs Al2O3
Pukaskwa
Nb (ppm)
Al2O3 (%)
2
4
6
8
12
14
16
18

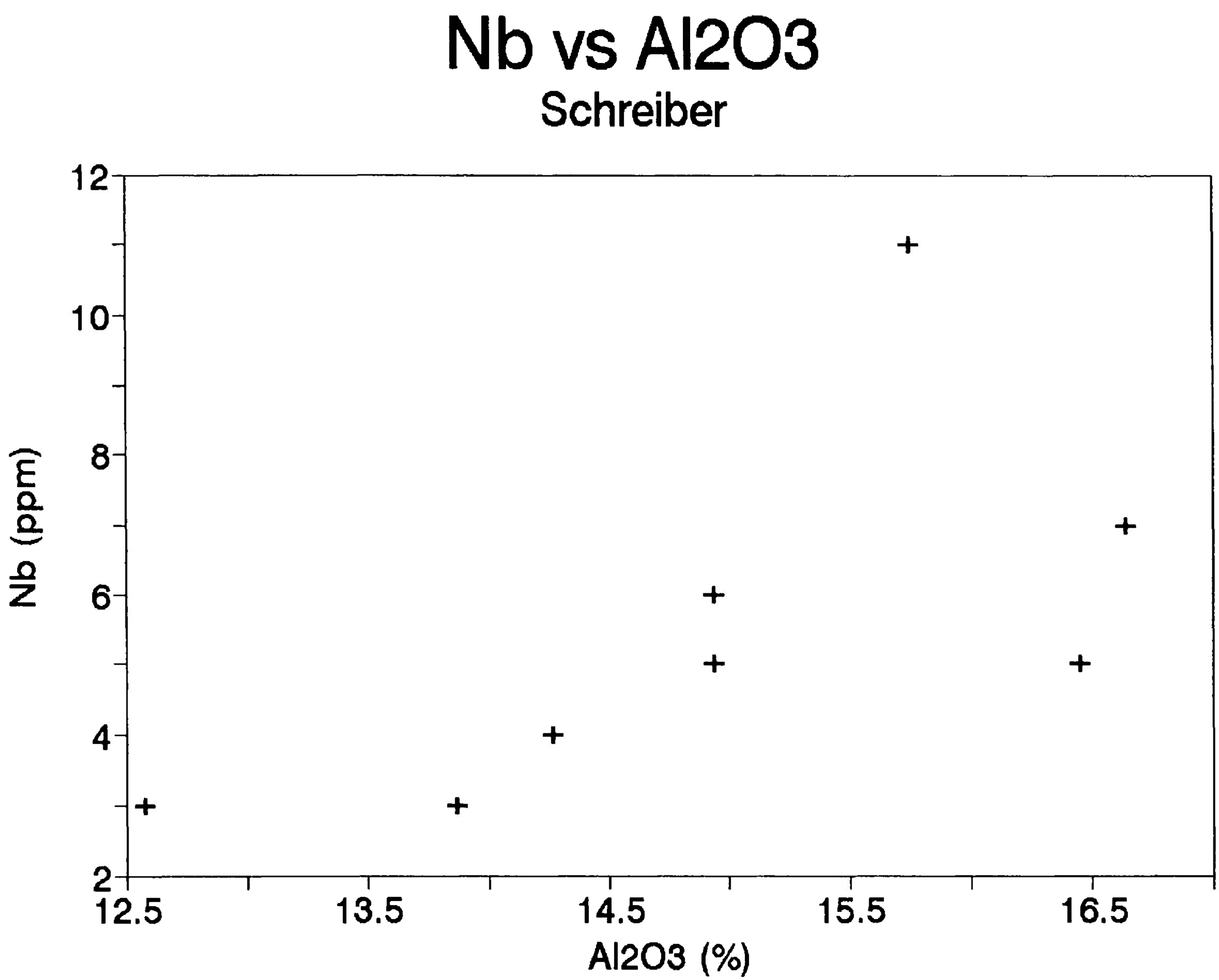
Nb vs Al2O3
Schreiber
Nb (ppm)
12
10
8
6
4
2
12.5
13.5
14.5
15.5
16.5
Al2O3 (%)

# Nb vs Al2O3
## Winston Lake

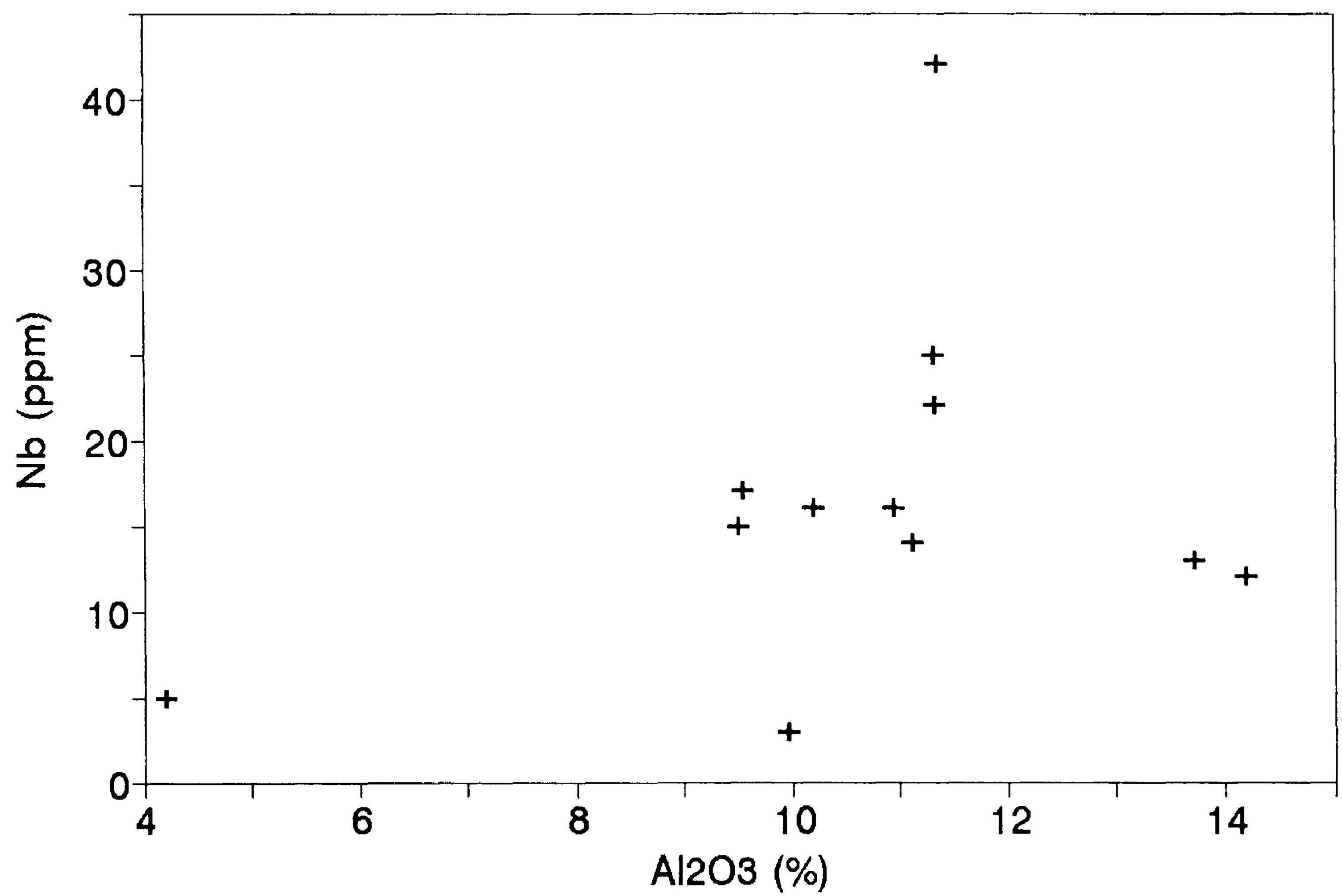

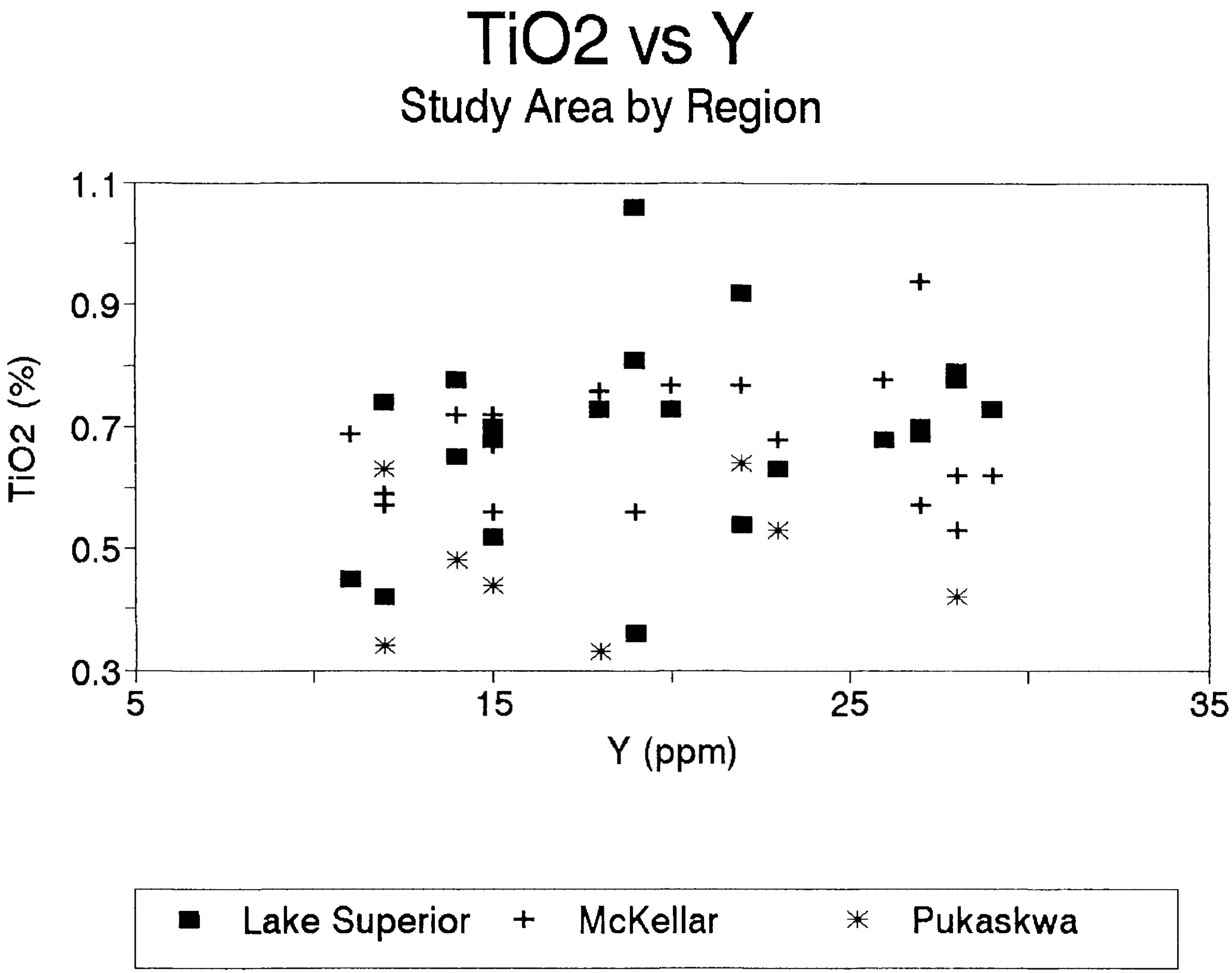
TiO2 vs Y
Study Area by Region
TiO2 (%)
1.1
0.9
0.7
0.5
0.3
5
15
25
35
Y (ppm)
Lake Superior
McKellar
Pukaskwa

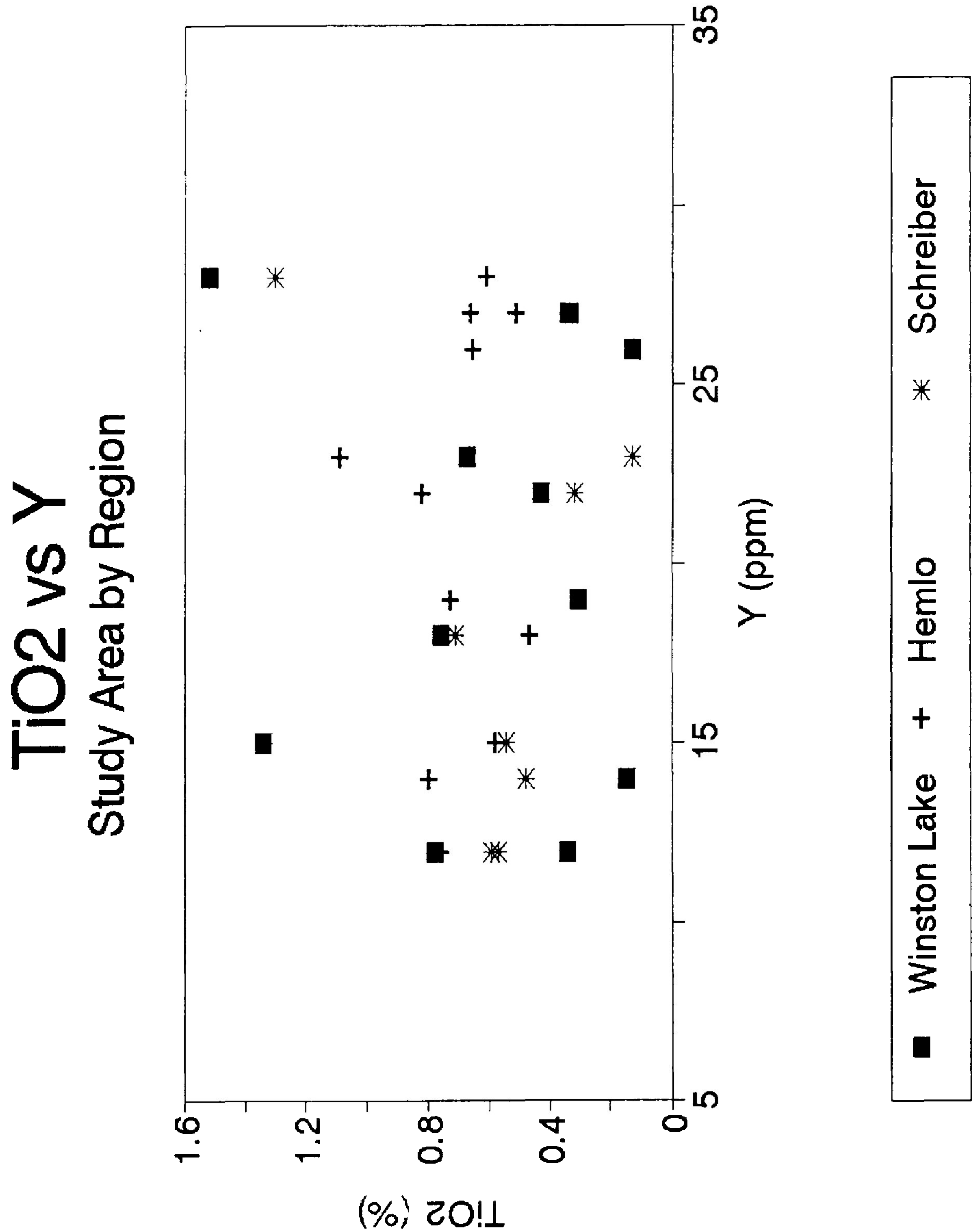

TiO2 vs Y
Study Area by Region
TiO2 (%)
1.6
1.2
0.8
0.4
0
5
15
25
35
Y (ppm)
Winston Lake
Hemlo
Schreiber

# Al2O3 vs Y

## Study Area by Region

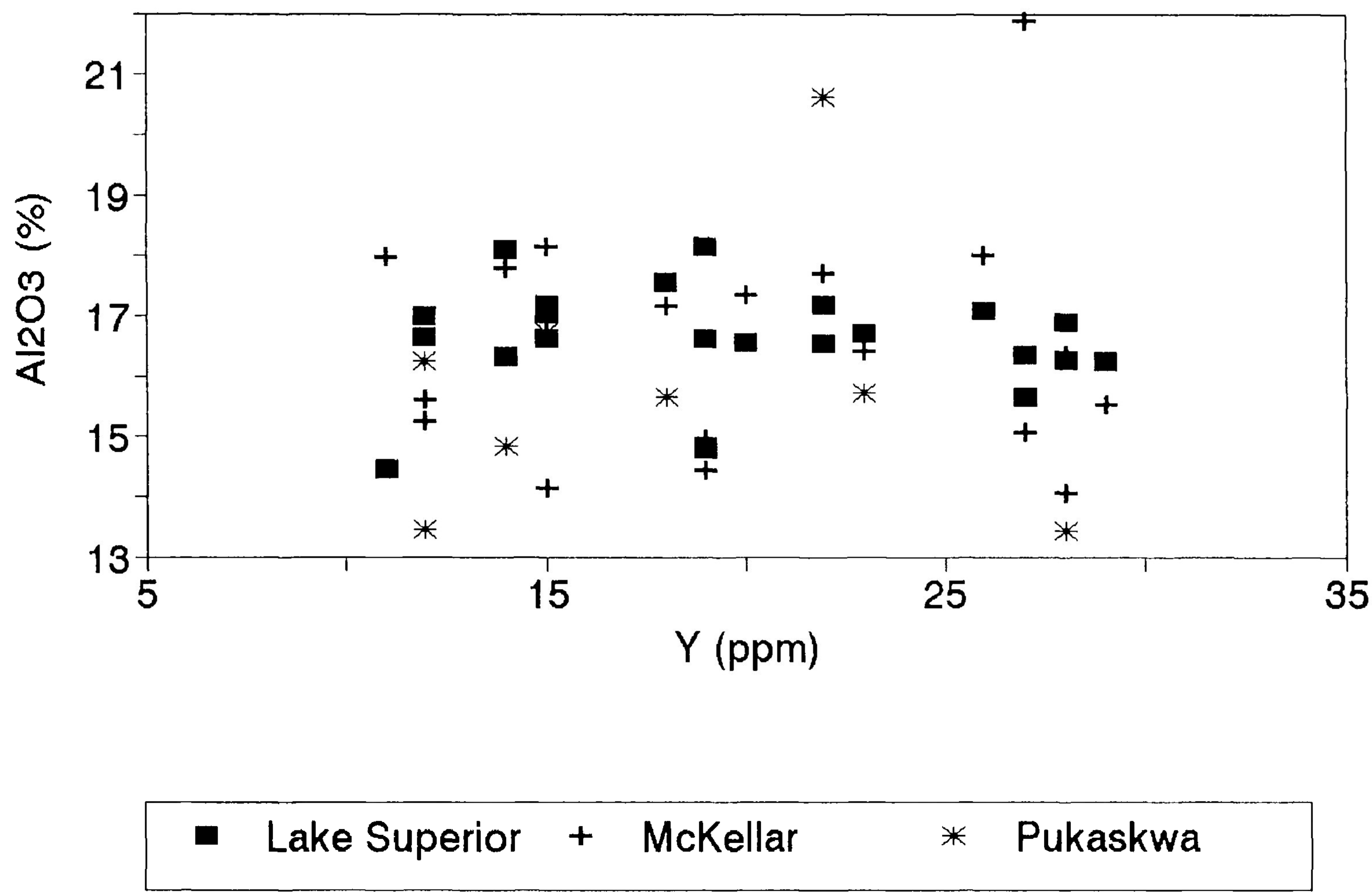

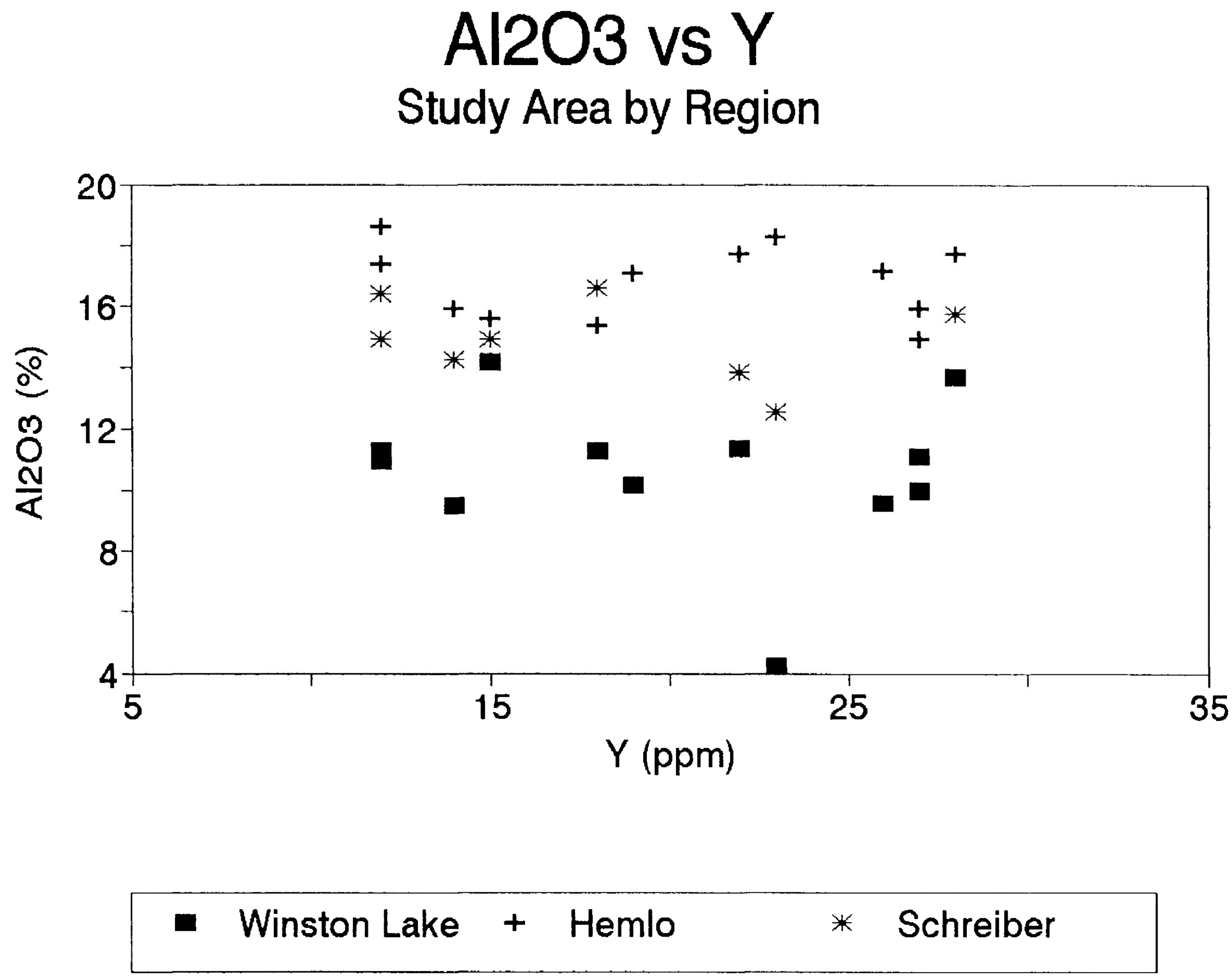

Al2O3 vs Y
Study Area by Region
20
16
12
8
4
Al2O3 (%)
5
15
25
35
Y (ppm)
Winston Lake
Hemlo
Schreiber

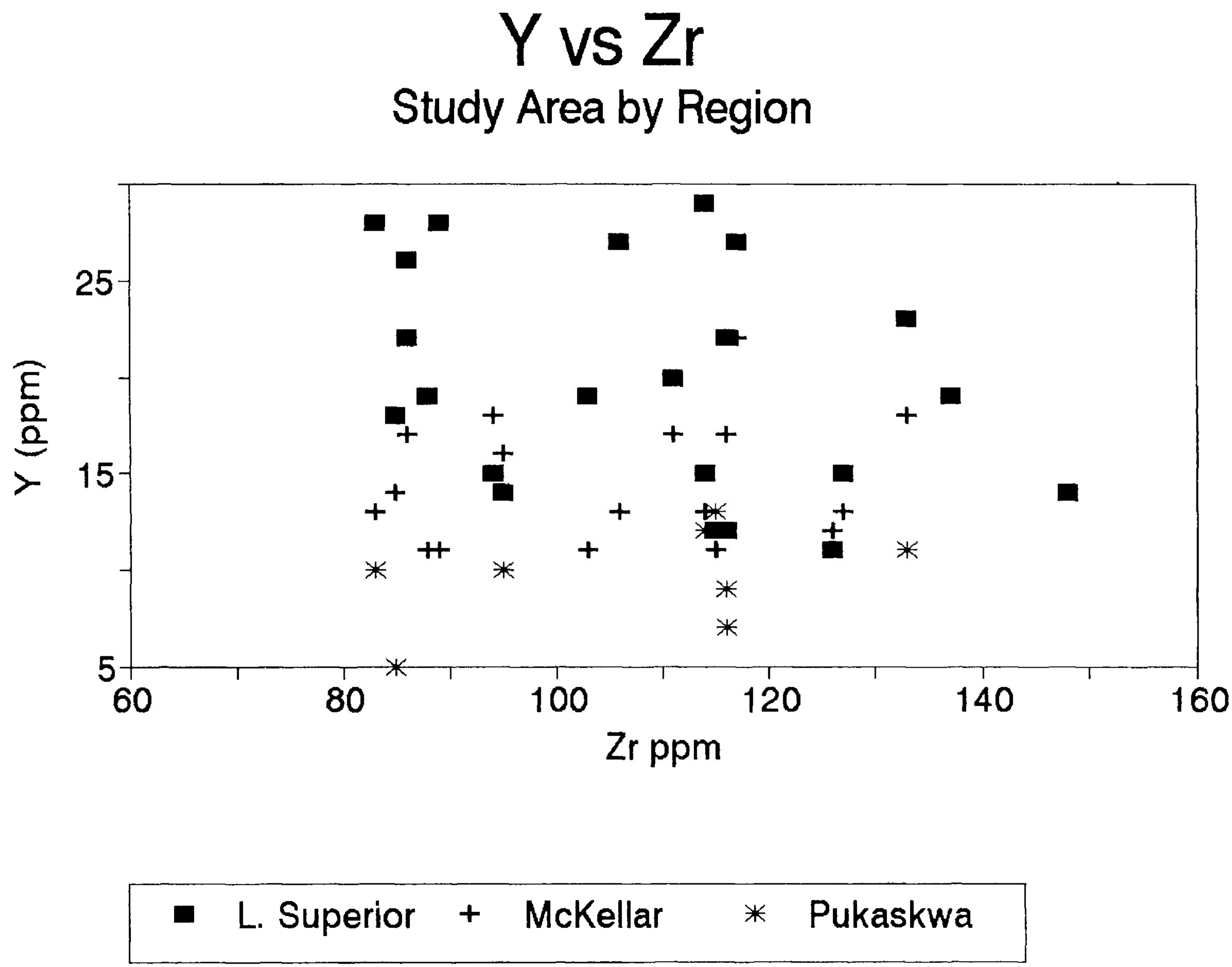

Y vs Zr
Study Area by Region
25
15
5
Y (ppm)
60
80
100
120
140
160
Zr ppm
L. Superior
McKellar
Pukaskwa

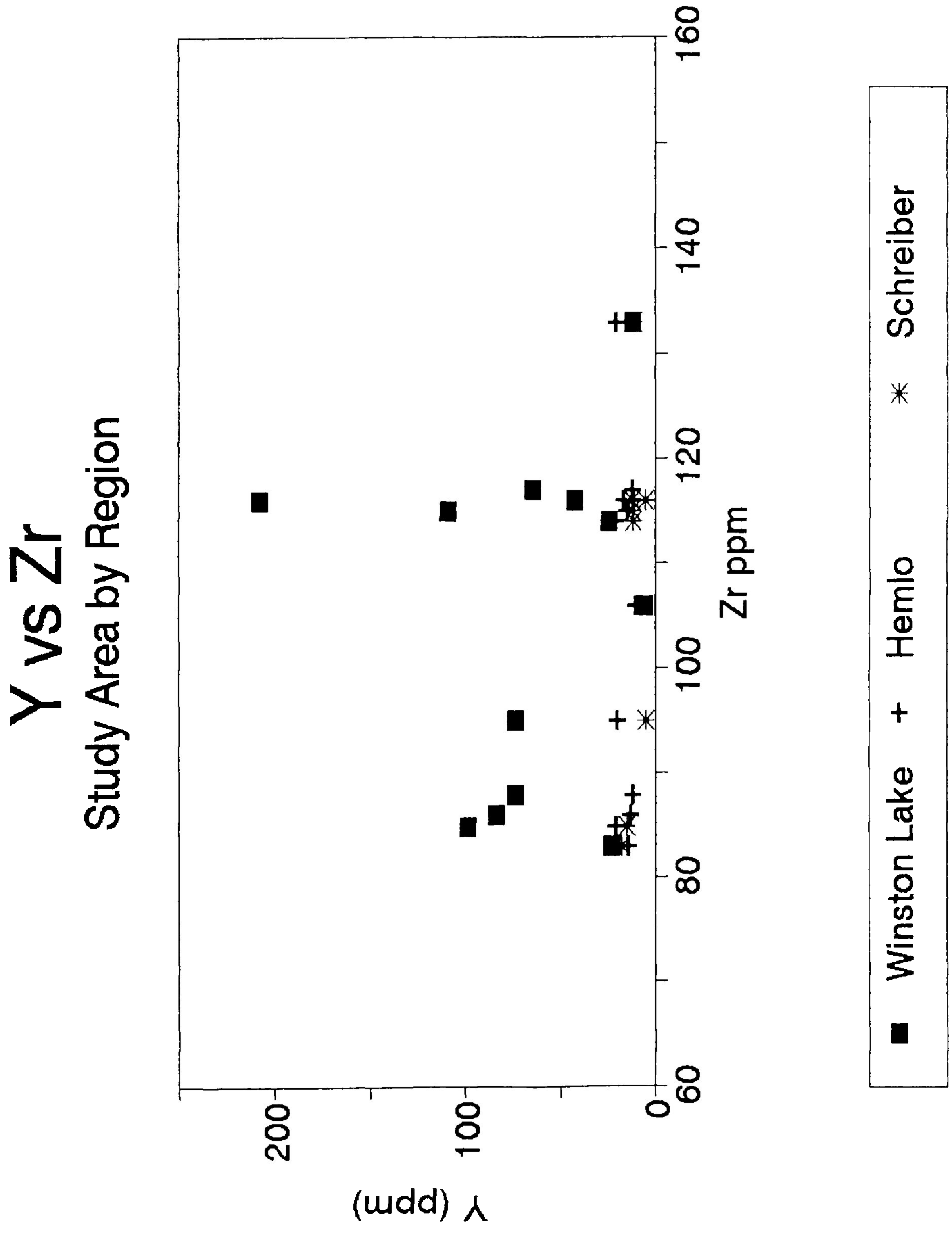
Y vs Zr
Study Area by Region
Y (ppm)
0
100
200
Zr ppm
60
80
100
120
140
160
Winston Lake
Hemlo
Schreiber

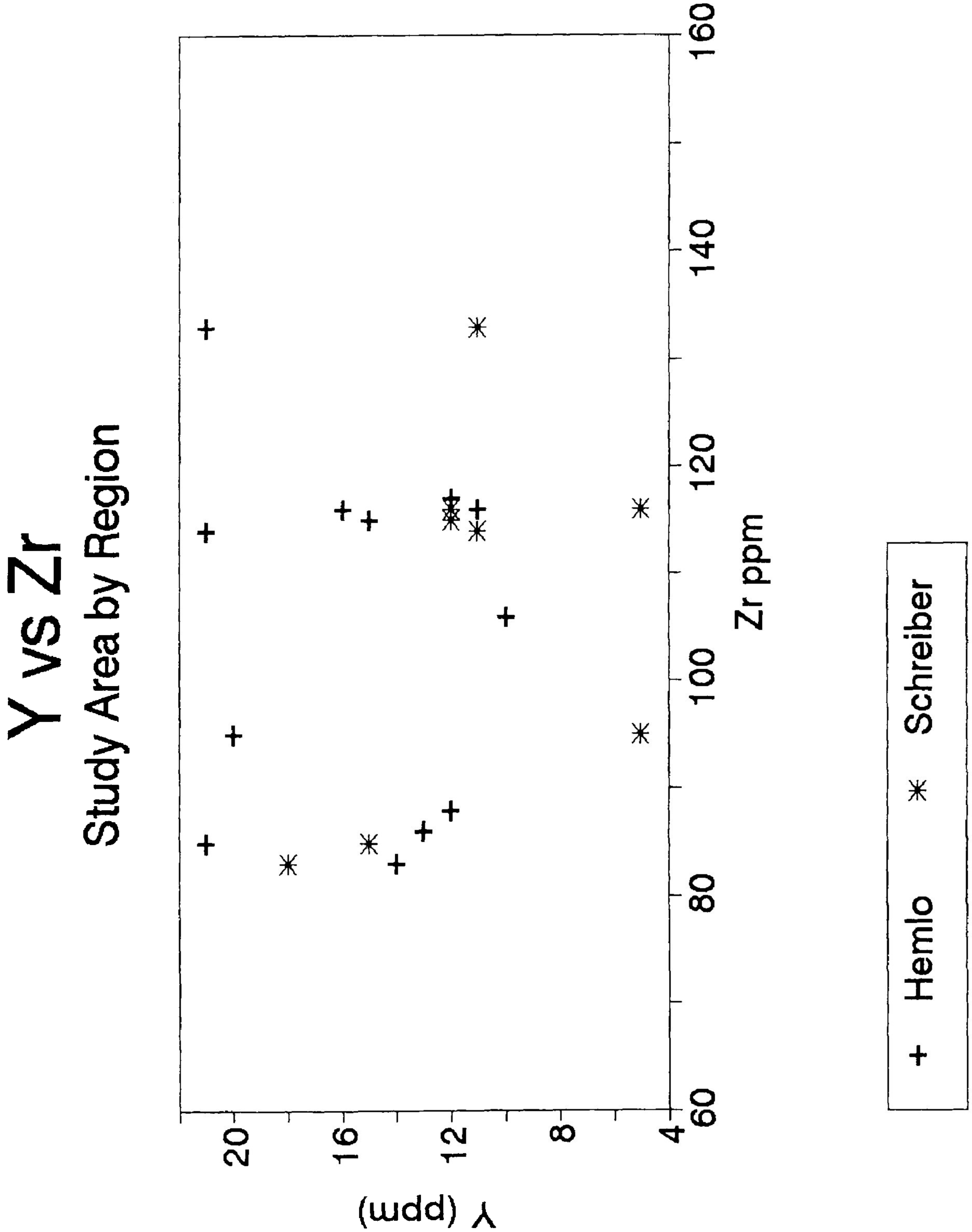

Y vs Zr
Study Area by Region
Y (ppm)
20
16
12
8
4
60
80
100
120
140
160
Zr ppm
Hemlo
Schreiber

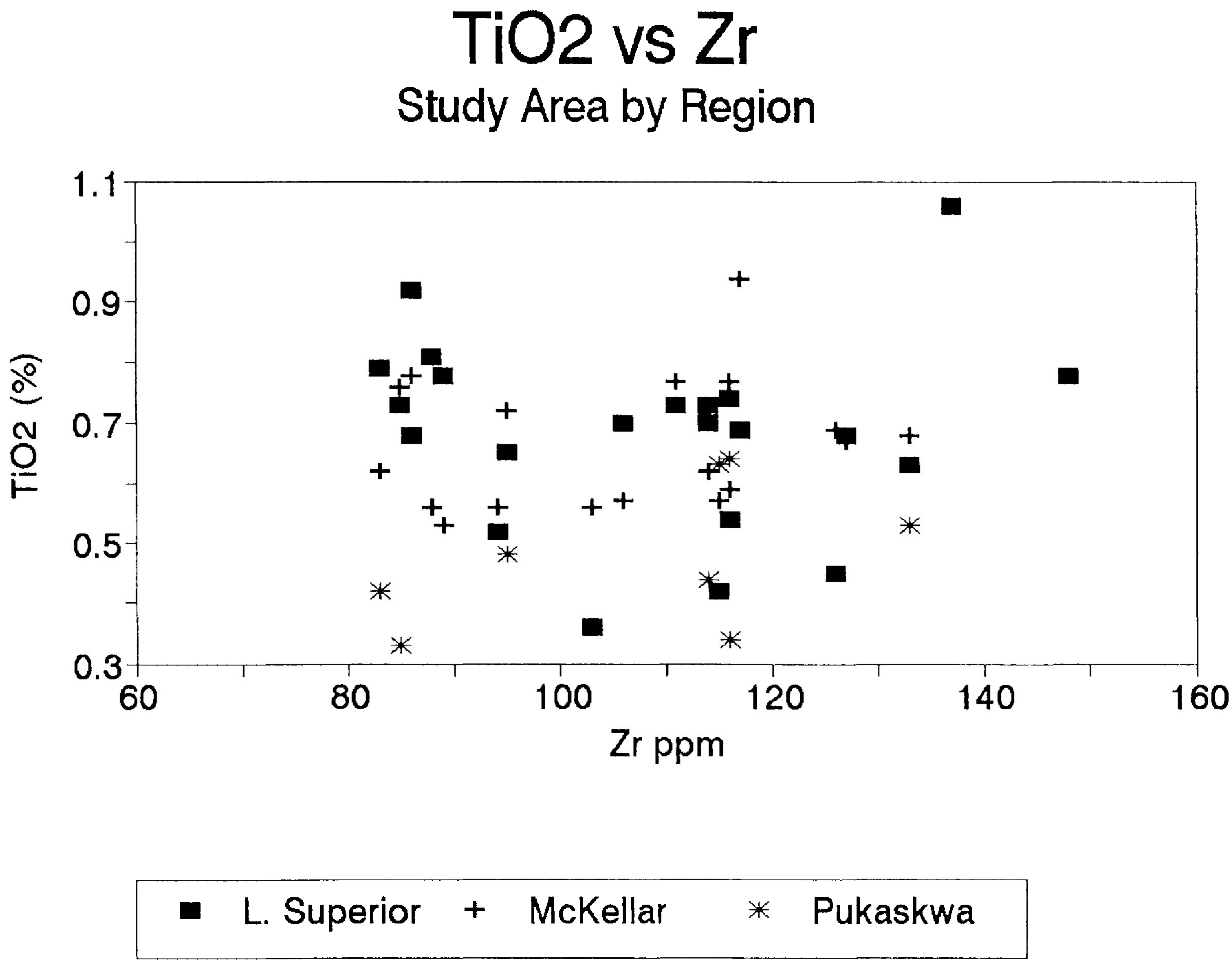

TiO2 vs Zr
Study Area by Region
TiO2 (%)
1.1
0.9
0.7
0.5
0.3
60
80
100
120
140
160
Zr ppm
L. Superior
McKellar
Pukaskwa

# TiO2 vs Zr

## Study Area by Region

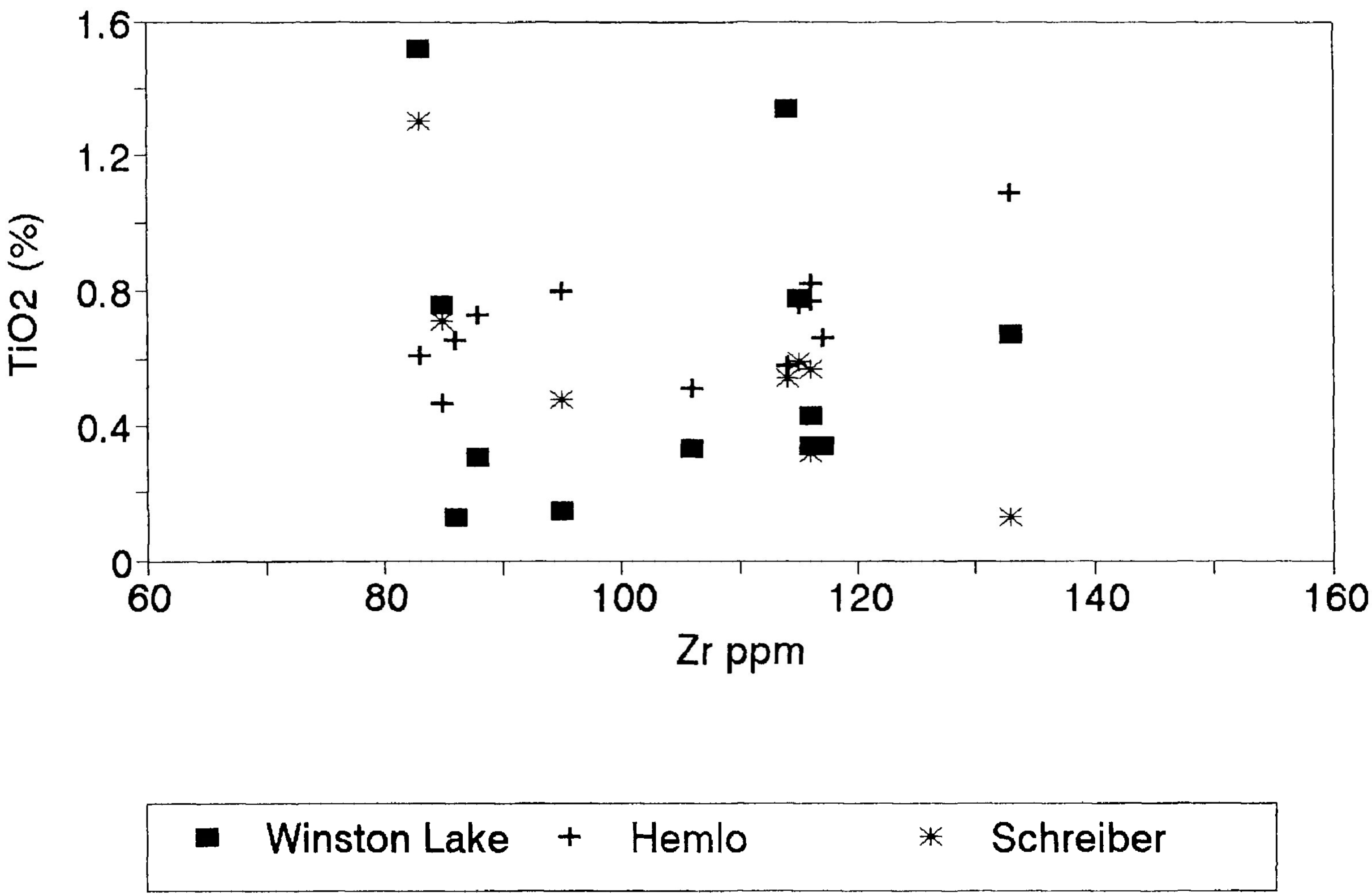

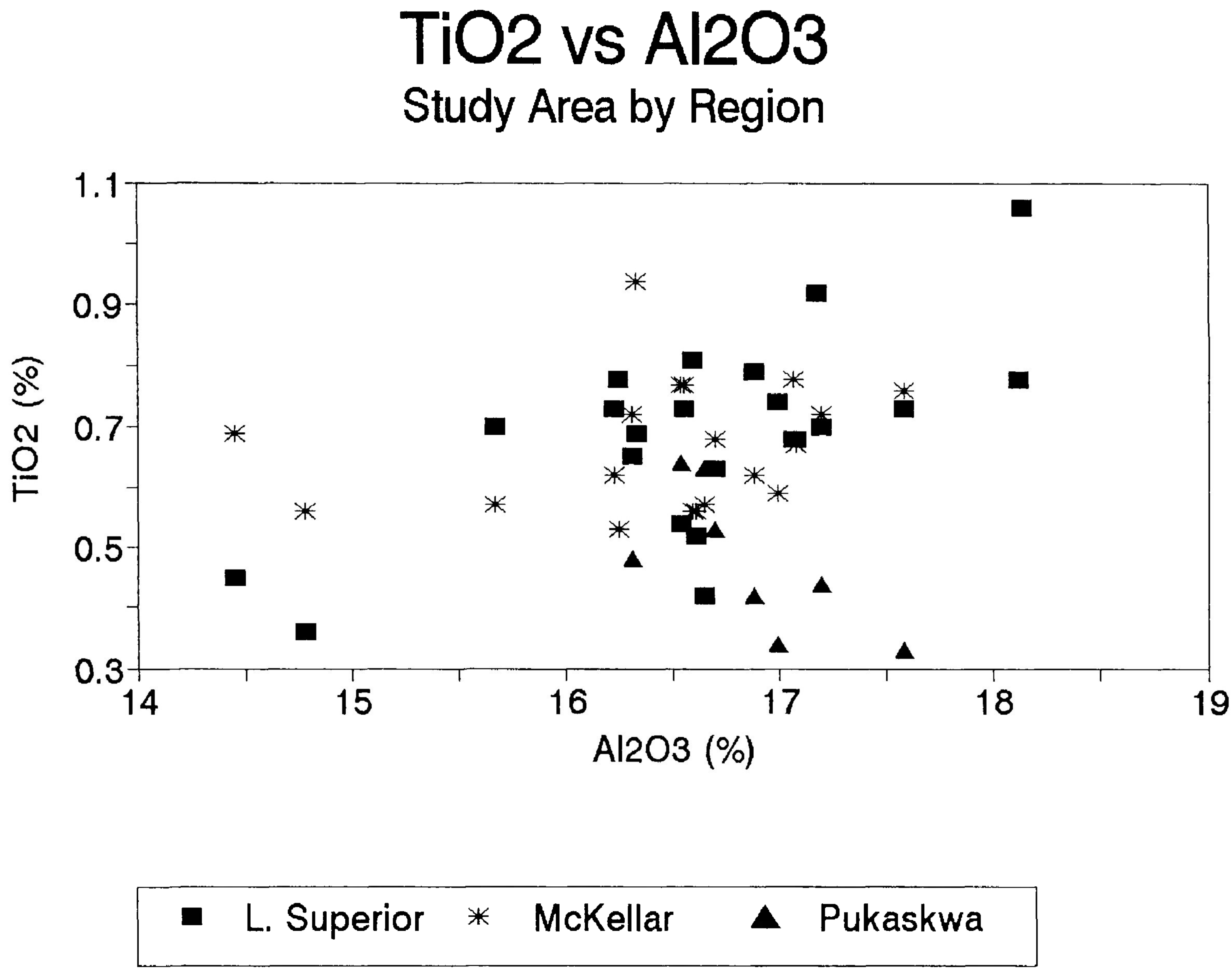
TiO2 vs Al2O3
Study Area by Region
1.1
0.9
0.7
0.5
0.3
14
15
16
17
18
19
TiO2 (%)
Al2O3 (%)
L. Superior
McKellar
Pukaskwa

## TiO2 vs Al2O3

### Study Area by Region

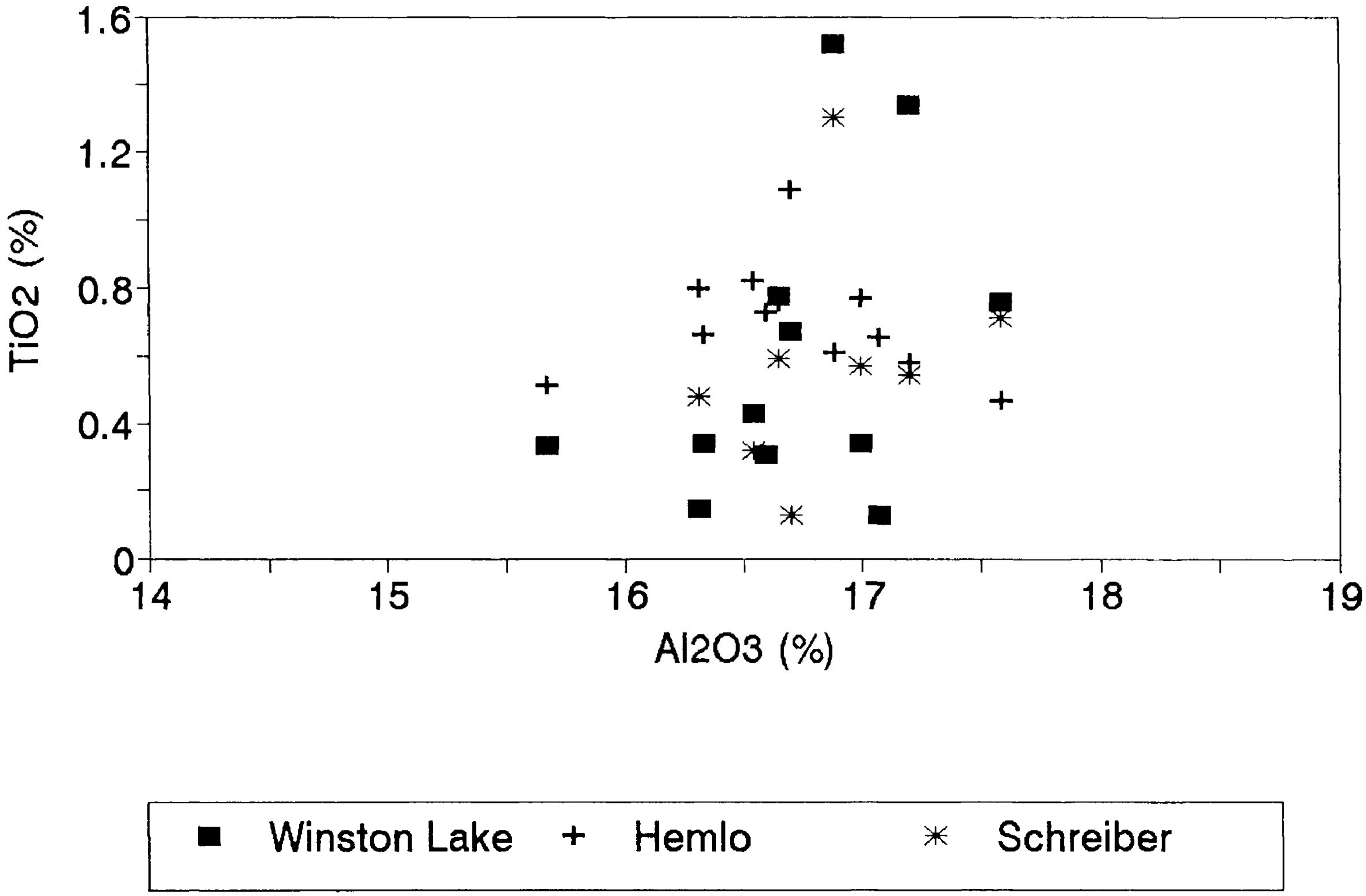

# Zr vs Al2O3

## Study Area by Region

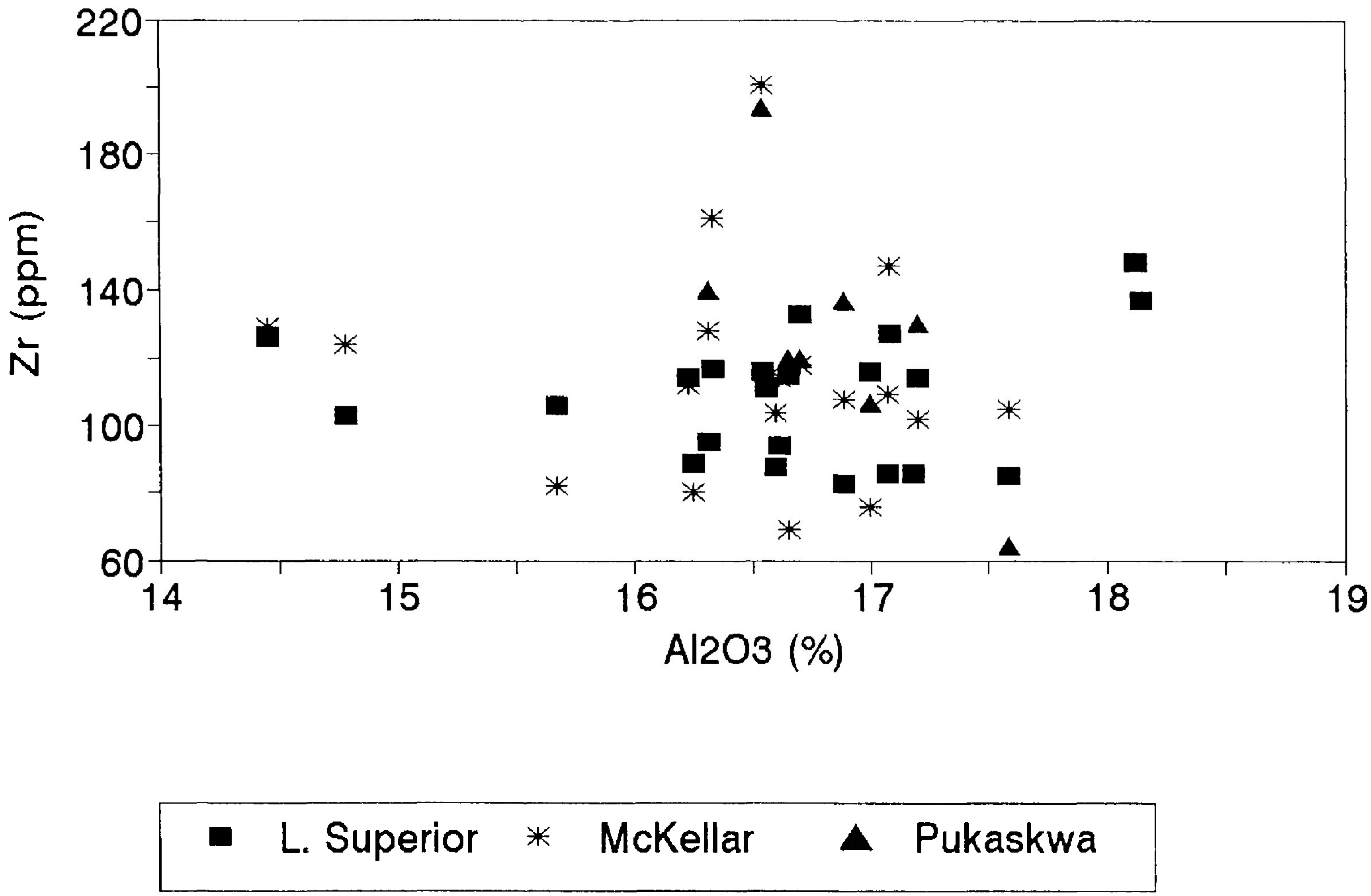

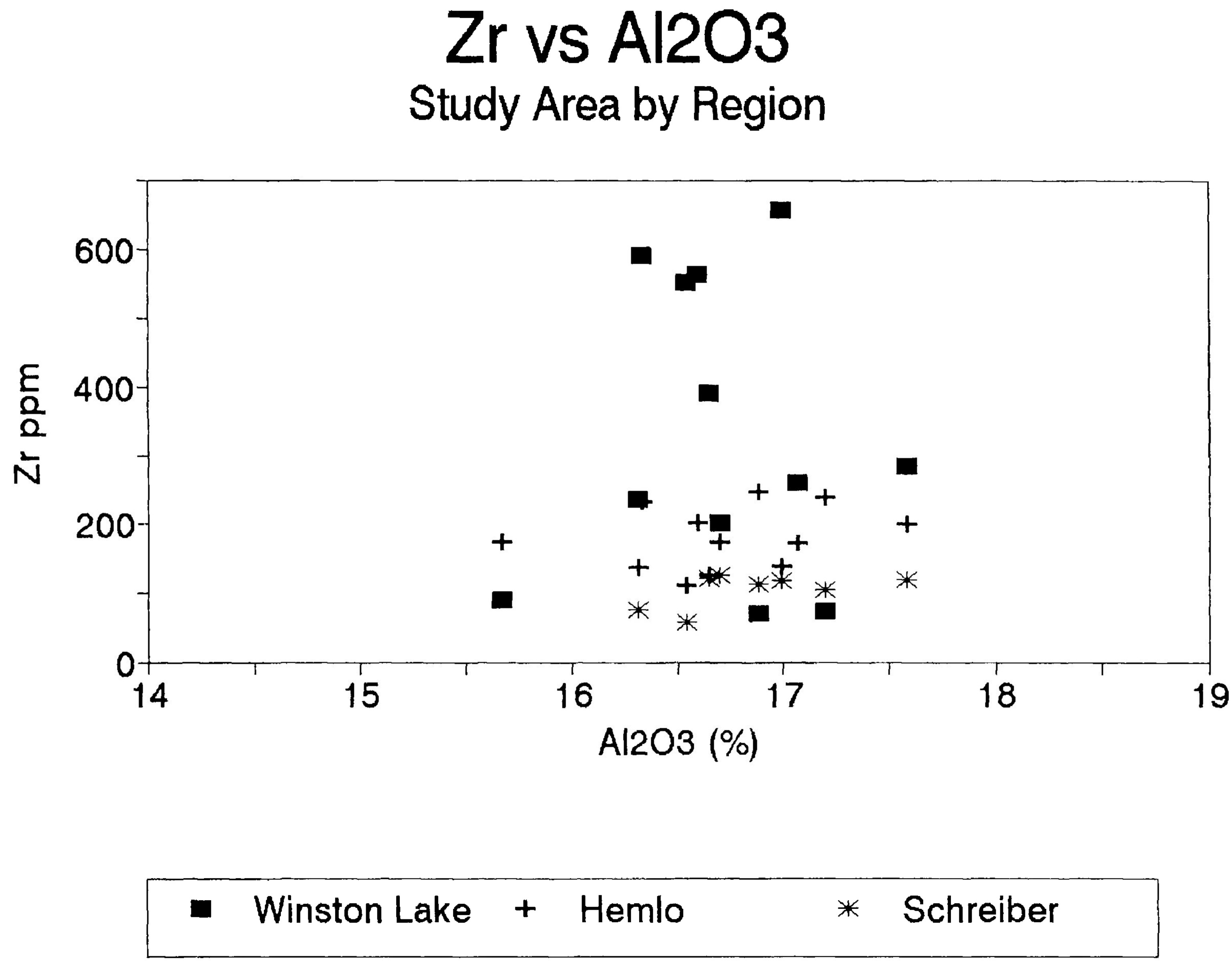
Zr vs Al2O3
Study Area by Region
Zr ppm
0
200
400
600
14
15
16
17
18
19
Al2O3 (%)
Winston Lake
Hemlo
Schreiber

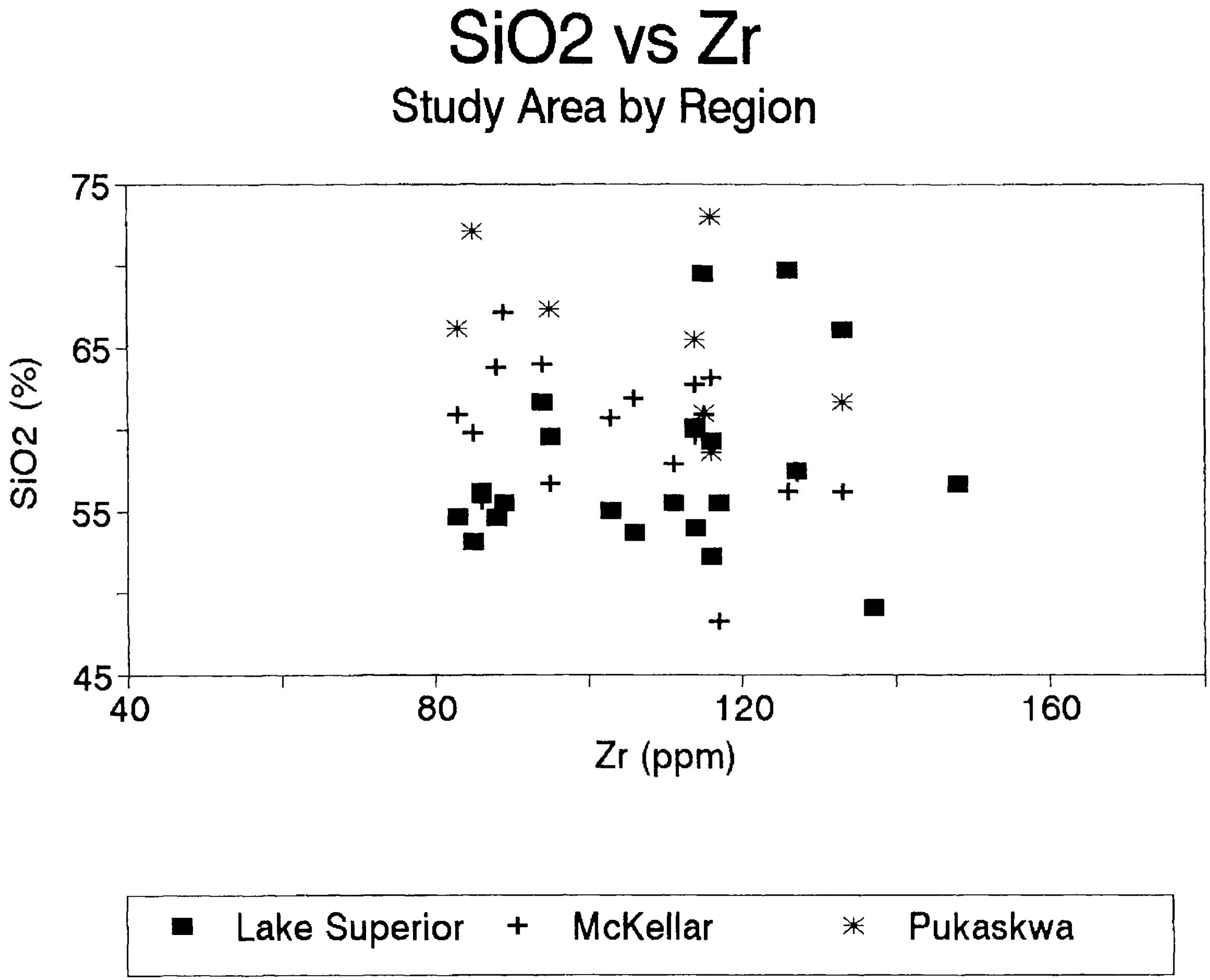
SiO2 vs Zr
Study Area by Region
75
65
55
45
SiO2 (%)
40
80
120
160
Zr (ppm)
Lake Superior
McKellar
Pukaskwa

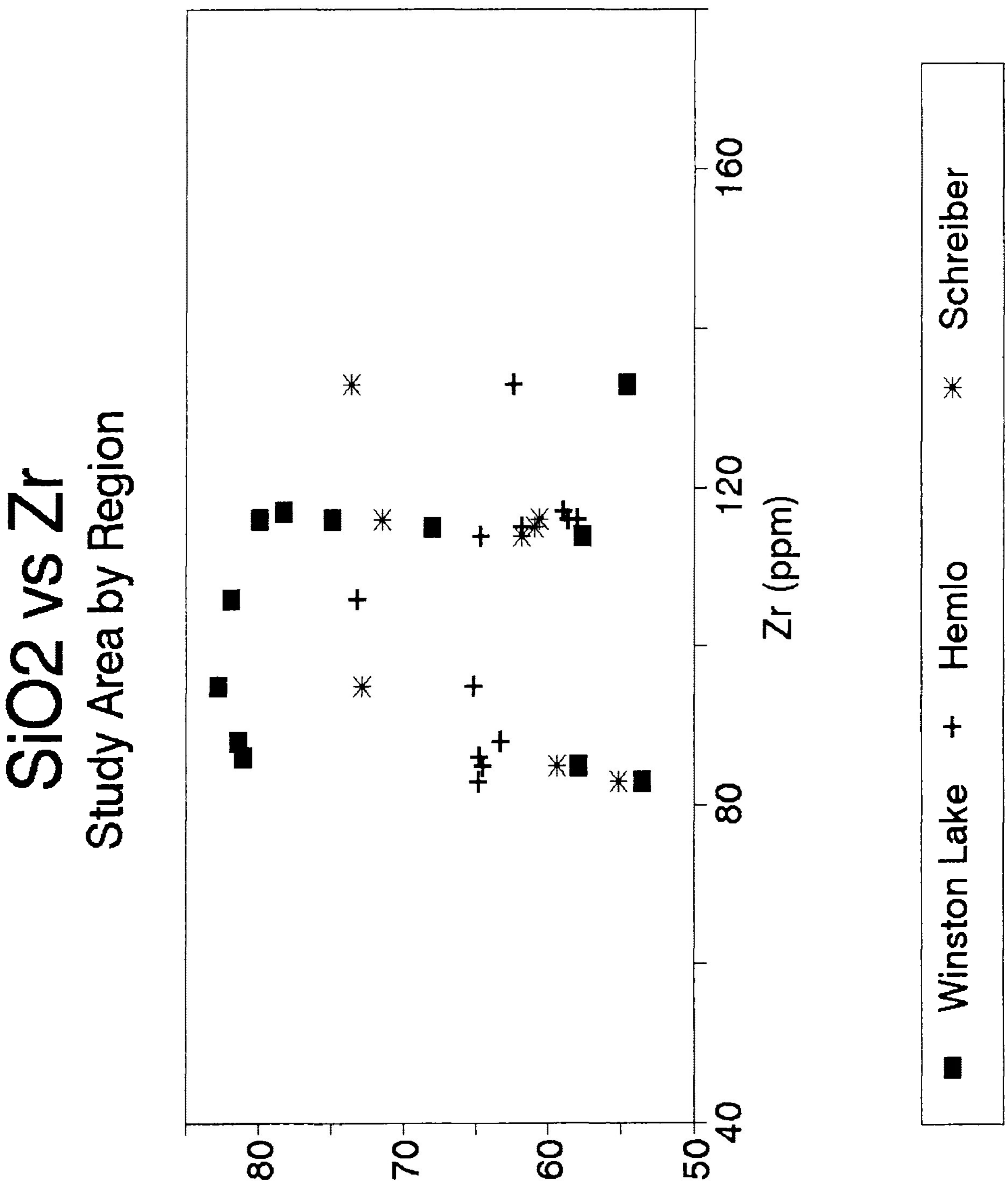

SiO2 vs Zr
Study Area by Region
SiO2 (%)
80
70
60
50
40
80
120
160
Zr (ppm)
Winston Lake
Hemlo
Schreiber

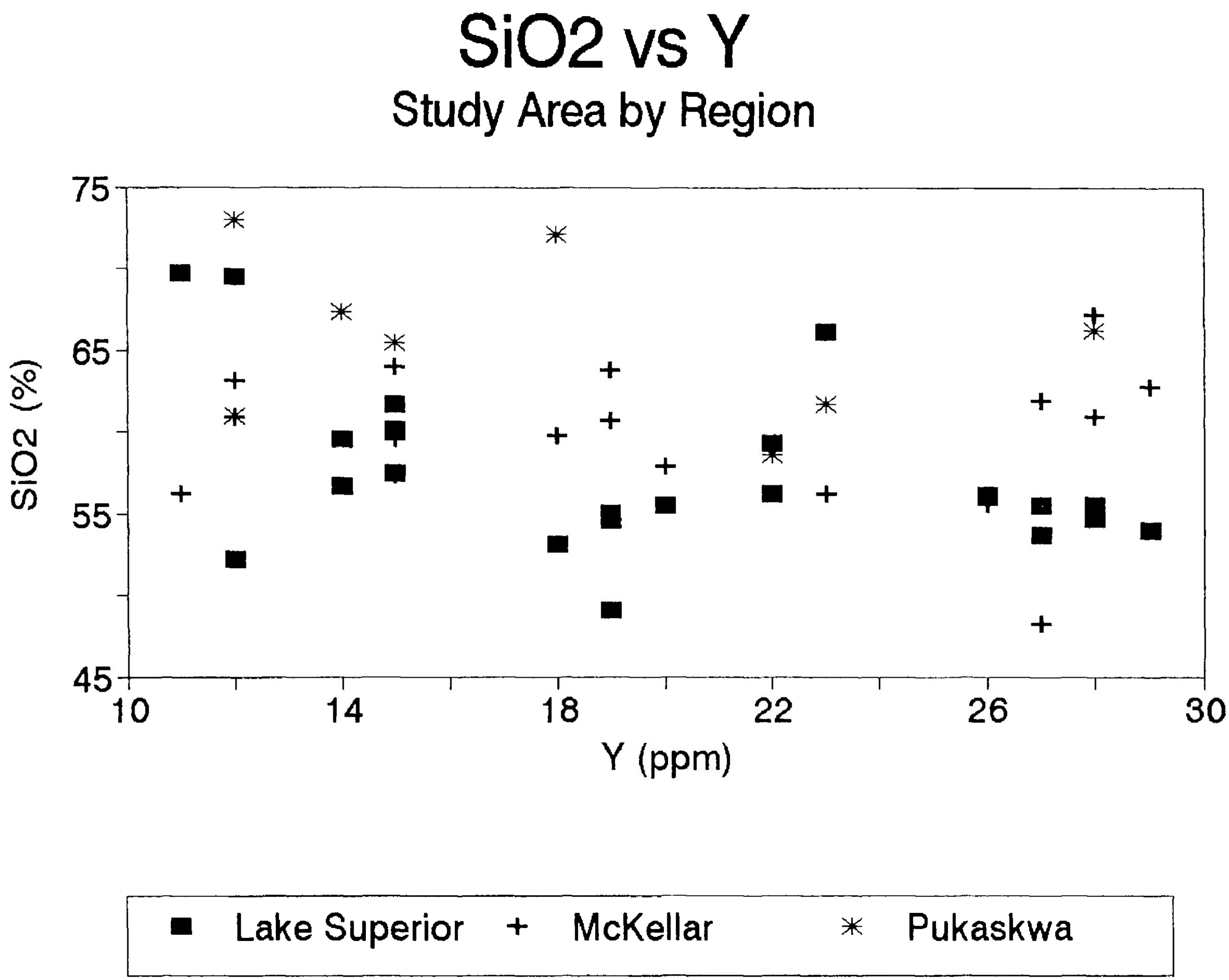
SiO2 vs Y
Study Area by Region
75
65
55
45
SiO2 (%)
10
14
18
22
26
30
Y (ppm)
Lake Superior
McKellar
Pukaskwa

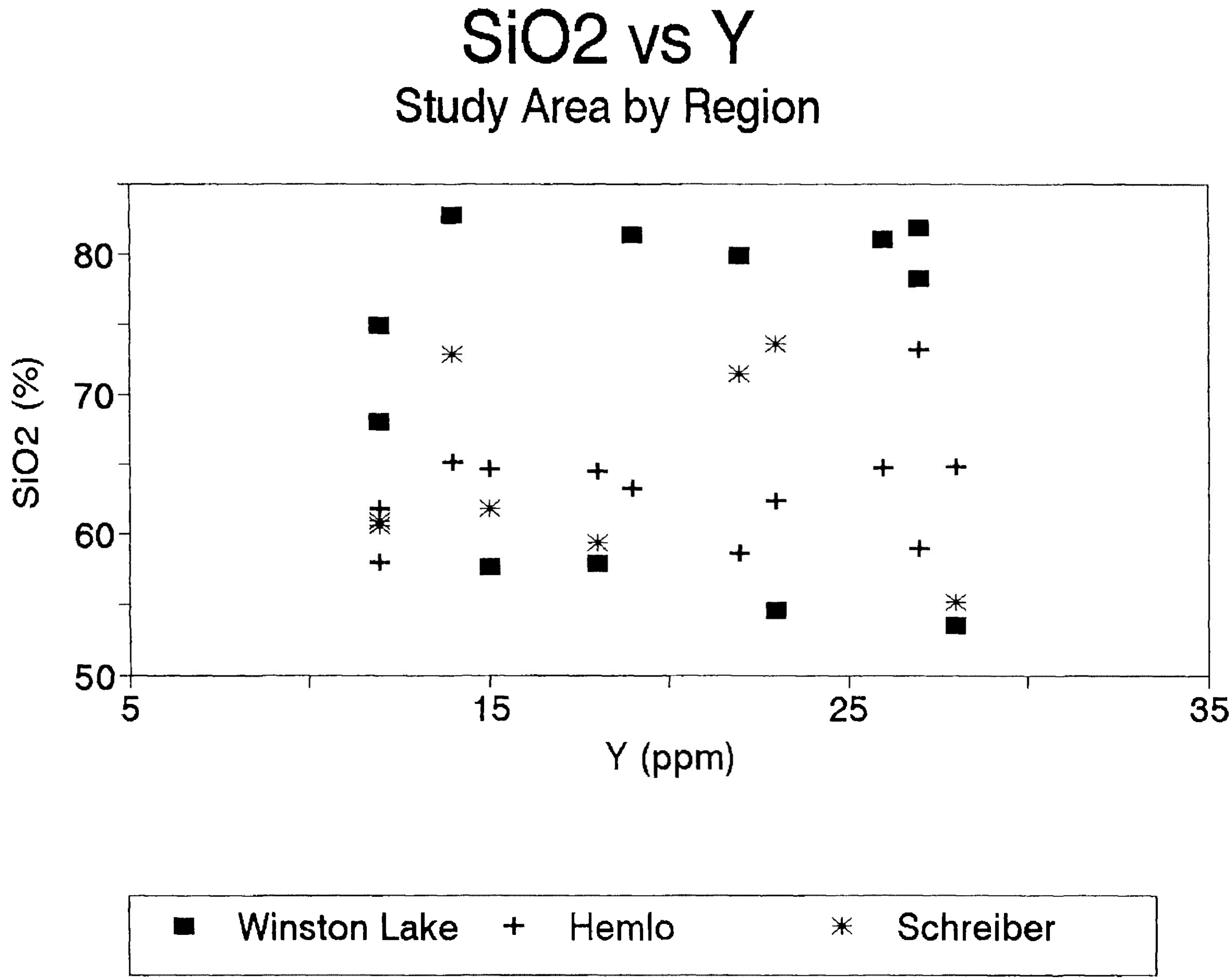
SiO2 vs Y
Study Area by Region
SiO2 (%)
80
70
60
50
5
15
25
35
Y (ppm)
Winston Lake
Hemlo
Schreiber

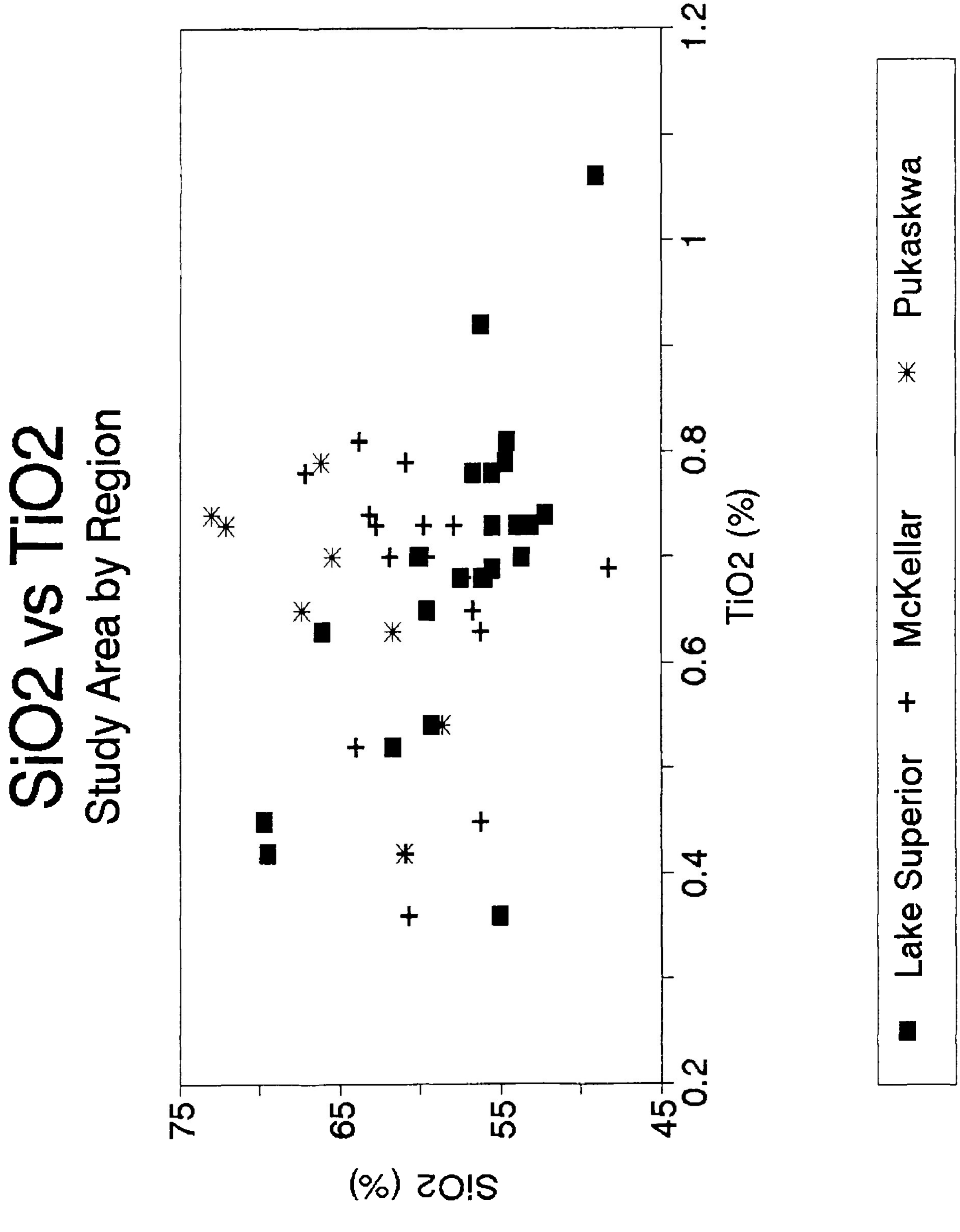

SiO2 vs TiO2
Study Area by Region
SiO2 (%)
75
65
55
45
TiO2 (%)
0.2
0.4
0.6
0.8
1
1.2
Lake Superior
McKellar
Pukaskwa

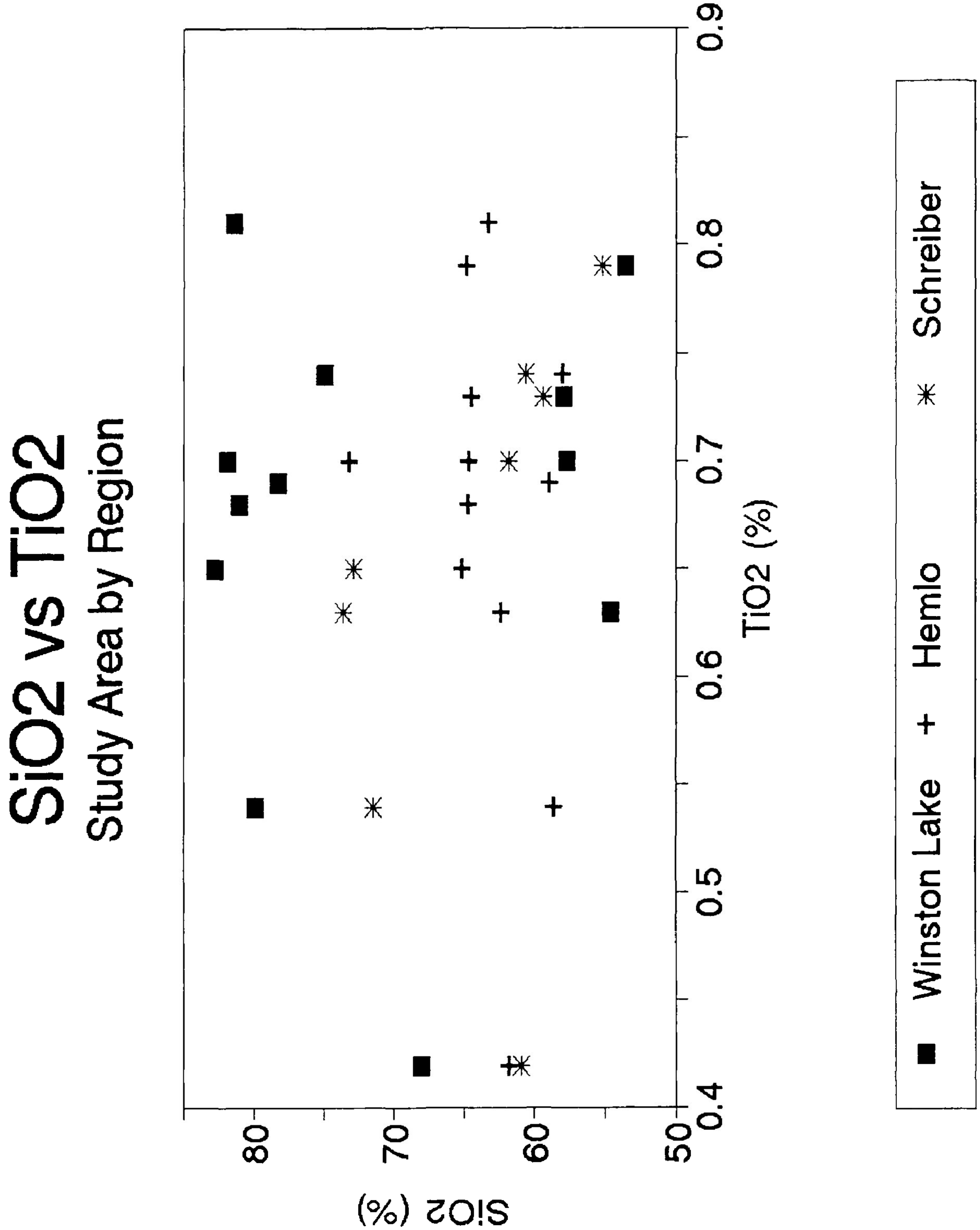
SiO2 vs TiO2
Study Area by Region
SiO2 (%)
80
70
60
50
0.4
0.5
0.6
0.7
0.8
0.9
TiO2 (%)
Winston Lake
Hemlo
Schreiber

# SiO2 vs Rb

## Study Area by Region

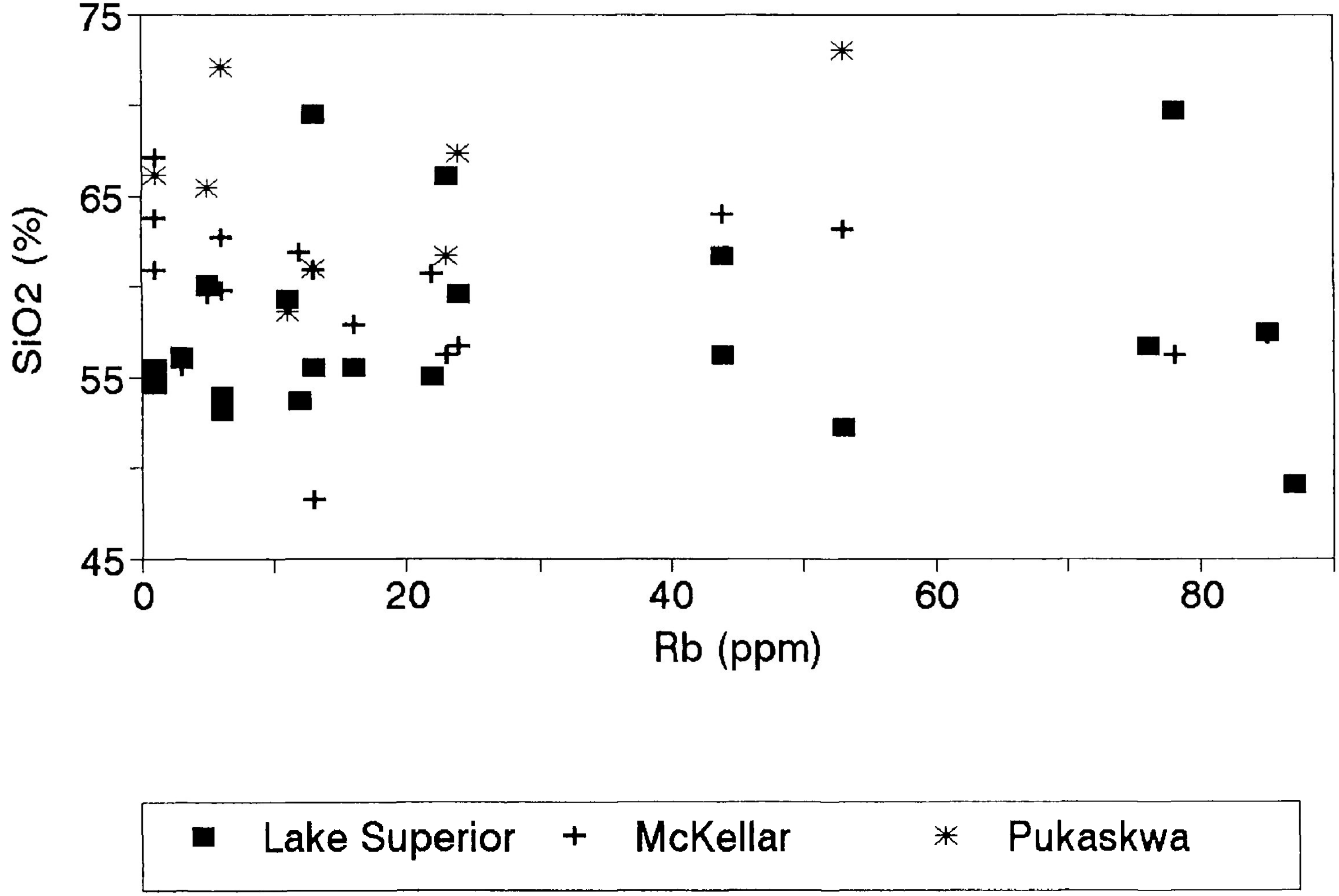

# SiO2 vs Rb

## Study Area by Region

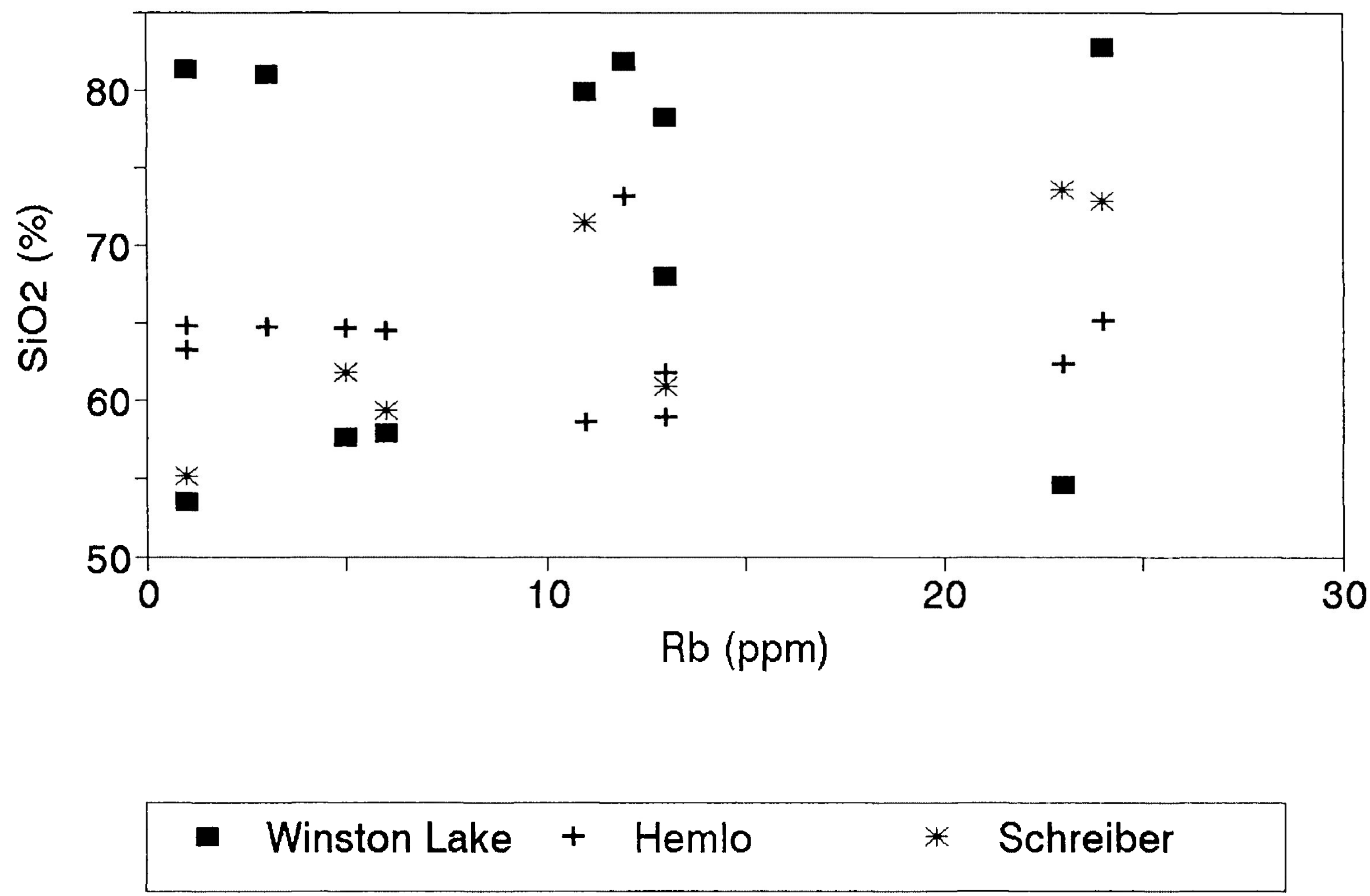

# SiO2 vs Nb

## Study Area by Region

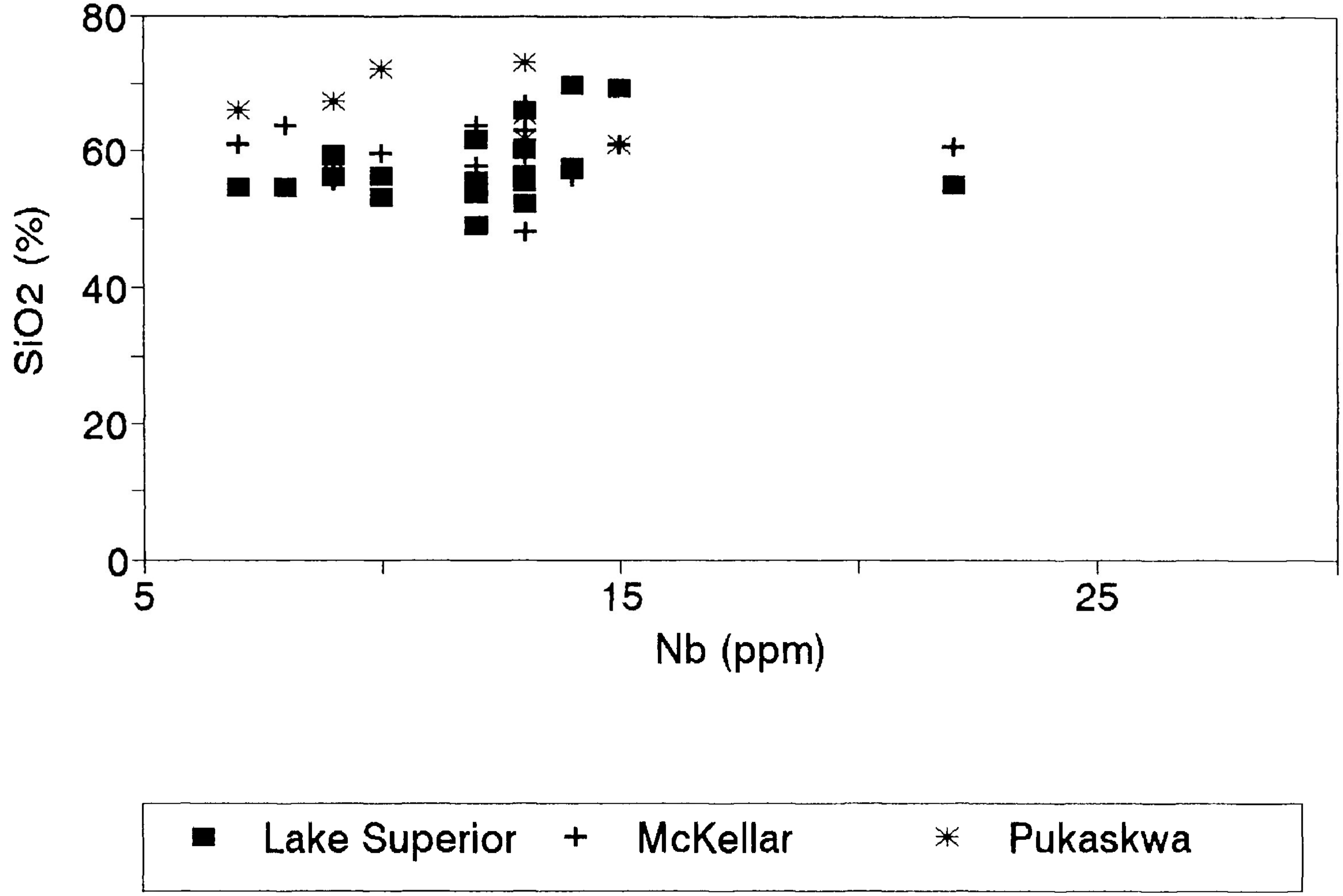

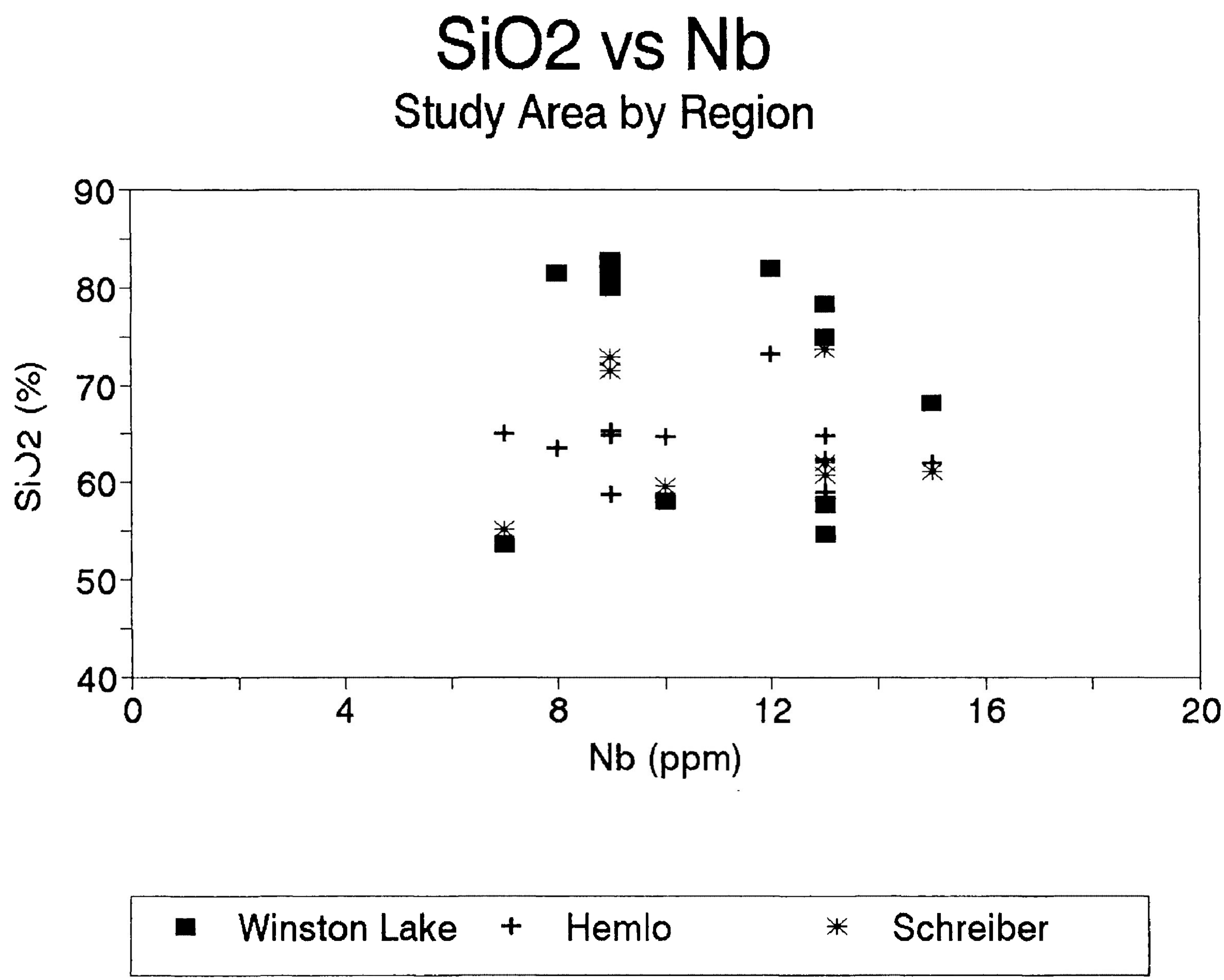
SiO2 vs Nb
Study Area by Region
SiO2 (%)
90
80
70
60
50
40
0
4
8
12
16
20
Nb (ppm)
Winston Lake
Hemlo
Schreiber

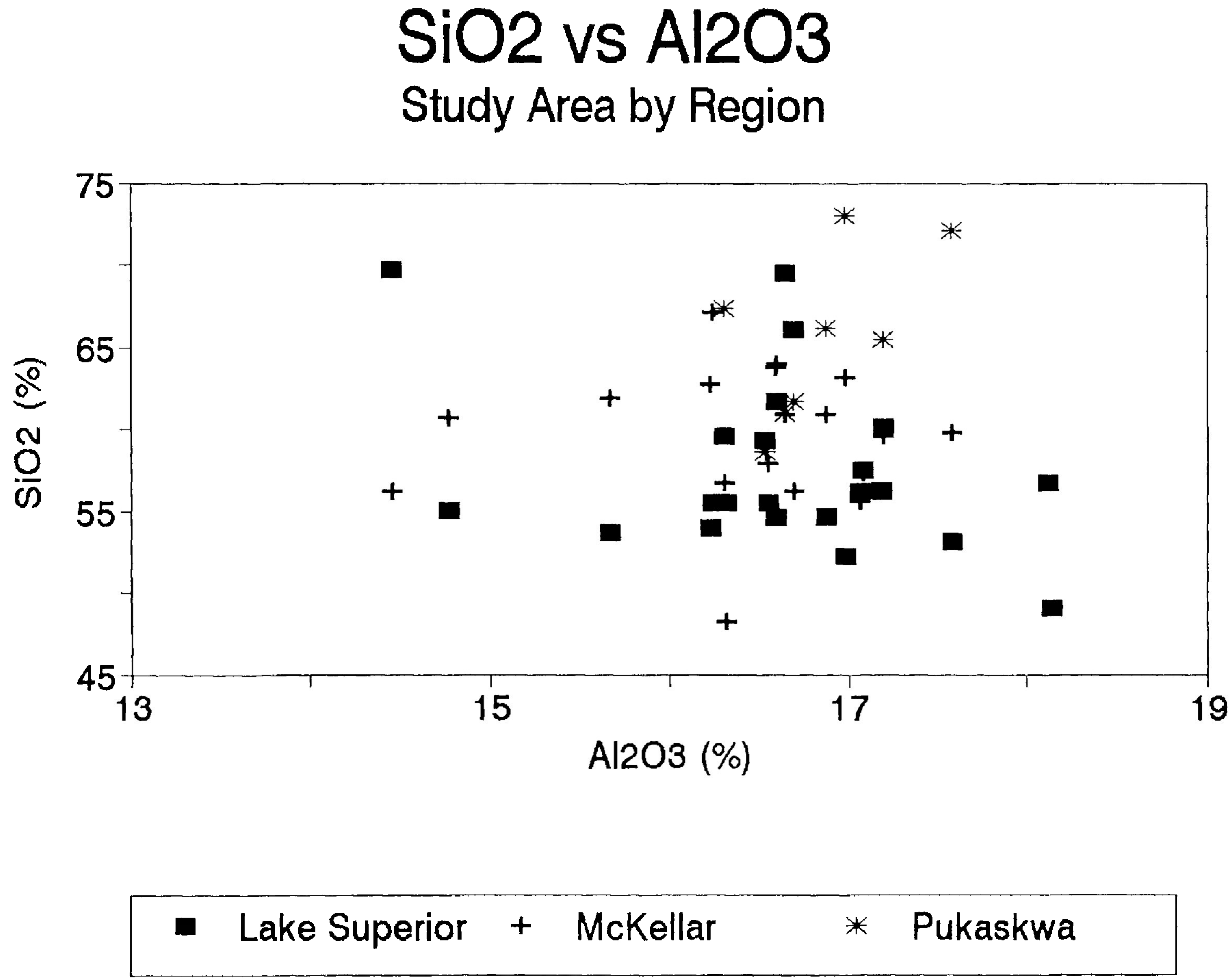
SiO2 vs Al2O3
Study Area by Region
SiO2 (%)
75
65
55
45
13
15
17
19
Al2O3 (%)
Lake Superior
McKellar
Pukaskwa

# SiO2 vs Al2O3

## Study Area by Region